Mohamed Khider University - Biskra

Faculty of Science and Technology

Department: Industrial Chemistry

Ref:...........................

جـــامعة محمد خيضر بـــسكرة

كـلية الـعلـــوم و التكـــنولوجـيا

قـسم : الكيمياء الصنــاعية

المرجع : ....

Thesis presented with a view to obtaining

LMD Doctorate in Chemical Process

Option: Chemical Engineering

Behavior of the dispersed phase in a biphasic liquid-liquid contactor

Comportement de la phase dispersé dans un contacteur diphasique liquide-liquide

Presented by:

Khaled ATHMANI

publicly defended on: 26/06/2022

before the jury composed of:

Mr. Abdelkrim MERZOUGUI	**Pr**	Chairman	University of Biskra
Mr. Abdelmalek HASSEINE	**Pr**	Reporter	University of Biskra
Mr. Hakim MADANI	**Pr**	Examiner	University of Batna 2
Mr. Zohir NEDJAR	**Pr**	Examiner	University of Khenchela

2021/2022

بسم الله الرحمن الرحيم

Abstract

In this work two major hydrodynamic parameters: the holdup of the dispersed phase and the Sauter diameter are considered. In the first part, this is done for describing the hydrodynamics of interacting liquid–liquid dispersions with using different drop breakup, coalescence and growth models in a droplet population balance model. Based on the variational iteration method, different process cases have been performed and, it is possible to find the exact solution or a closed approximate solution of a problem. For the simultaneous growth and the coalescence terms a comparison between the present method and projection method which include discontinuous Galerkin and collocation techniques are made respectively. The results are encouraging and the new method has proven to be suitable to predict holdup and Sauter diameter profiles.

In the second part, we extended the dual quadrature method of generalized moments (DuQMoGeM) to solve the population balance model for the hydrodynamics of liquid-liquid extraction columns using a multi-compartment model. The DuQMoGeM results were compared to analytical solutions for batch and continuous well-mixed vessels and extraction columns, showing that it is accurate for predicting the evolution of the low order moments and the drop number distribution along with the column height. We also modeled a Kühni column for which the simulation accurately predicted the steady-state experimental holdup, encouraging the DuQMoGeM usage to solve the population balance equation for heterogeneous systems and different columns.

Keywords: Population balance, Variational iteration method, DuQMoGeM, liquid-liquid dispersion, numerical modeling.

Resumé

Dans ce travail, deux paramètres hydrodynamiques majeurs : la rétention de la phase dispersée et le diamètre de Sauter sont considérés. Dans la première partie, ceci est fait pour décrire l'hydrodynamique des dispersions liquide-liquide en interaction en utilisant différents modèles de rupture, de coalescence et de croissance des gouttes dans un modèle de bilan de population de gouttes. Basé sur la méthode d'itération variationnelle, différents cas de processus ont été réalisés et il est possible de trouver la solution exacte ou une solution approximative fermée d'un problème. Pour les termes de croissance et de coalescence simultanées, une comparaison entre la méthode actuelle et la méthode de projection qui inclut des techniques de Galerkin discontinu et de collocation est faite respectivement. Les résultats sont encourageants et la nouvelle méthode s'est avérée adaptée à la prédiction des profils de Holdup et de diamètre de Sauter.

Dans la deuxième partie, nous avons étendu la méthode de double quadrature des moments généralisés (DuQMoGeM) pour résoudre le modèle de bilan de population pour l'hydrodynamique des colonnes d'extraction liquide-liquide en utilisant un modèle multi-compartiments. Les résultats de DuQMoGeM ont été comparés à des solutions analytiques pour des vessels et des colonnes d'extraction en batch et en continu bien mélangés, montrant qu'elle est précise pour prédire l'évolution des moments d'ordre faible et la distribution du nombre de gouttes en fonction de la hauteur de la colonne. Nous avons également modélisé une colonne Kühni pour laquelle la simulation a prédit avec précision la rétention expérimentale en régime permanent, ce qui encourage l'utilisation de DuQMoGeM pour résoudre l'équation de bilan de population pour des systèmes hétérogènes et des colonnes différentes.

Mots clés : Bilan de population, Méthode d'itération variationnelle, DuQMoGeM, dispersion liquide-liquide, modélisation numérique.

ملخـــــص

في هذا العمل تم الأخذ بعين الاعتبار معاملين هيدروديناميكيين رئيسيين: احتجاز الطور المشتت (Holdup) وقطر Sauter. في الجزء الأول، يتم إجراء ذلك لوصف الهيدروديناميكية للتشتت سائل-سائل المتفاعل باستخدام نماذج مختلفة لتفكك القطرات والاندماج والنمو في نموذج توازن الكثافة للقطيرات. بناءً على طريقة الحل الشبه التحليلية لتوازن الكثافة ، المسماة طريقة التكرار المتغير ، تم إجراء حالات عملية مختلفة ، ومن الممكن العثور على حل تحليلي أو حل تقريبي مغلق لمشكلة ما. بالنسبة للنمو المتزامن مع الاندماج ، يتم إجراء مقارنة بين الطريقة الحالية وطريقة الإسقاط التي تتضمن تقنيات جالركين المتقطعة (Discontinuous Galerkin) وتقنيات التجميع (Collocation) على التوالي. كانت النتائج مشجعة ، وقد أثبتت الطريقة الجديدة أنها مناسبة للتنبؤ بمنحنى احتجاز المرحلة المشتتة و كذلك قطر Sauter.

وفي الجزء الثاني ، قمنا بتوسيع نطاق استعمال الطريقة الرباعية المزدوجة للحظات المعممة (DuQMoGeM) لحل نموذج توازن الكثافة للهيدروديناميكية لأعمدة استخلاص سائل-سائل باستخدام نموذج متعدد المقصورات. وقورنت نتائج DQMoGeM بالحلول التحليلية للمفاعلات المغلوقة والمستمرة الجد مخلوطة وأعمدة الاستخلاص ، مما يبين أنها دقيقة للتنبؤ بتطور اللحظات ذات الرتب المنخفضة وتوزيع كثافة القطيرات على طول ارتفاع العمود. كما قمنا بنمذجة عمود Kühni حيث تنبأت المحاكاة بدقة للـ Holdup التجريبي في الحالة المستقرة، مما شجع استخدام DQMoGeM لحل معادلة توازن الكثافة للأنظمة الغير متجانسة والأعمدة المختلفة.

كلمات مفتاحية: توازن الكثافة، طريقة التكرار التغييري، DuQMoGeM، تشتت سائل-سائل , نمذجة عددية.

Acknowledgment

Khaled ATHMANI   Biskra, June 27, 2022

Contents

Nomenclature

a inverse of the residence time $[s^{-1}]$

A column cross-section area $[m^2]$

$\mathcal{A}_{jkli}$ aggregation matrix for compartment j $[m^{k+i+l}]$

B daughter drop conditional probability distribution $[m^{-1}]$

c coefficient in polynomial approximation of $\tilde{n}$ $[m^{-k-3}]$

c_v form factor $[-]$

C_1 collision frequency model parameter $[-]$

C_2 coalescence efficiency model parameter $[m^{-2}]$

d drop diameter as internal variable $[m]$

d_0 mother drop diameter on breakage $[m]$

d_1, d_2 diameters of coalescing drops $[m]$

D column diameter $[m]$

D_R rotor diameter $[m]$

$\mathcal{D}_{ef}$ effective dispersion coefficient $[m^2/s]$

f collision frequency $[m^3/s]$

F advective-dispersive flux $[m^{-3}s^{-1}]$

g breakage frequency $[s^{-1}]$

g_0 — breakage frequency model parameter $[-]$

G — growth rate

G — generic function (in the chapter IV)

$\mathcal{G}$ — gravitational acceleration $[m/s^2]$

h — column height $[m]$

h_j — compartment height $[m]$

H — breakage and coalescence source terms $[m^{-4}s^{-1}]$

$\mathcal{H}$ — Heaviside step function $[-]$

J — number of compartments $[-]$

$\mathcal{J}$ — Jacobian of the transformation of internal coordinates $[-]$

k_v — slowing factor $[-]$

$\mathcal{L}_{jki}$ — breakage matrix for compartment j $[m^{i+k}/s]$

m — mean of the Gaussian distribution $[m]$

M — number of Gauss-Legendre quadrature points $[-]$

n — drop number distribution in d variable $[m^{-4}]$

n_{in} — normalized drop number distribution of the feed $[m^{-1}]$

$\tilde{n}$ — drop number distribution in x variable $[m^{-3}]$

N_p — power number $[-]$

N_q — number of Gauss–Christoffel quadrature points $[-]$

N_R — rotor speed in revolutions per second $[s^{-1}]$

N_T — total number of droplets $[m^{-3}]$

N_0 — total number density of drops in the feed $[m^{-3}]$

p — volume distribution function $[m^{-1}]$

$P(d)$ breakage probability $[-]$

$\mathcal{P}$ power input per compartment $[W]$

Q phase volumetric flowrate $[m^3/s]$

r_d dispersed phase fraction (hold-up) $[-]$

Re_R Reynolds number of rotor/agitator $[-]$

s, u drop diameter values $[m]$

S source term $[m^{-4}s^{-1}]$

t time $[s]$

t_h hydrodynamic residence time $[s]$

v phase velocity $[m/s]$

v Droplet volume $[m^3]$

v_r relative velocity $[m/s]$

v_t terminal velocity $[m/s]$

V_d compartment volume $[m^3]$

$\mathcal{V}_{jki}$ convection matrix for compartment j $[m^{k+i+1}/s]$

w weight of the quadrature rule $[-]$

We_m modified Weber number $[-]$

We_R rotor Weber number $[-]$

x dimensionless diameter coordinate $[-]$

Y auxiliary variable

y, q dimensionless diameter values $[-]$

z height coordinate $[m]$

z_c continuous feed inlet $[m]$

z_d dispersed feed inlet $[m]$

Greek letters

α standard deviation of the Gaussian distribution $[m]$

β auxiliary function (in chapter IV)

β daughter droplet distribution $[m^{-1}]$

$\delta(X)$ Dirac delta function $[X^{-1}]$

$\delta_{i,j}$ Kronecker delta

$\Delta\rho$ density difference between phases $[kg/m^3]$

Δz height above disperse phase inlet, $z - z_d$ $[m]$

ϵ mechanical power dissipation $[W/kg]$

ζ dimensionless height variable, $\zeta = z/h$

η dynamic viscosity $[Pa\,s]$

θ plate free area fraction $[-]$

κ exponent in the swarm effect factor $[-]$

λ coalescence probability $[-]$

Λ auxiliary function

$\mu_k^{(\phi)}$ generalized moment of order k using the ϕ polynomial family $[m^{k-3}]$

μ_k regular moment of order k $[m^{k-3}]$

ν mean number of daughter droplets $[-]$

ξ abscissa of the quadrature rule $[-]$

ϖ angular velocity $\varpi = 2\pi N_R$ $[s^{-1}]$

$\Pi_k^{(\phi)}$ moments of the daughter distribution function of order k $[m^k]$

ρ density $[kg/m^3]$

σ	interfacial tension $[N/m]$
$v(d)$	drop volume corresponding to drop of diameter d $[m^3]$
$v'(d)$	derivative of drop volume function, $dv/d(d)$ $[m^2]$
$\bar{v}_{in}$	mean drop volume of the feed distribution $[m^3]$
Φ, Φ	auxiliary functions
$\phi_k(d)$	k-degree orthogonal polynomial in d variable $[m^k]$
$\varphi_k(x)$	k-degree orthogonal polynomial in terms of the x variable $[m^k]$
χ	auxiliary function
ψ	generic function
ω	coalescence frequency $[m^3/s]$
ω_0	coalescence frequency model parameter $[-]$

Subscripts

a	coalescence
b	breakage
c	continuous phase
$crit$	critical
d	dispersed phase
g	growth
in	inlet
max	maximum
min	minimum

Abbreviations

ADM	Adomian decomposition method

DG   discontinuous Galerkin

DQMOM   Direct quadrature method of moments

DuQMoGeM dual quadrature method of generalized moments

HPM   Homotopy perturbation method

LLEC   Liquid-liquid extraction columns

MOM   Method of moments

PBE   Population balance equation

PBM   Population balance model

QMOM   Quadrature method of moments

SQMOM   Sectional quadrature method of moments

VIM   variational iteration method

Superscripts

(a) analytical solution

(ϕ) relative to ϕ polynomial family

(φ) relative to φ polynomial family

List of Figures

List of Tables

General introduction

Liquid–liquid extraction is an important separation technique in chemical engineering, it finds many applications in hydrometallurgy, pharmaceuticals, petrochemical industry, environmental protection, and nuclear industry. Recently, it has gained more attention due to many reasons: increasing demand for heat-sensitive products in pharmaceutical industries, availability of selective low cost solvents and chelating agents has improved, the growing interest in products those must be separated from dilute aqueous solutions Laitinen et al., 2019.

In general, a liquid-liquid extraction system consists of two almost immiscible phases, with one dispersed in the form of fine droplets in the other continuous liquid phase. Several relevant properties of the dispersed phase come from the number density distribution that may change due to several mechanisms such as coalescence, breakage, and growth. However, the number density distribution evolution comes from solving a population balance equation. Consequently, population balance modeling is a powerful tool for predicting the dispersed phase behavior in liquid-liquid extraction equipment, such as columns and reactors Ramkrishna, 2000. In this sense, many scientific papers accomplished modeling and simulation of liquid-liquid extraction columns by the population balance equation. It became essential for modeling multiphase flow, mainly when a strong coupling exists between the number density distribution and the phase velocity fields Bart et al., 2020.

The determination of the total number dispersed phase hold-up and the particle size distributions in biphasic contactors is a key of chemical engineering processes in chemical industries, such as drops or bubbles columns, dispersed phase polymerization and reactions in organic chemistry. Such systems have been modelled using population

balance modelling, a method that describes the variations in size distribution of the dispersed phase as an averaged function of the behavior of individual particles, drops or bubbles. This approach requires description of the interactions of the dispersed phase such as breakage, aggregation and growth.

Mathematically, the population balance equation (PBE) is an integro-differential equation that is usually difficult enough to solve analytically. Therefore, it has solutions just for a few simple cases. Several researchers have developed numerical methods to find approximated solutions. A possible classification groups these methods into the following categories: methods of moments, stochastic methods, and discretization (or class) methods.

The most common discretization methods are the finite difference, finite element, and finite volume methods. They all discretize the domain of the internal coordinate (for instance, droplet diameter) Bart et al., 2020; Su et al., 2009. Although straightforward and accurate for calculating the particle size distribution, they have high computational costs to guarantee mass conservation Bart et al., 2020. These methods can approximate the distribution function in each discretization interval by a unique value (zero-order methods) or use high-order polynomials (higher-order methods) Bart et al., 2020.

Gelbard and Seinfeld, 1978 applied the orthogonal collocation on finite elements to the population balance equation. Nicmanis and Hounslow, 1996 solved a continuous crystallizer's steady-state population balance model using the Galerkin method and the orthogonal collocation methods on finite elements. Mantzaris et al., 2001a, 2001b used the finite difference and finite element methods to solve multivariate cell population balance models. S. Kumar and Ramkrishna, 1997; S. Kumar and Ramkrishna, 1996a, 1996b proposed three new approaches: the fixed pivot, the moving pivot, and the Lagrangian-moving pivot discretization methods. Campos and Lage, 2003 simulated a bubble extraction column using the Lagrangian-moving pivot technique. M. M. Attarakih et al., 2004 developed the extended fixed pivot technique (EFPT) to solve the PBE describing the hydrodynamics of interacting liquid-liquid phases.

Hulburt and Katz, 1964 introduced the method of moments. It has various advantages, such as efficiency, accuracy, and low computational cost, making it widely

used to solve the PBE. On the other hand, it does not give an approximation for the particle number distribution Bart et al., 2020. However, some mathematical techniques for reconstructing the size distribution function from its moments exist in the literature John et al., 2007. One of the most famous moments methods is the quadrature method of moments. It was first introduced and applied by McGraw, 1997 to describe the growth of aerosols and then extended to models with aggregation and breakage by Marchisio et al., 2003b. The main idea behind this method is the approximation of the integrals by the Gaussian quadrature constructed from the number density distribution moments. Marchisio and Fox, 2005 introduced the direct quadrature method of moments, whose central idea is the solution of transport equations for the quadrature weights and abscissas, avoiding their computation along the solution. M. M. Attarakih, Bart, and Faqir, 2006a introduced the sectional quadrature method of moments (SQMOM), which is a hybrid method involving the methods of classes and moments. The SQMOM discretizes the particle size domain in sections. The so-called primary particle represents the particle size in each one, being calculated from the secondary particles that are the abscissas of a local low-order quadrature. These local quadratures compute the breakage and coalescence terms.

The method of moments lacks a representation of the particle number distribution. P. L. Lage, 2011 introduced the dual quadrature method of generalized moments that gives a series approximation for the number density distribution using an orthogonal polynomial family whose coefficients are related to the generalized moments of the distribution for this polynomial family. The usage of high-order fixed-point Gaussian quadratures based on the same polynomial family controls the accuracy of the integral terms. Santos et al., 2013 introduced the direct version of DuQMoGeM that solves transport equations for the weights and abscissas of the Gauss-Christoffel quadrature. Another method that provides an approximation for the distribution is the extended quadrature method of moments (EQMOM), introduced by Yuan et al., 2012. It represents the number density distribution by a series of kernel density functions (KDF) whose locations are the abscissas of the Gauss-Christoffel quadrature. The EQMOM employs secondary Gaussian quadratures based on the KDFs to control the solution accuracy.

Recently much attention has been given to develop some semi analytical methods namely Adomian decomposition method and variational iteration method for solving PBE in stirred tank Hasseine, Barhoum, et al., 2015; Hasseine et al., 2011; Hasseine, Senouci, et al., 2015 and successive generation method Liou et al., 1997 for the one-dimensional gas-phase model in a bubble column reactor with simplifed hydrodynamics Campos and Lage, 2003.

The variational iteration method was first proposed by He J. He, 1997 and it is well known that VIM provide the most versatile tools available in nonlinear analysis problems J.-H. He, 2000b, 2004b, 2006, 2007; Mohyud-Din et al., 2017 . This method has been shown to be effective, easy and can accurately solve a large class of nonlinear problems. Generally, one or two iterations lead to high accurate solutions. This method is, in fact, a modification of the general Lagrange multiplier method into an iteration method, which is called correction functional.

This work developed a semi analytical methodology to solve the dynamic multi-dimensional PBE including advection in the internal and external coordinates, breakage, aggregation and growth that is based on the variational iteration method and solved also the PBE for the growth process by the discontinuous Galerkin method, which first was applied by Sandu and Borden, 2003 for the aerosol dynamics. The discontinuous Galerkin method was designed as an effective numerical method for solving hyperbolic conservation laws, which may have discontinuous solutions Cockburn, 2003; Cockburn and Shu, 1989.

This work also represented a numerical study that is the application of the DuQMo-GeM to solve the population balance equation for liquid-liquid columns using a multi-compartment model that represents a well-mixed vessel as a particular case.

Apart from this introduction which gives the aim objectives of this study ,this thesis is structured as follows:

The first chapter is a bibliographical study of the population balance equation. It touches upon the basic model for breakage, coalescence, growth and transport mechanisms. It also discusses the resolution methods of the population balance equation.

The second chapter represents the equations of the model and details the model-

ing of the liquid-liquid extraction columns. In particular, the model equation for both dispersed and continuous phases, drop breakage, drop coalescence, drop transport and axial dispersion.

The third chapter represents the results of solving the one-dimensional population balance equation involving breakage, coalescence, growth and simultaneous phenomenon by using the variational iteration method (VIM). For the simultaneous growth and the coalescence, a comparison between (VIM) and projection method which includes discontinuous Galerkin and collocation techniques are carried out graphically Hasseine et al., 2018.

The fourth chapter clearly explains how the DuQMoGeM is used to simulate the Liquid-Liquid extraction columns. We first applied it to solve such population balance models for test cases with analytical solutions. These include models for well-mixed reactors in both continuous and closed systems and a liquid-liquid extraction column without diffusion and with constant phase velocities. Finally, a realistic case of a Kühni column was modeled and solved, and the results were compared to available experimental data Athmani et al., 2022. The obtained results were carried out in collaboration with the laboratory Programa de Engenharia Quimica, Instituto Alberto Luis Coimbra de Pós-Graduação e Pesquisa de Engenharia, Universidade Federal do Rio de Janeiro (UFRJ).

Finally, a broad conclusion highlights all of the major findings from both analytical and numerical parts of this study.

Chapter I

A bibliographic review

I.1   Introduction

In general, multi-phase process consists of two phases with one dispersed in the form of fine particles (droplet, bubble, crystal..) in the other continuous liquid phase. The dispersed phase properties may be changed due to several mechanisms such as coalescence, breakage and mass transfer. A particle is distinguished by two kinds of coordinates (internal and external). The particle's internal coordinates give a quantitative characterization of its distinguishing characteristics, while the particle's external coordinates simply indicate where the particles are in physical space. However, the evolution of particles in gas-liquid, gas-solid and liquid-liquid systems is modelled successfully by the population balance equation. Consequently, it is regarded as a powerful tool to predict the dispersed phase behavior in process equipment columns and reactors Ramkrishna, 2000.

The first application of the PBE is according to the earlier work of Hulburt and Katz, 1964 where they studied nucleation and growth of crystals, and then it had extensions to liquid-liquid interaction in continuous and batch flow systems Valentas and Amundson, 1966, aerosol aggregation Gelbard and Seinfeld, 1978, cell biology Liou et al., 1997. Ramkrishna and Singh, 2014 reviewed the application area of population balance with other statistical information like the number of published articles on population balances per year. Mathematically, the population balance equation is defined as

an integro-partial differential equation, usually, it is difficult enough to solve analytically. Therefore, it has solutions just for some few simple cases, and several numerical methods were proposed to find approximated solutions.

The first parts of this chapter are concerned with the population balance equation and its solution methods, while in the last part, some exact solutions that come from previous research are presented.

I.2   Population balance equation

The PBE in one-dimensional can be expressed in terms of the number density function $n\left(t, z, v\right)$ using droplet volume v as the internal coordinate Ramkrishna, 2000:

$$\frac{\partial n\left(t, z, v\right)}{\partial t} + \nabla v_d n\left(t, z, v\right) = \nabla\left(D_d \nabla n\left(t, z, v\right)\right) + H\left(t, z, v\right) \tag{I.1}$$

The second term on the left-hand side represents the droplet transport by convection with a dispersed phase velocity v_d, the first term on the right-hand side is the droplet transport by diffusion, where D_d is the dispersion coefficient of the dispersed phase. Breakage, coalescence and growth terms are collected in $H\left(t, z, v\right)$:

$$H\left(t, z, v\right) = H_b\left(t, z, v\right) + H_a\left(t, z, v\right) + H_g\left(t, z, v\right) \tag{I.2}$$

The population balance equation describing the hydrodynamic behavior of the dispersed phase in a continuous well-mixed system could be written as Ramkrishna, 2000:

$$\frac{\partial n\left(t, v\right)}{\partial t} = \frac{1}{t_h}\left(n_{in}\left(t, v\right) - n\left(t, v\right)\right) + H\left(t, v\right) \tag{I.3}$$

Where $n_{in}\left(t, v\right)$ and $n\left(t, v\right)$ is the number density function and the inflow distribution, respectively. t_h is the mean residence time of the dispersed phase. For a batch reactor, the equation (I.3) takes this form:

$$\frac{\partial n\left(t, v\right)}{\partial t} = H\left(t, v\right) \tag{I.4}$$

In order to understand this equation, we must explain its source terms in details, these will be discussed under the relevant subsections:

I.2.1   Breakage

Breakage is the result of viscous shear forces and turbulent pressure fluctuations in the vicinity of a droplet. Drop breakage occurs when a single droplet (mother drop) divides into several daughter droplets, which reduces droplet volume and increases the number of droplets. The breakage frequency $g(z,v)$ and the distribution of droplet sizes resulting from the breakage of a mother drop $\beta(v/v')$ are adequate to describe the breakage process, its term is given by Valentas et al., 1966:

$$H_b = \int_v^\infty \beta\left(v/v'\right) g\left(z,v'\right) n\left(t,z,v'\right) dv' - g\left(z,v\right) n\left(t,z,v\right) \tag{I.5}$$

The integral term represents droplet formation due to breakage, while the other term represents droplet loss due to breakage. The function $\beta(v/v')$ must satisfy: $\beta(v/v') = 0, \ v > v'$.

I.2.2   Coalescence:

This breakage process is balanced by coalescence. It is a complicated mechanism where two or more drops merge into a larger drop. However, it has been discussed in detail in the paper of Valentas and Amundson, 1966. In Muralidhar and Ramkrishna, 1986 the drop coalescence mechanism in a turbulent flow field was considered as a problem of film drainage under the action of turbulent forces. In general, the coalescence phenomena are characterized by coalescence frequency $\omega(z,v,v')$, and consist of two terms birth (+) and death (-), which are rewritten as Valentas and Amundson, 1966:

$$\begin{aligned}
H_a(t,z,v) = & \frac{1}{2}\int_0^v \omega\left(z,v-v',v'\right) n(t,z,v) n\left(t,z,v-v'\right) dv' \\
& - \int_0^\infty \omega\left(z,v,v'\right) n(t,z,v) n\left(t,z,v'\right) dv'
\end{aligned} \tag{I.6}$$

The first introducing of this function is related to the study of Marian Smoluchowski Smoluchowski, 1916.
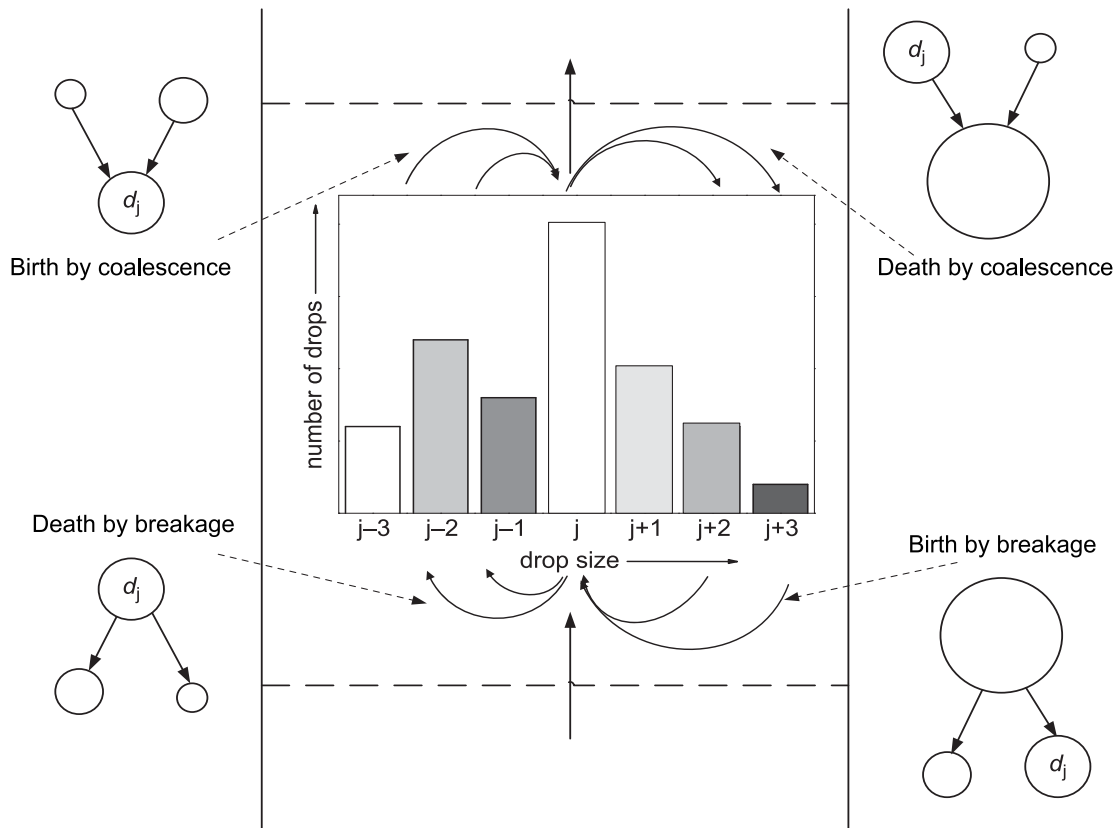
Figure I.1: Graphical representation of the breakage and coalescence terms, balance of a drop with diameter d_j Kopriwa et al., 2012

In Marchisio et al., 2003b the most common employed aggregation kernels (constant, Brownian, sum...) and breakage kernels (constant, power law, exponential) were listed, the PBE was also formulated in terms of the number density function using particle length as the internal coordinate.

The breakage and coalescence terms (birth and death) are presented graphically in the Figure I.1, which shows how each term affects the number of drops.

I.2.3   Growth

Due to mass transfer between phases, droplet volume may be changed. Growth is the process by which non-particulate matter becomes incorporated within a particle, it is defined as movement along the particle volume, this phenomenon is described by a

rate, this is often called growth rate $G\left(v\right)$, the growth term is reckoned as M. Hounslow, 1998:

$$H_g\left(t,z,v\right) = \frac{\partial\left(G\left(v\right)n\left(t,z,v\right)\right)}{\partial v} \tag{I.7}$$

where:

$$G\left(v\right) = \frac{\partial v}{\partial t} \tag{I.8}$$

In the crystallization process, anotheranother phenomenon, so-called nucleation is taken into account. It is a generation of the particles of size l_0 from a supersaturated solution with a rate of nucleation B_{nuc} (it is the rate of appearance of particles of zero size) M. Hounslow et al., 1988; Marchal et al., 1988.

I.3 Methods for solving the population balance equation

This section will be concerned with solution methods for population balance equations. Since the population balance equation solution is important, several solution methods have been proposed to solve it. However, its difficulty, especially in the analytical way, M. M. Attarakih et al., 2004; Kopriwa et al., 2012; Su et al., 2009 reviewed several methods for solving PBE. The numerical techniques can be grouped into the following categories: Method of moments, stochastic methods, high-order and zero-order methods. Both numerical and analytical methods are discussed below. In order to facilitate their classification, they are represented schematically in Figure.I.2.

I.3.1 Direct discretization methods

The most common discretization methods (also called class method) are: the finite difference method, finite element method and finite volume method. They discretize directly the internal coordinate (droplet diameter, concentration, ...) in the solution domain. Bart et al., 2020; Su et al., 2009. They are straightforward methods with accurate calculation of particle size distribution. Their mean drawbacks are the long computational time while guaranteeing the conservation of mass Bart et al., 2020. The direct discretization methods are classified into two categories: zero-order methods and
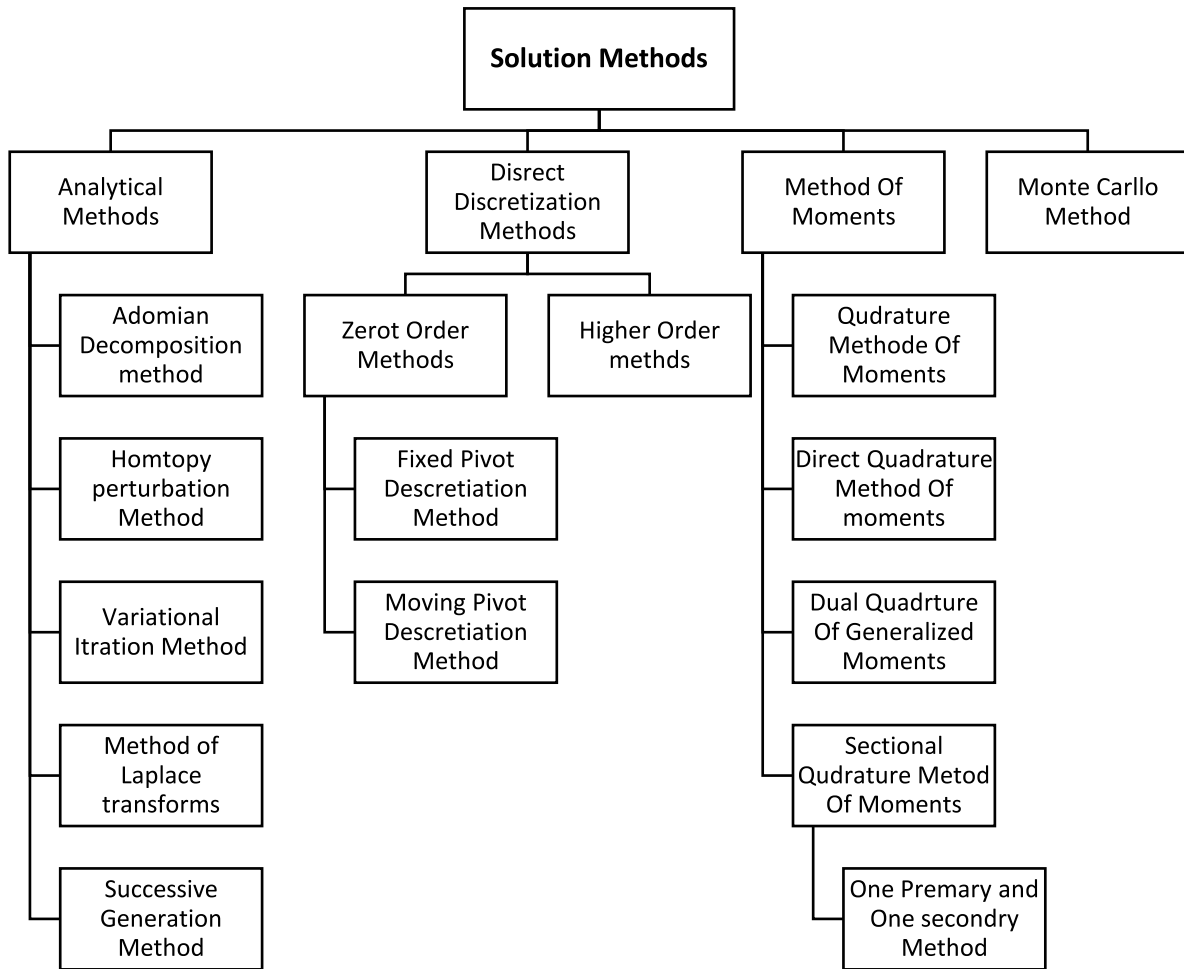
Figure I.2: Numerical and analytical methods to solve the population balance equation

Higher-order methods.

In zero-order methods, the droplet size is divided into a finite number of classes. In each class, the distribution is represented by a constant value (zero-order polynomial).

Higher-order methods approximate the drop-size distribution by higher-order polynomials, usually, the cubic polynomials are used.

In the earliest work of Gayler et al., 1953, they applied the orthogonal collocation on finite elements to the solution of the population balance equation for particulate systems. Nicmanis and Hounslow, 1998 solved steady-state population balance equation for continuous crystallizer using the Galerkin and the orthogonal collocation methods on finite elements. Mantzaris et al., 2001a, 2001b used the finite difference method and finite element method for multi-variable cell population balance models. Two promise ap-

proaches were proposed by S. Kumar and Ramkrishna, 1996a, 1996b: the fixed pivot discretization method and the moving pivot discretization method. These methods have been used in the commercial CFD software ANSYS CFX§and ANSYS Fluent§Bart et al., 2020. In Campos and Lage, 2003 they used the fixed-pivot technique to simulate a bubble column. In M. M. Attarakih et al., 2004 they have extended the fixed-pivot technique (EFPT) to solve the PBE describing the hydrodynamics of interacting liquid-liquid.

I.3.2   Monte Carlo method (MC)

Monte Carlo method is a stochastic method. It is easy to program and can be applied to multivariate PBE with respect to internal coordinate M. M. Attarakih et al., 2004. It is difficult to couple this method with CFD code due to its discrete features and high computational expense. based on the driven pattern of the discrete physical events this method is classified into time-driven algorithms and event-driven algorithms Su et al., 2009. Altunok et al., 2006 Developed a simulator named ReDrop for LLEC. In the ReDrop algorithm, individual drops and their ways are followed along an extraction column. The ReDrop approach is a Monte-Carlo method to solve the drop-population balances.

I.3.3   Method of moments MOM

The method of moments was initially introduced in 1963 by Hulburt and Katz, 1964. It has various advantages such as efficiency, accuracy, and low computational time. Because of them, it is widely utilized to solve the PBE, but on the other hand, it loses the size distribution function Bart et al., 2020. However, some mathematical techniques for reconstructing the size distribution function from its moments have been proposed in the literature John et al., 2007.

The population balance equation can be reduced to be a set of moment equations using the following expression Hulburt and Katz, 1964:

$$\mu_k\left(t,z\right) = \int_0^\infty v^k n\left(t,z,v\right) dv \tag{I.9}$$

Where μ_0, μ_1 are the total number of particles and the total volume of particles, respectively.

In order to assume the particle length is the internal variable, Marchisio et al., 2003b transformed the PBE from volume form to length-based form using these considerations:

The particle volume has a cubic form $v \propto l^3$ and $dv = 3l^2 dl$, where l is the particle length.

For a constant droplet velocity, they obtained this general form:

$$\frac{\partial n\,(t,z,l)}{\partial t} + v_d \frac{\partial n\,(t,z,l)}{\partial z} = \frac{\partial}{\partial z}\left(D_{ax}\frac{\partial n\,(t,z,l)}{\partial z}\right)$$
$$+ H_a\,(t,z,l) + H_b\,(t,z,l) + H_g\,(t,z,l) \tag{I.10}$$

Where, $n\,(t,z,l)$ is the length-based number density function.

The aggregation term is:

$$H_{a,k}(t,z) = \frac{1}{2}\int_0^\infty n\,(t,z,l')\int_0^\infty \omega\,(z,u,l')\left(u^3 + l'^3\right)^{k/3} n(t,z,u)\,du\,dl'$$
$$- \int_0^\infty l^k n(t,z,l)\int_0^\infty \omega\,(z,l/l')\,n\,(t,z,l')\,dl'\,dl \tag{I.11}$$

Breakage term:

$$H_{b,k}(t,z) = \int_0^\infty l^k \int_l^\infty \beta\,(l/l')\,g\,(z,l')\,n\,(t,z,l')\,dl'\,dl$$
$$- \int_0^\infty g(z,l)l^k n(t,z,l)\,dl \tag{I.12}$$

The growth term is:
$$H_g\,(t,z,l) = -\frac{\partial\,(G\,(l)\,n\,(t,z,l))}{\partial l} \tag{I.13}$$

The kth moment of $n\,(t,z,l)$ is defined as M. Hounslow et al., 1988:

$$\mu_k\,(t,z) = \int_0^\infty l^k n\,(t,z,l)\,dl \tag{I.14}$$

The first four moments have the following physical meanings:

μ_0: is the total number of particles.

μ_1: is the total length of particles.

μ_2: is the total area of particles.

μ_3: is the total volume of particles.

Applying the moment transformation given by equation (I.14) , we obtain Marchisio et al., 2003a:

$$\frac{\partial \mu_k(t,z)}{\partial t} + v_d \frac{\partial \mu_k(t,z)}{\partial z} = \frac{\partial}{\partial z}\left(D_d \frac{\partial \mu_k(t,z)}{\partial z}\right)$$
$$+ H_{a,k}(t,z) + H_{b,k}(t,z) + H_{g,k}(t,z)$$

(I.15)

This model has found wide uses in the description of the dispersed phase, especially in the crystallization process. Source terms of the moments of $n(t,z,l')$ are written as:

Using the variable u: $u^3 = l^3 - l'^3$ and $dl = u^2/l^2 du$, the aggregation term becomes:

$$H_{a,k}(t,z) = \frac{1}{2}\int_0^\infty n(t,z,l') \int_0^\infty \omega(z,u,l') \left(u^3 + l'^3\right)^{k/3} n(t,z,u)\, du dl'$$
$$- \int_0^\infty l^k n(t,z,l) \int_0^\infty \omega(z,l/l')\, n(t,z,l')\, dl' dl$$

(I.16)

Breakage term:

$$H_{b,k}(t,z) = \int_0^\infty l^k \int_l^\infty \beta(l/l')\, G(l')\, n(t,z,l')\, dl' dl$$
$$- \int_0^\infty g(l)\, l^k\, n(t,z,l)\, dl$$

(I.17)

The growth term is simplified as (disappearance of the derivative):

$$H_{g,k}(t,z) = -\int_0^\infty k\, l^{k-1} G(l)\, n(t,z,l)\, dl$$

(I.18)

There are several methods are derived from the method of moments, such as QMOM, DQMOM and SQMOM; these will be discussed as follows:

QMOM

One of the most moments methods is the quadrature method of moments. It was first introduced and applied by McGraw, 1997 to describe the growth of aerosols. The main idea behind this method is the approximation of the integrals by Gaussian quadrature. Furthermore, the weights w_i and the abscissas l_i are completely specified in terms of the lower-order moments of the distribution function $n\,(t,z,l)$.

For n quadrature point, the first $2n$ moments are calculated by McGraw, 1997:

$$\mu_k\,(z,t) = \int_0^\infty l^k n\,(t,z,l)\,dl = \sum_{i=1}^n l_i^k w_i \tag{I.19}$$

After applying the above quadrature rule, we obtain Marchisio et al., 2003a:

$$\frac{\partial \mu_k\,(t,z)}{\partial t} + v_d \frac{\partial \mu_k\,(t,z)}{\partial z} = \frac{\partial}{\partial z}\left(D_d \frac{\partial \mu_k\,(t,z)}{\partial z}\right)$$
$$+ H_{a,k}\,(t,z) + H_{b,k}\,(t,z) + H_{g,k}\,(t,z) \tag{I.20}$$

The moments of the birth and death rates become:

$$H_{a,k}\,(t,z) = \frac{1}{2}\sum_{i=1}^n w_i \sum_{j=1}^n w_j \left(l_i^3 + l_j^3\right)^{k/3} \omega_{ij} - \sum_{i=1}^n l_i^k w_i \sum_{j=1}^n w_j \omega_{ij} \tag{I.21}$$

$$H_{b,k}\,(t,z) = \sum_{i=1}^n g_i \bar{\beta}_i^k - \sum_{i=1}^n g_i w_i \tag{I.22}$$

Where:

$$\bar{\beta}_i^k = \int_0^\infty l^k \beta(l/l_i)\,dl \tag{I.23}$$

The growth term is given by:

$$H_{g,k}\,(t,z) = k \sum_{i=1}^n w_i\; l^{k-1} G_i \tag{I.24}$$

Gordon, 1968 proposed an algorithm so-called product-difference algorithm to determine the weights and the abscissas that are needed for the quadrature.

DQMOM

The principal idea of the direct quadrature method of moments is the direct solution of the transport equations for weights and abscissas Fox, 2003. In DQMOM the distribution function $n\,(v, z, t)$ and its moments $\mu_k(z, t)$ are approximated by the following summations Marchisio and Fox, 2005:

$$n\,(t, z, v) = \sum_{i=1}^{n} v_i^k w_i\,(z, t)\, d\,[v - v_i\,(t, z)] \tag{I.25}$$

$$\mu_k\,(t, z) = \int_0^\infty v^k n\,(t, z, v)\, dv = \sum_{i=1}^{n} v_i^k w_i \tag{I.26}$$

Using these approximations, the general formula of DQMOM is these two transport equations for the weights w_i and weighted abscissas ς_i Marchisio and Fox, 2005 :

$$\frac{\partial w_i}{\partial t} + \frac{\partial(\langle v_{d,j}\rangle_i w_i)}{\partial z_j} - \frac{\partial}{\partial z_j}\left(D_d \frac{\partial w_i}{\partial z_j}\right) = a_i \tag{I.27}$$

$$\frac{\partial \varsigma_i}{\partial t} + \frac{\partial(\langle v_{d,j}\rangle_i \varsigma_i)}{\partial z_j} - \frac{\partial}{\partial z_j}\left(D_d \frac{\partial \varsigma_i}{\partial z_j}\right) = b_i \tag{I.28}$$

Where a_i and b_i are the source terms and $\varsigma_i = w_i v_i$.

DuQMoGeM

The dual-quadrature method of generalized moments is a new numerical method for solving the PBE, it was proposed first by P. L. Lage, 2011, and it was shown good accuracy than the QMOM for breakage and aggregation problems. The key advantage of the DuQMoGeM is its ability to reconstruct the distribution function.

In order to understand the principal idea of DuQMoGeM, we must define the generalized moment of the PBE firstly, those are given by:

$$\mu_k^{(\phi)} = \int_0^{v_{max}} n\,(t, v)\, \phi_k\,(v)\, dv \tag{I.29}$$

Where:

$\phi_k(v)$, is an orthogonal polynomial of k order.

If $\phi_k(v) = v^k$, $\phi_k(v)$ become the regular moments μ_k.

After applying the moments transformation (I.29) to the PBE, with some manipulation we get P. L. Lage, 2011:

$$
\frac{\partial \mu_k^{(\phi)}}{\partial t} + \underbrace{\int_0^{v_{max}} G(t,v)n(t,v)\phi_k(v)dv + [G(t,v)n(t,v)\phi_k(v)]_0^{v_{max}}}_{\text{growth term}}
$$

$$
+ \underbrace{\int_0^{v_{max}} \int_0^{v_{max}} \left[\phi_k(v) - \frac{1}{2}\phi_k(v+v')\right] \omega(t,v,v')\, n(t,v)n(t,v')\, dv dv'}_{\text{aggregation term}} \tag{I.30}
$$

$$
+ \underbrace{\int_0^{v_{max}} g(t,v)\left[\phi_k(v) - \vartheta(t,v)\Pi_k^\phi(t,v)\right] n(t,v)dv}_{\text{breakage term}}
$$

$$
= \underbrace{\int_0^{v_{max}} \phi_k(v)S(t,v)dv}_{\text{nucleation term}}
$$

Where:
$$
\Pi_k^\phi(t,v) = \int_0^{v_{max}} \phi_k(v')\, B(t,\frac{v'}{v})dv' = \int_0^v \phi_k(v')\, B(t,\frac{v'}{v})dv' \tag{I.31}
$$

$\vartheta(t,v)$: is the number of daughters upon breakage. $g(t,v)$: is breakage frequency. $B\left(t,\frac{v'}{v}\right)$: is the daughter probability density function for particle breakage. It must satisfy the normalization condition Ramkrishna, 2000:

$$
\int_0^{v_{max}} B(\frac{v'}{v},t)dv = 1 \tag{I.32}
$$

Conservation of mass requires that:

$$
B\left(\frac{v'}{v},t\right) = 0, \quad \text{if } v \geq v' \tag{I.33}
$$

The dual-quadrature method of generalized moments consists of two quadrature rules, one is a discretization of the particulate system, and the other is an accurate calculation of the integrals in the equations for the generalized moments P. L. Lage, 2011. The

number density function is approximated by:

$$n\left(t,v\right) = w\left(v\right)\sum_{i=0}^{2n-1} c_i\left(t\right)\phi_i\left(v\right) \tag{I.34}$$

The coefficient c_i is calculated by:

$$c_i = \frac{1}{\|\phi_i\|_{d\bar{\lambda}}^2} \int_0^{v_{max}} \phi_i n\left(v\right) dv \tag{I.35}$$

We can write:

$$c_i = \frac{\mu_i^{(\phi)}}{\|\phi_i\|_{d\bar{\lambda}}^2} \tag{I.36}$$

By applying n-point Gaussian quadrature to the (I.35), the coefficient c_i can be written as:

$$c_i = \frac{1}{\|\phi_i\|_{d\bar{\lambda}}^2} \sum_{j=1}^{n} w_j \varphi_i\left(\xi_j\right) \tag{I.37}$$

The choice of the polynomial ϕ_i is according to the v interval:

1. For a finite interval,$v \in [0,\ v_{max}]$, $w\left(v\right) = 1$, the Legendre polynomials shifted to the given interval must be taken.

2. For a semi-infinite interval, $v \in [0,\ \infty]$, $w\left(v\right) = v^a e^{-v}$, the generalized Laguerre polynomials must be used.

3. For an infinite interval, $v \in [-\infty,\ +\infty]$, $w\left(v\right) = e^{-a^2 v^2}$, which results in the Hermite polynomials.

Here, a short discerption of the weighted residual method based on the generalized moments:

Substituting $n\left(v,t\right)$ by its approximation, the equation (I.30) becomes P. L. Lage, 2011:

$$\frac{\partial}{\partial t}\sum_{i=0}^{2n-1} P_{ki}\, c_i + \sum_{i=0}^{2n-1} G_{ki}\, c_i + \sum_{i=0}^{2n-1} L_{ki}\, c_i + \sum_{i=0}^{2n-1}\sum_{j=0}^{2n-1} A_{kij}\, c_j c_i = s_k \tag{I.38}$$

Where:

$$\mu_i^{(\phi)} = \sum_{i=0}^{2n-1} P_{ki}\, c_i \tag{I.39}$$

More details about these terms G_{ki}, L_{ki}, A_{kij} and s_k in both integral and quadrature forms, are provided and discussed in P. L. Lage, 2011. In Santos et al., 2013, they coupled the Dual Quadrature Method of Generalized Moments (DuQMoGeM) with the Direct Quadrature Method of Moments to be D^{2}uQMoGeM.

SQMOM

The Sectional Quadrature Method of Moments is a combined method between the classes method and the method of moments, where the particle size is discretized to be N_{pp} sections, the population in each section is called primary particle that is formed from the secondary particles, the latter are responsible for droplet breakage and droplet coalescence. The population in the ith section $[d_{i-1/2}, d_{i+1/2}]$ is represented in term of weights $w_j^{\langle i \rangle}$ and abscissas $d_j^{\langle i \rangle}$ as M. M. Attarakih, Bart, and Faqir, 2006a; M. M. Attarakih et al., 2009:

$$n^{\langle i \rangle}(t,d) = \sum_{j=1}^{N_{sp}} w_j^{\langle i \rangle}(t)\, d\left(d - d_j^{\langle i \rangle}(t)\right), \quad i = 1, 2, 3, \ldots, N_{pp} \tag{I.40}$$

In SQMOM the distribution can be reconstructed from the primary particles, this is one of its advantages M. M. Attarakih et al., 2009.

$$n(t,d) = \sum_{i=1}^{N_{pp}} \tilde{w}_j(t)\, d\left(d - \tilde{d}_j(t)\right), \quad i = 1, 2, 3, \ldots, N_{pp} \tag{I.41}$$

Where, $\tilde{d}_j$ and $\tilde{w}_j$ are the mean abscissas and weights, respectively. Thus, the sectional moments of order k are calculated by M. M. Attarakih et al., 2009:

$$\mu_k^{\langle i \rangle} = \sum_{j=1}^{N_{sp}} w_j^{\langle i \rangle} \left(d_j^{\langle i \rangle}\right)^k, \quad k = 0, 1, 2 \ldots, 2N_{sp} - 1 \tag{I.42}$$

OPOSPM

The One Primary and One Secondary Particle Model (OPOSPM) was developed by M. M. Attarakih, Bart, and Faqir, 2006b. It is a special case of the sectional quadrature method of moments where only one primary particle and one secondary particle are

considered. This model is a system of two differential equations, usually by selection. They are the total number N_T and the total volume concentrations r_d. Its advantages are: retains the simplicity in structure, ease of explanation and efficient in coding M. M. Attarakih, Bart, and Faqir, 2006b, the OPOSPM can be described by M. Attarakih et al., 2013 :

$$\frac{\partial}{\partial t}\begin{pmatrix} N_T \\ r_d \end{pmatrix} + \frac{\partial}{\partial z}\begin{pmatrix} v_d N_T - D_d\frac{\partial N_T}{\partial z} \\ v_d r_d - D_d\frac{\partial r_d}{\partial z} \end{pmatrix} = \begin{pmatrix} v_{d,in}/v_{in} \\ v_{d,in} \end{pmatrix}\delta\left(z - z_d\right) + \begin{pmatrix} H \\ \dot{v}\left(\bar{d}\right)N_T \end{pmatrix} \tag{I.43}$$

S term on the right-hand side of the above equation represents a spatial point source term. While $\dot{v}\left(d\right)N_T$ is the source term for volume concentration, which represents particle growth or contraction due mass transfer M. M. Attarakih, Bart, and Faqir, 2006b.

$$H = \left(\vartheta\left(d_{30}\right) - 1\right)g\left(d_{30}\right)N_T - \frac{1}{2}\omega\left(\left(d_{30}\right),\left(d_{30}\right)\right)N_T^2 \tag{I.44}$$

The mean diameter d_{30} is given as:

$$d_{30} = \sqrt[3]{\frac{\pi}{6}\frac{r_d}{N_T}} \tag{I.45}$$

I.3.4   Semi-analytical methods

In this part, we present the most common approaches that were used to solve the population balance equation analytically. The semi-analytical methods like Adomian method, variational iteration method and Homotopy perturbation method had attention in recent years because of their simplicity in implementation and accuracy in solving. Following the work of Pr Hasseine, they were used to solve the PBE in the batch system and were extended for the continuous one (dynamic and steady-state) Hasseine, Barhoum, et al., 2015; Hasseine et al., 2011; Hasseine et al., 2017; Hasseine et al., 2020; Hasseine, Senouci, et al., 2015, where their exact solutions were found.

Adomian decomposition method (ADM)

In 1980, George Adomian introduced an efficient analytical method, so-called Adomian decomposition method to solve easily and accurately algebraic, differential, integral and integro-differential equations. It is based on giving the solution as an infinite power series, which usually converges to exact solution Adomian and Rach, 1986; Adomian, 2013. Recently, ADM was used by many researchers to solve a wide range of mathematical problems in engineering, chemistry, biology and physics Babolian and Biazar, 2002; Momani and Odibat, 2006; Reddy et al., 2017.

The general form of a differential equation can be written as follows:

$$Fu = g \tag{I.46}$$

$$F = L + R + N \tag{I.47}$$

By substituting Eq. (I.46) into (I.47) one gets:

$$Lu + Ru + Nu = g \tag{I.48}$$

where L is easily invertible operator, R is the remainder of the linear operator and N corresponds to the non-linear terms.

We can write Eq. (I.48) as

$$Lu = g - Ru - Nu \tag{I.49}$$

By multiplying Eq. (I.49) by L^{-1} we obtain:

$$L^{-1}(Lu) = L^{-1}(g) - L^{-1}(Ru) - L^{-1}(Nu) \tag{I.50}$$

Where $L^{-1} = \int \ldots \int (.)(dt)^n$ is the inverse of operator L.

Therefore,

$$u = u_0 - L^{-1}(Ru) - L^{-1}(Nu) \tag{I.51}$$

Where:

$$L^{-1}(Lu) = u - u(0) - tu'(0) \tag{I.52}$$

and

$$u_0 = u(0) + tu'(0) + L^{-1}g \tag{I.53}$$

the decomposition method consists of decomposing $u(x)$ into a sum of components given by the infinite series:

$$u(x) = \sum_{n=0}^{\infty} u_n \tag{I.54}$$

and the nonlinear function $N(u)$ is decomposed by the infinite series as:

$$Nu = \sum_{n}^{\infty} A_n \tag{I.55}$$

Where A_n is the Adomian's polynomials are given by:

$$A_n = \frac{1}{n!} \frac{d^n}{d\lambda^n} \left[N \left(\sum_{i=0}^{\infty} \lambda^i u_i \right) \right] \Bigg|_{\lambda=0} \quad , n = 0, 1, 2, \dots \tag{I.56}$$

The convergence of the Adomian decomposition method, it has been intensively studied by Adomian, 1990; Adomian, 1988.

Homotopy perturbation method (HPM)

Homotopic perturbation method is a coupling of the perturbation method and the homotropy method with conserving the full advantages of the traditional perturbation techniques. It is proposed for nonlinear equations and does not depend upon a small parameter in the equation J.-H. He, 1999a, 2000a, 2004a, 2005b. The Homotopic perturbation method has been successfully applied to solve : heat conduction and convection equation Rajabi et al., 2007, gas dynamics equation Jafari et al., 2008, biological population model Roul, 2010 and nonlinear wave equation J.-H. He, 2005a.

To illustrate the basic concept of this method, the following nonlinear differential equation is considered J.-H. He, 1999a, 2000a:

$$L(u) + N(u) = f(r), r \in \Omega \tag{I.57}$$

with boundary conditions

$$B(u, \partial u / \partial n) = 0, r \in \Gamma \qquad (I.58)$$

where L is a linear operator while N is a nonlinear operator, B is a boundary operator, Γ is the boundary of the domain Ω and $f(r)$ is a known analytic function.

He's homotopy perturbation technique [12-22] El-Shahed, 2005; J.-H. He, 1999a, 2000a, 2003, 2004a, 2005b; Odibat and Momani, 2008 defines homotopy as: $v(r, p) : \Omega \times [0; 1] \to \Re$, which satisfies:

$$H(v; p) = (1 - p) \left[l(v) - l(u_0) \right] + p[l(v) + N(v) - f(r)] = 0 \qquad (I.59)$$

or it can be written in an equivalent form:

$$H(v, p) = l(v) - l(u_0) + pL(u_0) + p[N(v) - f(r)] = 0 \qquad (I.60)$$

In the above equations, $r \in \Omega$ and $p \in [0, 1]$ are embedding parameters and u_0 is an initial approximation which satisfies the boundary conditions. From Eqs. (I.59) and (I.60), it follows:

$$H(v, 0) = L(v) - L(u_0) = 0 \qquad (I.61)$$

$$H(v, 1) = L(v) + N(v) - f(r) = 0 \qquad (I.62)$$

The changing process of p from zero to unity is just that of $v(r, p)$ from u_0 to $u(r)$. In topology, this is called deformation; $L(v) - L(u_0)$ and $L(v) + N(v) - f(r)$ are homotopic. The basic assumption is that the solution of Eqs. (I.59) and (I.60) can be expressed as a power series in p :

$$v = v_0 + p v_1 + p^2 v_2 + \cdots \qquad (I.63)$$

Therefore, the approximate solution of Eq. (I.57) can be readily obtained as:

$$u = \lim_{p \to 1} v = v_0 + v_1 + v_2 + \cdots \qquad (I.64)$$

The convergence of the series (I.64) was proven in Abbasbandy, 2006; J.-H. He, 1999a.

Variational iteration method (VIM)

The variational iteration method is an analytical technique that was developed first by J.-H. He, 1998; J. He, 1997, which is a modified general Lagrange multiplier method. It was proposed as an efficient and accurate method to solve a large class of nonlinear differential equations with approximations converging rapidly to exact solutions J.-H. He, 1998. It found many applications to solve various kinds of differential equations like: KdV, the K(2,2), the Burgers, and the cubic Boussinesq equations coupled Wazwaz, 2007, Schrodinger-KdV, generalized KdV and shallow water equations Abdou and Soliman, 2005, Helmholtz equation Momani and Abuasad, 2006.

We can write the general form of the differential equation see equation (I.46) as follows J.-H. He, 1999b:

$$F = L + N \tag{I.65}$$

Substituting equation (I.46) into equation (I.65) we obtain:

$$Lu + Nu + g \tag{I.66}$$

Where L a linear operator, N a non-linear operator, g an inhomogeneous term.
According to the variational iteration method, we can build a functional correction as follows J.-H. He, 1998:

$$U_{n+1} = U_n(t) + \int_0^t \lambda \left(U_n(\xi) + N\tilde{U}(\xi) - g(\xi) \right) d\xi \tag{I.67}$$

Where, λ is a general lagrange multiplier that can be optimally identified by the variational theory, and $\tilde{u}_n$ is a restricted variation which means $\delta\tilde{u}_n = 0$.

Other analytical methods

Laplace transform and successive generations methods are regarded as suitable methods for obtaining analytical solutions for certain forms of population balance equations. These are discussed in Ramkrishna, 2000, where some obvious examples are provided. In order to solve PBE in simple forms, apart from numerical ways, some suc-

cessful attempts have been made in the past to solve PBE analytically. Using the multi-dimensional Laplace transform Multicomponent aggregation population balance equation was solved analytically for constant aggregation kernel, Gelbard and Seinfeld, 1978 and for additive kernel Fernandez-Diaz and Gomez-Garcia, 2007. While using Laplace transforms exact solutions were obtained for size-independent aggregation M. J. Hounslow, 1990 and for simultaneous aggregation with breakage P. Lage, 2002; McCoy and Madras, 2003; Patil and Andrews, 1998. Liou et al., 1997 applied successive generations method to solve mass structured and age-mass structured cell population balances.

I.4 Available analytical solutions of the spatially distributed PBE:

In M. M. Attarakih et al., 2004 the spatially distributed PBE with some considerations was solved analytically using a methodology that uses relative time and chain rule for only breakage and only coalescence and using Laplace transform for no breakage and no coalescence. The obtained exact solutions are presented below. To get these solutions, they assumed a stagnant continuous phase with no diffusion and zero initial condition.

Case 1: LLEC without breakage and coalescence

In this case, the droplet velocity was taken as a function of the droplet diameter. Using Laplace transform with respect to time followed by solving the resulting linear ODE with respect to spatial, they found this exact solution:

$$p\left(t, z, d\right) = \frac{Q_d}{A v_t\left(d\right)} P_{in} u\left[t - \tau(d, z)\right] \tag{I.68}$$

Where: $u\left[.\right]$ Is the *unit step* function is defined by:

$$u\left[t - \tau(z, d)\right] = \begin{cases} 1, & t - \tau(d, z) \geq 0, \\ 0, & otherwise \end{cases} \tag{I.69}$$

$$\tau(z,d) = \begin{cases} \frac{z-z_d}{v_d}, & z-z_d \geq 0, \\ 0, & \textit{otherwise,} \end{cases} \tag{I.70}$$

Case 2: LLEC with droplet breakage

Here, they used the following assumptions:

The feed flow distribution is taken as:

$$n_{in} = \frac{N_0^f e^{-\frac{v(d)}{v_0}}}{v_0} \tag{I.71}$$

Breakage functions are:

$$\Gamma = k_b' v_d v(d), \ \beta_n(d/d') = 6d^2/d'^3. \tag{I.72}$$

The analytical solution is given as:

$$
\begin{aligned}
p(t,z,d) = & \left(\frac{d}{d_0}\right)^3 \left(\frac{\pi d^2}{2}\right) \left[\frac{\alpha + k_b'(z-z_d)}{\alpha}\right]^2 \\
& \times \exp\left[-(\alpha + k_b'(z-z_d))\left(\frac{d}{d_0}\right)^3\right] \\
& \times u[t - \tau(d,z)]
\end{aligned} \tag{I.73}
$$

Case 3: LLEC with droplet coalescence

For only coalescence, they used the same assumptions were considered in the above case except that the breakage functions are equal to zero, the coalescence frequency is $\omega = k_c \, v_d$ with $v_d = constant$, an exact solution was provided as:

$$
\begin{aligned}
p(t,z,d) = & N_0^f \left(\frac{d}{d_0}\right)^3 \left(\frac{\pi d^2}{2}\right) \left(\frac{2}{2 + N_0^f k_c (z-z_d)}\right)^2 \\
& \times \exp\left[\frac{-2\left(\frac{d}{d_0}\right)^3}{2 + N_0^f k_c (z-z_d)}\right] u[t - \tau(d,z)]
\end{aligned} \tag{I.74}
$$

Additionally, in Campos and Lage, 2003, analytical and semi-analytical solutions of the spatially distributed PBE were provided using the successive generation method for pure advection, advection with absorption and advection with breakage and with ab-

sorption. They also assumed a uniform dispersed phase velocity.

I.5   Conclusion

As discussed above, the population balance equation finds many applications in different engendering fields, and a large number of scientific papers concerning this equation have been published. These prove clearly that the population balance models are more convenient for describing a wide range of chemical, physical and biological processes.

The spatially distributed population balance equation is a partial integro- differential equation and is not easy to solve analytically. However, few ideas were proposed to overcome its difficulty and find exact solutions. Unfortunately, the exact solutions of spatially distributed population balance equation are still very rare. Alternatively, numerical methods were proposed and applied to get approximated solutions. Other approaches are called semi-analytical methods were shown recently as adequate mathematical techniques to solve the PBE in batch and continuous system flow, but in this work, we will extend one of them (VIM) to solve the population balance equation in one dimension (see chapter III).

Chapter II

Modeling of Liquid-Liquid extraction columns

II.1   Introduction

The solvent extraction is an interesting alternative to distillation, especially when the latter is inadequate or uneconomic, like in these cases: the components of the solution have close boiling points, separation of heat-sensitive materials (antibiotic and vitamins), recovery of non-volatile solutes from aqueous solution in hydro-metallurgy, recovery a solute from a very dilute solution in bioseparation and removal of phenol from aqueous wastes Dutta, 2007. Nowadays, liquid-liquid extraction columns are widely used in a wide range of the separations industries such as: chemical, biochemical, pharmaceutical, and nuclear industries because of their advantages of high efficiency and low cost in respect of the number of stages, solvent inventory, site area, settler area, maintenance Hasseine et al., 2005.

The population balance equation was found as a powerful tool for predicting extraction column behavior. Consequently, in many scientific studies, different types of extraction columns were modeled and simulated using population balance equations like pulsed packed, pulsed sieve tray, RDC and Kühni extraction column Bart et al., 2020; Garthe, 2006. The extraction column design and control have not yet been com-

pleted and still needs to be improved. It is based on laboratory scale pilot plants and is dependent on scale up method that is time consuming and expensive Jaradat, 2012. Usually, the population balance model is used to find specific proprieties of the dispersed phase along the column at an instant t, these can be changed due to different complex drop mechanisms: breakage, coalescence and mass transfer. To achieve the modeling, their rates must be described. Therefore, several attempts have been made in the literature to model conveniently these phenomena Garthe, 2006; Kopriwa et al., 2012.

This chapter provides background information on the modeling of liquid-liquid extraction columns, in particular Kühni column and Rotating Disc Contactor (RDC). We discuss obviously the model for both dispersed and continuous phases, drop breakage, drop coalescence as well as drop transport (liquid velocities and axial dispersion).

II.2   Modeling of liquid-liquid extraction column

In order to understand how the model was established, we must first describe the liquid-liquid extraction column. For two phases system, in a countercurrent column, the light phase must be the dispersed phase; it enters the column at $z = z_d$ and leaves at the top of the column. While the other phase is continuous, it enters the column at $z = z_c$ and leaves at the bottom of the column; it moves downwards from the top. In general, the column can be divided into three parts: the active zone, where the phases are brought into contact, and the two settling zones, at the bottom and the top of the column, where the phases are separated Casamatta, 1981 (Figure II.1). Based on the type of agitation the extraction columns are classified into three categories Dutta, 2007:

1. **Unagitated columns:** Spray column, Packed column and Perforated plate or Sieve tray.

2. **Pulsed columns:** Pulsed, Packed column and Sieve tray.

3. **Mechanically agitated columns:**

(a) **Rotary agitated contactors:** Scheibel column, Oldshue-Rushton column, Rotating Disk Contactor (RDC) and Kühni column.

(b) **Reciprocating plate columns:** Perforated plate or Sieve plate.

The centrifugal extractor is a different column extractor. It is based on the usage of the centrifugal force to create a countercurrent radial flow of the two phases.
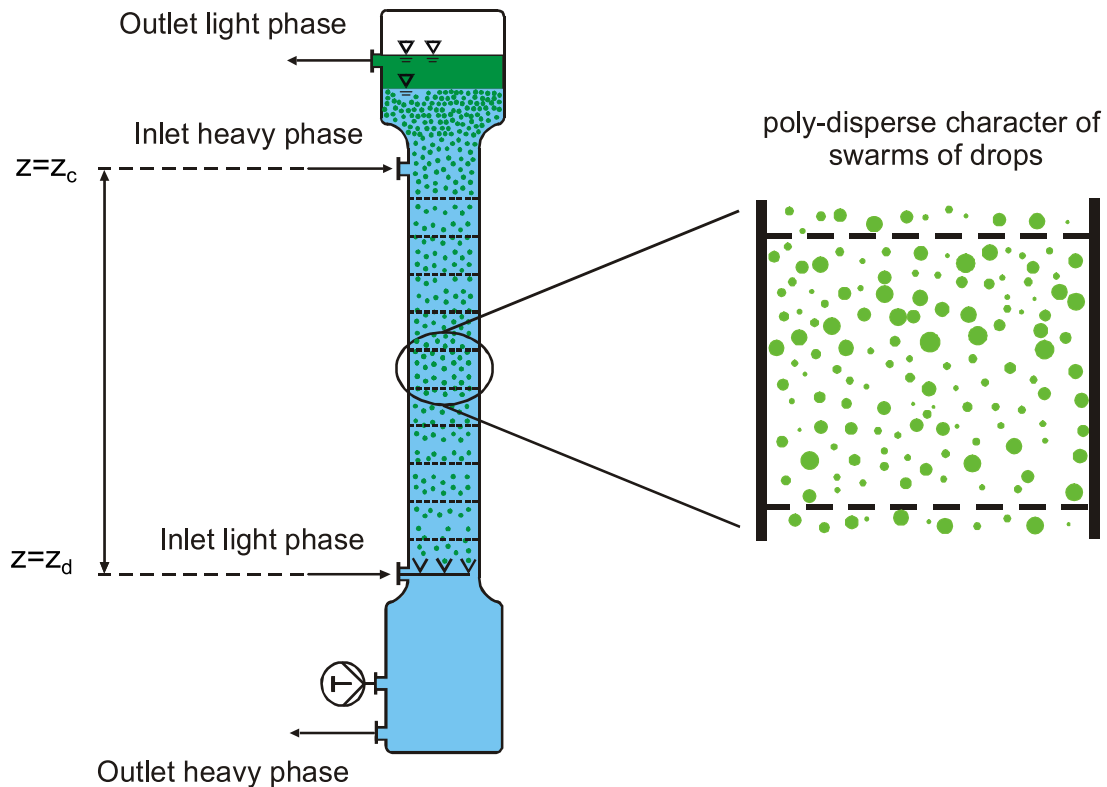
Figure II.1: Schematic of a countercurrent liquid-liquid extraction column Garthe, 2006

II.2.1   Model development

A knowledge of dispersed-phase hold-up is necessary in the design of extraction columns. The hold-up is needed to compute the interfacial area per unit volume A. Kumar and Hartland, 1995. The local holdup of the dispersed phase at time t at column heigh z is calculated by integrating $p(t,z,d)$ as follows:

$$r_d(t,z) = \int_0^{d_{max}} p(t,z,d)dd \qquad \text{(II.1)}$$

d_{max} represents the maximum droplet diameter.

Drop size and distribution have a considerable impact on extractor throughput and mass transfer. The hydrodynamics can be presented by a diameter d_{43} and the mass transfer by a diameter d_{32}. The most widely used drop size is the mean Sauter diameter d_{32}, it is volume-surface diameter Casamatta, 1981; Dutta, 2007; Garthe, 2006:

$$d_{32} = \frac{\int_0^{d_{max}} d^3 n(t,z,d)dd}{\int_0^{d_{max}} d^2 n(t,z,d)dd} \tag{II.2}$$

It is needed to calculate the interfacial area:

$$\bar{a} = \frac{6r_d}{d_{32}} \tag{II.3}$$

II.2.2   Balance on the dispersed phase

In Casamatta, 1981 proposed a general model for liquid-liquid extraction column, for the dispersed phase, the balance consists of four different terms: inlet, outlet, production and accumulation, as shown in the figure. II.2 :
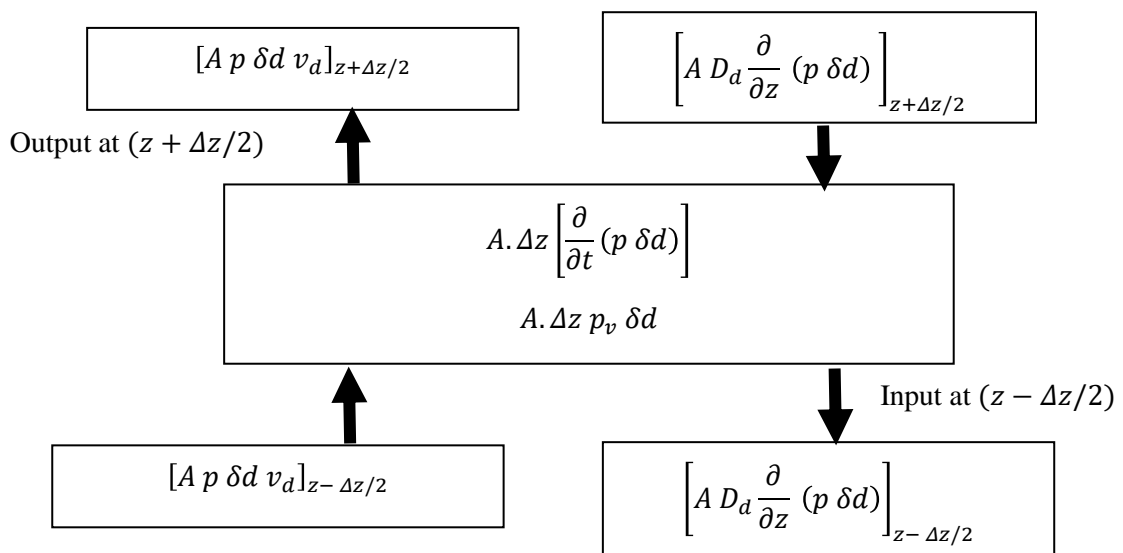
Figure II.2: Balance on a reference volume $A.\Delta z$ for the dispersed phase

It is assumed in the following a dispersed ascending phase (light phase). Thus,

for particles of size $d \pm \delta d/2$, for a volume defined between $z + \Delta z/2$ *and* $z - \Delta z/2$ the various terms involved in the balance are:

Inlet (E):

$$\left[A\, p\, \delta d\, v_d\right]_{z-\ \Delta z/2} - \left[A\, D_d \frac{\partial}{\partial z}\, \left[p\, \delta d\right]\right]_{z-\ \Delta z/2} \tag{II.4}$$

Outlet (S):

$$\left[A\, p\, \delta d\, v_d\right]_{z+\ \Delta z/2} - \left[A\, D_d \frac{\partial}{\partial z}\, \left[p\, \delta d\right]\right]_{z+\ \Delta z/2} \tag{II.5}$$

Production (G):

$$A\, \Delta z\, p_v \delta d \tag{II.6}$$

Accumulation (A):

$$A\, \Delta z \left[\frac{\partial}{\partial t} p \delta d\right] \tag{II.7}$$

By writing that, **E-S+G=A**. And by passing the limit $\Delta z \to 0$, $\Delta t \to 0$ the volume balance on the dispersed phase for particles of size thus leads to the following equation:

$$\frac{\partial p(t,z,d)}{\partial t} = \frac{\partial}{\partial z}\left(D_d \frac{\partial}{\partial z} p(t,z,d)\right) - \frac{\partial}{\partial z}\left(v_d(t,z,d,r_d)p(t,z,d)\right)$$
$$+ \frac{Q_d}{A} p_{in}(d)\delta\left(z - z_d\right) + p_v(t,z,d) \tag{II.8}$$

The breakage and coalescence process of drops are taken into account in the term p_v, which is given by:

$$p_v(t,z,d) = \frac{v(d)}{2} \int_0^{d/\sqrt[3]{2}} \omega\left(t,z,d_1,d_2\right) \frac{p\left(t,z,d_1\right)}{v\left(d_1\right)} \frac{p\left(t,z,d_2\right)}{v\left(d_2\right)} \left(\frac{d}{d_2}\right)^2 dd_1$$
$$- p(t,z,v) \int_0^{\sqrt[3]{d_{max}^3 - d^8}} \omega\left(t,z,d_1,d_2\right) \frac{p\left(t,z,d_1\right)}{v\left(d_1\right)} dd_1$$
$$+ \int_0^{d_{max}} \beta\left(d_0,\quad d\right) g\left(t,z,d_0\right) p\left(t,z,d_0\right) dd_0$$
$$- g(t,z,d)p(t,z,d) \tag{II.9}$$

II.2.3   Balance on the continuous phase

Here the balance consists of three different terms: inlet, outlet and accumulation, as shown in the figure. II.3. For a volume defined between $z + \Delta z/2$ *and* $z - \delta z/2$ the various terms involved in the balance are:
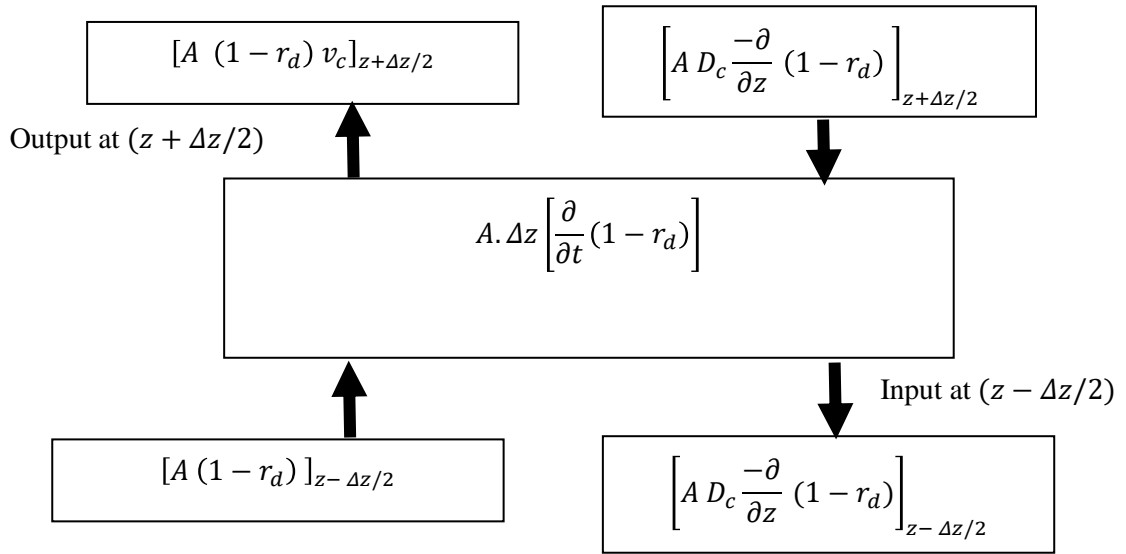
Figure II.3: Balance on a reference volume $A.\Delta z$ for continuous phase.

Inlet (E):

$$[A\ (1 - r_d)\ ]_{z+\ \Delta z/2} - \left[A\ D_c \frac{-\partial}{\partial z}\ (1 - r_d)\right]_{z-\ \Delta z/2} \tag{II.10}$$

Outlet (S):

$$[A\ \ (1 - r_d)\ v_c]_{z+\ \Delta z/2} - \left[A\ D_c \frac{-\partial}{\partial z}\ (1 - r_d)\ \right]_{z+\ \Delta z/2} \tag{II.11}$$

Accumulation (A):

$$A.\ \Delta z\left[\frac{\partial}{\partial t}\ (1 - r_d)\right] \tag{II.12}$$

By writing that, **E-S=A**. And by passing the limit $\Delta z \to 0$, $\Delta t \to 0$ the volume balance on the continuous phase leads to the following equation:

$$\frac{\partial}{\partial t}[1 - r_d(t,z)] + \frac{\partial}{\partial z}\ (v_c(t,z)[1 - r_d(t,z)]) = \frac{\partial}{\partial z}\left(D_c\frac{\partial}{\partial z}[1 - r_d(t,z)]\right)$$
$$+ \frac{Q_c}{A}\delta\ (z - z_c) \tag{II.13}$$

II.2.4   Initial and boundary conditions

The Danckwerts boundary condition can be used at the column ends:

At the bottom of the column, at $z = 0$ with $t > 0$:

$$v_d p - D_d \frac{\partial p}{\partial z} = 0 \tag{II.14}$$

Drops can be assumed to leave the column at $z = h$ with their own velocity, that is:

at $z = h$ for $t > 0$

$$D_d \frac{\partial p}{\partial z} = 0 \tag{II.15}$$

Initially (at $t = 0$), if the column is empty of dispersed phase:

$$p(0, z, d) = 0 \ \ \text{for} z \in [0, \ h] \tag{II.16}$$

II.2.5   Hydrodynamics

The holdup and the droplet sizes of the dispersed phase are changed temporally along the column height due to the following hydrodynamics processes:

Droplet Velocity

The velocity of drops in a swarm significantly depends on the drop diameter and the volume fraction of the dispersed phase. For countercurrent system, the rising velocity v_d of a droplet of diameter d, is expressed as Gayler et al., 1953:

$$v_d (t, z, d, r_d) = v_r (t, z, d, r_d) - v_c (t, z, d, r_d) \tag{II.17}$$

Where v_d and v_c are dispersed phase velocity and continuous phase velocity, respectively. v_r describes the relative velocity of droplets with diameter d, which is often called the relative swarm velocity or slip velocity. it is calculated from the single drop

terminal velocity v_t as the following:

$$v_r = k_v(d) \, v_t \, (1 - r_d)^m \tag{II.18}$$

Where: m is the swarm exponent which indicates the extent of the hold-up influence. $k_v(d)$ is the slowing factor its values must be in rang $(0, 1)$. For the RDC column, the slowing factor of droplets of diameter d is calculated by J. Godfrey, 1991 :

$$k_v(d) = 1 - 1.037 \left(N_R^3 \, D_R^5 \right)^{0.12} - 0.62 \left(\frac{d}{D_S - D_R} \right)^{0.44} \tag{II.19}$$

For the Kuhni column, the slowing factor correlation Fang et al., 1995 :

$$k_v(d) = 1 - (1 - \theta) \left(\frac{7.18 \; 10^{-5} \frac{Re_R}{\theta}}{1 + 7.18 \; 10^{-5} \frac{Re_R}{\theta}} \right) \tag{II.20}$$

Where:

N_R : is the rotor speed $[s^{-1}]$.

D_R : is the rotor diameter $[m]$.

D_S : is the stator diameter $[m]$.

θ : is the relative free cross-sectional stator area $[-]$.

In addition to the terminal velocity, it depends on the physical properties of both phases and droplet diameter Klee and Treybal, 1956. In the Figure II.4, the terminal velocity is presented graphically for four different types of droplet forms rigid, circulating, oscillating and deformed ones. The terminal velocity is associated with drop size, drop stability and drop form Garthe, 2006. Many terminal velocity correlations were proposed in the literature:

For rigid sphere with for $Mo^{-1} > 10^{11}$, J. Godfrey et al., 1994 provided this correlation:

$$v_t = \frac{d}{4.2} \left(\frac{g \Delta \rho}{\rho_c} \right)^{2/3} \left(\frac{\rho_c}{\eta_c} \right)^{1/3} \tag{II.21}$$

where:

η : is the dynamic viscosity.

$E\ddot{o}$ is Eötvös number $E\ddot{o} = \frac{g \Delta \rho d^2}{\sigma}$.

Mo is the Morton number $Mo = \frac{g \; \Delta \rho \eta_c^4}{\rho_c^2 \, \sigma^3}$.

For circulating droplets with $Mo^{-1} > 10^7$, a correlation is reported in Vignes and Globule, 1965:

$$v_t = \frac{d}{4.2}\left(\frac{g\Delta\rho}{\rho_c}\right)^{2/3}\left(\frac{\rho_c}{\eta_c}\right)^{1/3}\left(1 - \frac{E\ddot{o}}{6}\right) \tag{II.22}$$

For $Mo^{-1} > 10^5$, the critical diameter d_{crit} determines which correlation must be used Klee and Treybal, 1956:

$$v_t = 17.6\rho_x^{-0.55}\Delta\rho^{0.28}\eta_x^{0.1}\sigma^{0.18} \ \ d \geq d_{crit} \ \text{large drop} \tag{II.23}$$

$$v_t = 38.3\rho_x^{-0.45}\Delta\rho^{0.58}\eta_x^{-0.11}d^{0.7} \ \ d < d_{crit} \ \text{small drop} \tag{II.24}$$

where

$$d_{crit} = 0.3\rho_x^{-0.14}\Delta\rho^{-0.43}\eta_x^{0.3}\sigma^{0.24} \tag{II.25}$$

The application of Grace model according to the value of the parameter J_t Grace, TH, et al., 1976.

$$v_t = \frac{\eta_c 1/Mo^{0.149}}{\rho_c d}(J_t - 0.857) \tag{II.26}$$

In order to calculate the terminal velocity for all forms of drops, according to the value of Mo^{-1} Hasseine, 2007 they made an algorithm gives the values of v_t using rigid sphere Law, Klee and Treybal, Grac and Vignes low (see page 89).

The steady-state solution of the mass balance equation for the continuous phase for a column operated in counter-current operation provided as Kronberger et al., 1995:

$$v_c(t,z) = \frac{1}{1 - r_d(t,z)}\left\{(1 - \mathcal{H}(z - z_c))\frac{Q_c}{A} + \mathcal{D}_c(z)\frac{\partial r_d(t,z)}{\partial z}\right\} \tag{II.27}$$

Drop breakage

The breakage of a drop in a turbulent flow is influenced by drop size, density, interfacial surface tension, viscosity of both phases, holdup fraction, local flow and local energy dissipation Coulaloglou and Tavlarides, 1977. Based on the difference between energies, Coulaloglou and Tavlarides, 1977 consider the drop breakage to occur when an oscillating deformed drop has a surface energy less than turbulent kinetic energy transmitted by the turbulent eddies. In the liquid-liquid extraction columns, it also depends
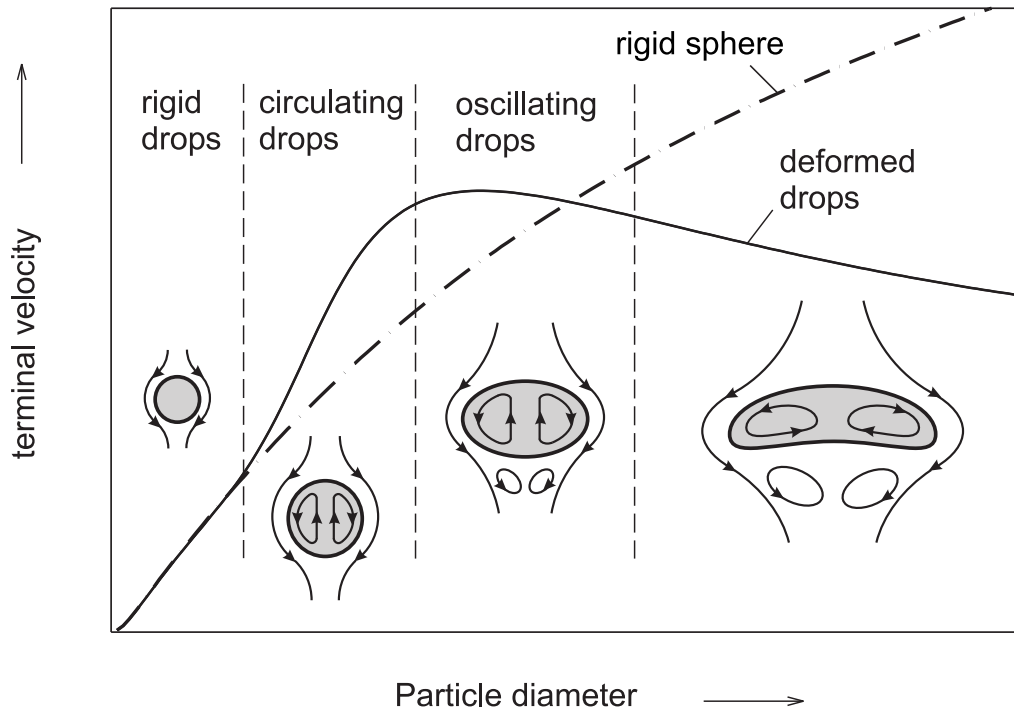
Figure II.4: terminal velocities of single drops and spheres Garthe, 2006

on the internals type. It occurs if the drop passes through the turbine outlet stream or the impellor blade in the Kühni column, while it occurs only if the drop touches the rotator disc in the RDC column Bart et al., 2020. The breakage frequency is a ratio between the number of breaking drops and the initial number of drops and time, the breakage frequency depends on the residence time of the droplets Coulaloglou and Tavlarides, 1977:

$$g\left(z,d\right) = \left(\frac{1}{breakage\ time}\right)\left(\frac{fraction\ of}{drops\ breaking}\right) \tag{II.28}$$

In the agitator column the breakage frequency depends on the drop breakage probability $P(d)$ Cabassud et al., 1990:

$$g\left(z,d\right) = \frac{P\left(d\right)v_d(z,d)}{h_j} \tag{II.29}$$

The ratio $\frac{v_d(z,d)}{h_j}$ can be defined as the inverse of the average residence time of a drop of diameter d diameter in a compartment of the column. The drop breakage probability $P(d)$ can be calculated by the correlation that was reported in Bahmanyar and Slater,

1991; Cauwenberg et al., 1997; Simon et al., 2003:

$$\frac{P(d)}{1 - P(d)} = c_1 \, We_m^{c_2} \tag{II.30}$$

where:

$$We_m = \frac{\rho_c^{0.8} \mu_c^{0.2} D_R^{1.6} (2\pi)^{1.8} (N^{1.8} - N_{crit}^{1.8})}{\sigma} \tag{II.31}$$

This model was frequently used to describe the breakage probability in the liquid-liquid extraction columns M. M. Attarakih et al., 2004; Hasseine et al., 2005; Schmidt et al., 2003; Simon et al., 2002. In contrast Garthe, 2006 used other correlation which based on Ohnesorge and modified Weber numbers:

$$\frac{P(d)}{1 - P(d)} = c_1 \cdot \left(\frac{We_{\text{mod}}}{1 + c_2 \cdot \eta_d \cdot [We_{\text{mod}} / (\sigma \cdot d \cdot \rho_d)]^{0.5}} \right)^{c_3} \tag{II.32}$$

The critical rotational speed $N_{R,crit}$ can be calculated by:

$$N_{R,crit} = \frac{c_4}{2} \frac{D_R^{-2/3} \eta_d d^{-4/3}}{(\rho_c \rho_d)^{1/2}} + \left[\left(\frac{c_4}{2} \frac{D_R^{-2/3} \eta_d d^{-4/3}}{(\rho_c \rho_d)^{1/2}} \right)^2 + c_5 \frac{\sigma}{\rho_c D_R^{4/3} d^{5/3}} \right]^{0.5} \tag{II.33}$$

The constant factors are determined by analysing a series of experiments.

For an RDC column:

$c_1 = 1.29.10^{-6}$, $c_2 = 0.33$, $c_3 = 2.78$, $c_4 = 0.02$, $c_5 = 0.13$

For a Kühni column:

$c_1 = 1.63.10^{-3}$, $c_2 = 0.48$, $c_3 = 3.05$, $c_4 = 0.13$, $c_5 = 1.21.10^{-2}$

The size distribution of the daughter droplets is given by a beta distribution function, based on the mother droplet diameter d_0 Bahmanyar and Slater, 1991:

$$\beta(d_0, d) = 3\nu(\nu - 1) \left(1 - \frac{d^3}{d_0^3} \right)^{(\nu - 2)} \frac{d^3}{d_0^2} \tag{II.34}$$

With ν the average number of daughter drops given by Hančil and Rod, 1988 :

$$\nu = 2 + p \left(\left(\frac{d_0}{d_{crit}} \right) - 1 \right)^q \tag{II.35}$$

The parameters p and q of the above equation are dependent on the column type Garthe, 2006:

For an RDC column: $p = 1.42.10^{-3}$, $q = 2.93$

For a Kühni column: $p = 0.03$, $q = 2.45$

d_{crit} is the critical diameter, at which the drops start to break.

Droplet coalescence

The coalescence complicity produces real difficulties in its modeling. However, a number of expressions for drop coalescence have been proposed in the past Chesters, 1991; Coulaloglou and Tavlarides, 1977; Henschke, 2004; Tsouris and Tavlarides, 1994. The theoretical model of Coulaloglou and Tavlarides, 1977 describes the binary coalescence as: it occurs if two droplets collide and then remain in contact for enough time and the fluid film between that droplets is drained and ruptured where the droplets are compressed by external forces. During these processes a turbulent eddy probably restrains the coalescence by separating the drops. Figure II.5 represents a binary collision of two uniform droplet in a continuous phase. The coalescence rate between two drops is considered to be given by the following product:

$$\omega(d_1, d_2, r_d) = f(d_1, d_2)\, \lambda(d_1, d_2) \tag{II.36}$$

Coulaloglou and Tavlarides, 1977 considered the collision rate between two droplets as the collision frequency between two gas molecules, they introduced the collision rate as:

$$f(d_1, d_2, r_d) = \frac{C_1 \sqrt[3]{\epsilon}\,(d_1 + d_2)^2 \sqrt{d_1^{2/3} + d_2^{2/3}}}{1 + r_d} \tag{II.37}$$

The film drainage model is described by:

$$\lambda(d_1,\ d_2, r_d) = \exp\left[\overline{\tau}/\overline{t}\right] \tag{II.38}$$

Where: $\overline{t}$: average coalescence time.

$\overline{\tau}$: average contact time.

The coalescence time is considered to be the time necessary for film drainage between

the drops. The coalescence succeeds if the contact time surpasses the coalescence time, the external force must act for a sufficient time. The coalescence efficiency is related to the physical phenomena, which is given by Coulaloglou and Tavlarides, 1977:

$$\lambda\left(d_1, d_2, r_d\right) = \exp\left[-\frac{C_2 \eta_c \rho_c \epsilon \left(\frac{d_1 d_2}{d_1 + d_2}\right)^4}{(1 + r_d)^3 \sigma^2}\right] \tag{II.39}$$
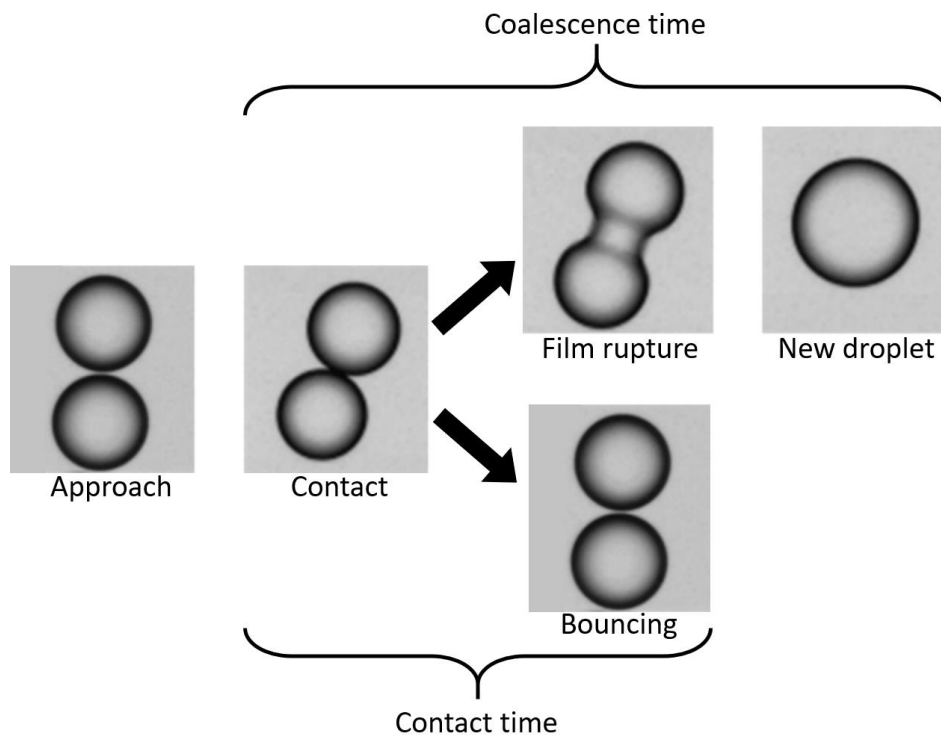
Figure II.5: Binary coalescence Dudek et al., 2020

Energy dissipation

In the agitator columns, the effect of agitation is taken into account in terms of power dissipation per unit mass ϵ, the latter is an essential parameter for comparison between columns efficiency A. Kumar and Hartland, 1995.

The mechanical power dissipation per unit mass ϵ is defined as:

$$\epsilon = \frac{\mathcal{P}}{m} = \frac{\mathcal{P}}{\rho_c V_c} = 4\frac{\mathcal{P}}{(\pi H_c D_c^2 \rho_c)} \tag{II.40}$$

where P is the power input, it is obtained from:

$$\mathcal{P} = N^3 N_p D_R^5 \rho_c \tag{II.41}$$

Where, the power number N_p expression has the following form A. Kumar and Hartland, 1995:

For Kühni column:

$$N_p = 1.08 + \frac{10.94}{Re_R{}^{0.5}} + \frac{257.37}{Re_R{}^{1.5}} \tag{II.42}$$

For RDC column:

$$N_p = \frac{109.36}{Re_R} + 0.74\left[\frac{1000 + 1.2\ Re_R{}^{0.72}}{1000 + 3.2\ Re_R{}^{0.72}}\right]^{3.3} \tag{II.43}$$

where, Re_R is rotor Reynolds number $Re_R = \dfrac{ND_R^2 \rho_c}{\eta_c}$.

Axial dispersions

Due to the turbulence imparted by the rising drops and the channeling flow due to the particular column geometry and other influences , a part of each liquid phase flow is mixed back. This phenomenon is named backmixing or axial mixing. In addition, axial mixing often reduces the mass transfer between phases. Garthe, 2006; Li and Ziegler, 1967. The axial dispersion model is given by Strand et al., 1962:

$$\frac{\partial c}{\partial t} = D_{ax}\frac{\partial^2 c}{\partial z^2} - u\frac{\partial c}{\partial z} \tag{II.44}$$

For an agitated RDC-column, continuous dispersion coefficient can be predicted by A. Kumar and Hartland, 1992:

$$\frac{D_c}{\bar{v}_c h_j} = 0.42 + 0.29 \left(\frac{v_d}{v_c}\right) + \left[c_1 \left(\frac{N\,D_R}{v_c}\right) + \frac{13.38}{3.18 + \left(\frac{N\,D_R}{v_c}\right)}\right]$$
$$\times \left(\frac{v_c\,\rho_c\,D_R}{\eta_c}\right)^{-0.08} \left(\frac{D_k}{D_R}\right)^{0.16} \left(\frac{D_k}{H_c}\right)^{0.1} A_r \tag{II.45}$$

Correlations for the dispersed axial dispersion coefficient for the RDC columns are listed and discussed in A. Kumar and Hartland, 1992.

For an agitated Kühni column, the dispersion coefficient correlations are given by Steiner et al., 1988. For the continuous phase, the correlation is applied to each compartment:

$$D_c = \bar{v}_c h_j \left[0.188 + 0.0267\theta^{0.5}\frac{D_R N_R}{\bar{v}_c}\right] \tag{II.46}$$

where h_j is the compartment height j in the Kühni column.

For the disperse phase, Steiner et al., 1988 also provided the following correlation:

$$D_d = -3.78 \times 10^{-4} + 0.068 \left[\frac{Q_c}{AN_R}\right]^{0.5} \tag{II.47}$$

II.2.6   Numerical solvers for LLEC

Certain numerical methods are developed to be sowftwar Bart et al., 2020:

LLECMOD (Liquid-Liquid Extraction Column MODule)

It is a Fortran window-based program, simulation based on the population balance approach to model the hydrodynamics of liquid-liquid extraction columns M. M. Attarakih, Bart, Lagar, et al., 2006.

PPBLAB (Particulate Population Balance Laboratory):

It is a windows-based MATLAB program, for modelling and numerical simulation of liquid-liquid extraction columns using a bivariate population balance model with respect to the particle internal properties: concentration and size M. Attarakih et al., 2012.

II.3   Conclusion

The solvent extraction is a mass transfer technique. The liquid-Liquid extraction column breaks up droplets to increase the interfacial area and improve the mass transfer and extraction efficiency. Mass transfer is strongly influenced by fluiddynamics and vice versa. Liquid-Liquid extraction column are modeled by drop population balance for predicting their performance Bart et al., 2020; Garthe, 2006.

The final population balance model was obtained by the collection of a number of different works of many scientists for dozens of years, where some theories and considerations were proposed. The knowledge of droplet interactions (breakage and coalescence), axial dispersions, slip velocity of the phases in particular column geometry and energy dissipation is very important for modeling liquid-liquid extraction columns. The population balance model was shown here as an efficient tool for describing the hydrodynamics behavior of the dispersed phase in liquid-liquid extraction column. The PBM is a highly complex equation. So, efficient and accurate methods are required to find its solutions (Hold-up, Sauter diameter, ...), those are discussed obviously in the previous chapter.

Chapter III

VIM application

III.1   Introduction

The population balance framework is regarded as an adequate tool for dealing with a dispersed phase system. Usually, the number of particles is used to describe the population but sometimes (with better reason) by other variables such as the mass or volume of particles. The population balance equations, despite their importance, rarely have an analytical solution. However, few cases with a simple form of breakage, aggregation and growth exist, where most of these solutions are for the stirred vessel Ramkrishna, 2000.

In this chapter, 1D population balance equation is solved analytically using variational iteration method for different particle breakage, coalescence and growth models in a particle population balance model, where a mathematic technique is used to simplify the model. In fact, variational iteration method generates a truncated part of the solution, but we could find exact solutions for eight problems. For the simultaneous growth and coalescence terms comparisons between VIM and projection method which includes discontinuous Galerkin and collocation techniques, are applied, respectively.

III.2   Model Equations

In the present model the basic variable is a drop size distribution function $p(t,z,v)$ that represents the volume fraction of drops with volume v in an unit volume of the column at level z and time t M. M. Attarakih et al., 2004. The local hold-up of the dispersed phase can be calculated from $p(t,z,v)$ as follows:

$$r_d (t,z) = \int_0^\infty p (t,z,v) \, dv \tag{III.1}$$

The volume balance equation of unit volume of the column can be expressed as:

$$\frac{\partial p (t,z,v)}{\partial t} + \frac{\partial v_d p (t,z,v)}{\partial z} = \frac{\partial}{\partial z} \left(D_d \frac{\partial p (t,z,v)}{\partial z} \right)$$
$$+ \frac{Q_d}{A} p_{in} d (z - z_d) + p_v (t,z,v) \tag{III.2}$$

with a transient and a convective term, where v_d is the dispersed phase velocity, balanced against a back mixing term expressed with the dispersion coefficient D_d . Q_d and A are the dispersed phase flow and the column cross-sectional area, respectively. The solvent feed entering at the level z_d of the column is handled as a point source by Dirac's $\delta - function$ Kronberger et al., 1995. The break-up, coalescence and growth process of drops are taken into account in the

$$p_v (t,z,v) = v \int_v^{+\infty} \beta \left(\frac{v}{u} \right) g (u) \frac{p (t,z,u)}{u} \partial u \quad - g (v) p (t,z,v)$$
$$+ \frac{v}{2} \int_0^v \omega (v - u, u) \frac{p (t,z,v - u)}{v - u} \frac{p (t,z,u)}{u} \partial u \tag{III.3}$$
$$- v \frac{\partial \left(\frac{G(v)p(\omega,x,v)}{v} \right)}{\partial v}$$

The first integral accounts for gain and loss due to break-up of the mother particle u according to the daughter particle distribution β. The second integral holds for similarly for aggregation according to the aggregation frequency ω. In order to apply the proposed method we reformulate Eq. (III.2) as follows:

$$\frac{\partial p (t,x,v)}{\partial t} + \frac{\partial v_d p (t,x,v)}{\partial x} = \frac{\partial}{\partial x} \left(D_d \frac{\partial p (t,x,v)}{\partial x} \right) + p_v (t,x,v) \tag{III.4}$$

where $x = z - z_d$ and the boundary condition is given by

$$p\left(t, 0, v\right) = \frac{Q_d}{A} P_{in} \tag{III.5}$$

Moreover, and by assuming the equation of motion with uniform particle velocity; negligible diffusion flux, and making the necessary variable transformation using the chain rule, Eq. (III.4) could be reduced to M. M. Attarakih et al., 2004:

$$\frac{\partial v_d p\left(\theta, x, v\right)}{\partial x} = p_v\left(\theta, x, v\right) \tag{III.6}$$

with θ define the relative time as:

$$\theta\left(t, x\right) = t - \frac{x}{v_d} \tag{III.7}$$

The following is the list of relevant combinations of processes for which the continuous PBE has been solved analytically.

Case study I. Pure breakage:

$$\frac{\partial v_d p\left(\theta, x, v\right)}{\partial x} = v \int_v^{+\infty} \beta\left(v/u\right) g(u) \frac{p\left(\theta, x, u\right)}{u} \partial u \quad - g\left(v\right) p\left(\theta, x, v\right) \tag{III.8}$$

Case study II. Pure aggregation:

$$\begin{aligned}
\frac{\partial v_d p(\theta, x, v)}{\partial x} &= \frac{v}{2} \int_0^v \omega(v - u, u) \frac{p(\theta, x, v - u)}{v - u} \frac{p(\theta, x, u)}{u} \partial u \\
&\quad - p(\theta, x, v) \int_v^{+\infty} \omega(v, u) \frac{p(\theta, x, u)}{u} \partial u
\end{aligned} \tag{III.9}$$

Case study III. Pure growth:

$$\frac{\partial v_d p\left(\theta, x, v\right)}{\partial x} + v \frac{\partial\left(G\left(v\right) p\left(\theta, x, v\right) / v\right)}{\partial v} = 0 \tag{III.10}$$

Case study VI. Aggregation and growth:

$$
\begin{aligned}
\frac{\partial v_d p(\theta, x, v)}{\partial x} = {} & \frac{v}{2} \int_0^v \omega(v-u, u) \frac{p(\theta, x, v-u)}{v-u} \frac{p(\theta, x, u)}{u} \partial u \\
& - p(\theta, x, v) \int_v^{+\infty} \omega(v, u) \frac{p(\theta, x, u)}{u} \partial u \\
& - v \frac{\partial \left(\frac{G(v) p(\theta, x, v)}{v} \right)}{\partial v}
\end{aligned}
\tag{III.11}
$$

Case study V. Breakage and growth:

$$
\begin{aligned}
\frac{\partial v_d p(\theta, x, v)}{\partial x} = {} & v \int_v^{+\infty} \beta\left(\frac{v}{u}\right) g(u) \frac{p(\theta, x, u)}{u} \partial u - g(v) p(\theta, x, v) \\
& - v \frac{\partial (G(v) p(\theta, x, v)/v)}{\partial v}
\end{aligned}
\tag{III.12}
$$

Case study VI. Simultaneous breakage and aggregation and growth:

$$
\begin{aligned}
\frac{\partial v_d p(\theta, x, v)}{\partial x} = {} & v \int_v^{+\infty} \beta\left(\frac{v}{u}\right) g(u) \frac{p(\theta, x, u)}{u} \partial u - g(v) p(\theta, x, v) \\
& + \frac{v}{2} \int_0^v \omega(v-u, u) \frac{p(\theta, x, v-u)}{v-u} \frac{p(\theta, x, u)}{u} \partial u \\
& - p(\theta, x, v) \int_v^{+\infty} \omega(v, u) \frac{p(\theta, x, u)}{u} \partial u \\
& - v \frac{\partial \left(\frac{G(v) p(\theta, x, v)}{v} \right)}{\partial v}
\end{aligned}
\tag{III.13}
$$

III.3   Variational iteration method

As a first step to obtain the solutions for the above set of population balance equation using the variational iteration method, we consider the following functional equation:

$$
Lp + Np = g(\theta, x, v)
\tag{III.14}
$$

Where L is a linear operator, N a nonlinear operator and $g(\theta, x, v)$ a source term. According to the variational iteration method, a functional correction can be constructed

as follows:

$$p_{n+1}(\theta, x, v) = p_n(\theta, x, v)$$
$$+ \int_0^x \lambda(\xi) \left(L p_n(\theta, \xi, v) + N \tilde{p}_n(\theta, \xi, v) - g(\xi) \right) d\xi \tag{III.15}$$

where $\lambda(\xi)$ is a general Lagrangian multiplier which can be identified optimally via variational theory and $\tilde{p}_n$ is a restrictive variation meaning $\widetilde{\partial p_n}$ J. He, 1997. Therefore, the solution is given by:

$$p(\theta, x, v) = \lim_{n \to \infty} p_n(\theta, x, v) \tag{III.16}$$

III.4   Projection method

The objective in this section is to develop the finite element expansion coefficients scheme based on discontinuous Galerkin and collocation methods for the solution of the simultaneous growth and coalescence process respectively.

III.4.1   Discontinuous Galerkin method for the growth equation

To introduce the basic idea of the discontinuous Galerkin method, consider the following initial value problem:

$$\frac{\partial p(\theta, x, v)}{\partial x} + v \frac{\partial (H(v) p(\theta, x, v))}{\partial v} = 0 \tag{III.17}$$

with the initial condition Eq. (III.5). which has the form of conservation law with flux function f and source terms

$$\frac{\partial p(\theta, x, v)}{\partial x} + \frac{\partial f(v, p(\theta, x, v))}{\partial v} = H(v) p(\theta, x, v) \tag{III.18}$$

with $f(v, p(\theta, x, v)) = v H(v) p(\theta, x, v)$.

It is assumed that the spatial domain Ω is periodic and partitioned into nonoverlapping intervals $I_j, j=1,..., N_j$. The center of bin I_j is denoted by v_j.

A weak formulation of the problem is obtained by multiplying (III.18) by an arbitrary smooth test function $\varphi(v)$ and integrating over an interval I_j

$$\int_{I_j} \left[\frac{\partial p(\theta,x,v)}{\partial x} + \frac{\partial f(v, p(\theta,x,v))}{\partial v} - H(v) p(\theta,x,v) \right] \varphi(v)\, dv = 0, \qquad \text{(III.19)}$$

Integrating the second term of (III.18) by parts yields

$$\int_{I_j} \frac{\partial p(\theta,x,v)}{\partial x} \varphi(v)dv - \int_{I_j} f(v, p(\theta,x,v)) \frac{\partial \varphi(v)}{\partial v} dv$$
$$+ f\left(v_{j+1}, p\left(\theta,x,v_{j+1}\right)\right) \varphi\left(v_{j+1}^{-}\right)$$
$$- f\left(v_{j}, p\left(\theta,x,v_{j}\right)\right) \varphi\left(v_{j}^{+}\right) \qquad \text{(III.20)}$$
$$= \int_{I_j} H(v) p(\theta,x,v)\varphi(v)dv$$

where $\varphi\left(v_{j+1}^{-}\right)$ and $\varphi\left(v_{j}^{+}\right)$ are the values of the function $\varphi(v)$ at the end points v_{j+1} and v_j of the element I_j respectively.

At an interface between elements (e.g., the points v_{j+1} and v_j), the flux function f is not uniquely defined, and a suitable numerical flux must be determined according to the classical finite-volume method. For example, the nonlinear flux function $f\left(v_{j+1}, p\left(\theta,x,v_{j+1}\right)\right)$ is replaced by a numerical flux $\hat{f}\left(v_{j+1}, p\left(\theta,x,v_{j+1}\right)\right)$ that depends on two values, the left and right limits of the discontinuous function p evaluated at the interface v_{j+1} such that

$$\hat{f}(f)_{j+1}(x) = \hat{f}\left(f\left(v_{j+1}^{-}, p\left(\theta,x,v_{j+1}^{-}\right)\right), f\left(v_{j+1}^{+}, p\left(\theta,x,v_{j+1}^{+}\right)\right)\right)$$

However, the Godunov numerical flux was chosen for the present study.

For the approximate solution $p_h(\theta,x,v)$, the DG space discretization based on the weak formulation (III.19) is written as follows Cockburn and Shu, 1989:

$$\int_{I_j} \frac{\partial p_h(\theta,x,v)}{\partial x} \varphi_h(v)dv - \int_{I_j} f(v, p_h(\theta,x,v)) \frac{\partial \varphi_h(v)}{\partial v} dv$$
$$+ \hat{f}\left(v_{j+1}, p_h\left(\theta,x,v_{j+1}\right)\right) \varphi_h\left(v_{j+1}^{-}\right) + \hat{f}\left(v_{j+1}, p_h\left(\theta,x,v_{j+1}\right)\right) \varphi_h\left(v_{j+1}^{-}\right) \qquad \text{(III.21)}$$
$$- \hat{f}\left(v_{j}, p_h\left(\theta,x,v_{j}\right)\right) \varphi_h\left(v_{j}^{+}\right) = \int_{I_j} H(v) p_h(\theta,x,v)\varphi_h(v)dv$$

We consider the approximations solutions p_h for each interval I_j, $p_h(x)|_j$ is a polynomial of degree k. We take as the local basis function the suitably scaled Legendre polynomials, that is, for $x \in I_j$, we write $p_h(\theta, x, v) = \sum_l^k u_j^l(x) f_j^l(v)$, where $f_j^l(v) = P_l\left(\frac{2(v - v_j)}{v_{j+1} - v_j}\right)$ and P_l is the lth Legendre polynomial. Since these polynomials are orthogonal, that is, since $\int_{-1}^{+1} P_l(\zeta) P_{l'}(\zeta) d\zeta = \frac{2}{2l+1} \delta_{ll'}$, the mass matrix is diagonal. Indeed, the weak formulation (III.21) takes the following simple form:

For each interval I_j and each $l = 0,...,k$, we have

$$
\begin{aligned}
\frac{\partial u_j^l(x)}{\partial x} = {} & \frac{2l+1}{v_{j+1} - v_j} \int_{I_j} f\left(v, p_h(\theta, x, v)\right) \frac{\partial \varphi_j^l(v)}{\partial v} dv \\
& - \frac{2l+1}{v_{j+1} - v_j} \left[h\left(p_h\left(\theta, x, v_{j+1}^-\right), p_h\left(\theta, x, v_{j+1}^+\right)\right) - \right. \\
& \left. (-1)^l h\left(p_h\left(\theta, x, v_{j-1}^-\right), p_h\left(\theta, x, v_{j-1}^+\right)\right) + \int_{I_j} H(v) p_h(\theta, x, v) \varphi_h(v) dv \right]
\end{aligned}
\tag{III.22}
$$

A high-order Gaussian quadrature rule is applied to evaluate the integral on the right-hand side of Eq. (III.22).

In order to obtain the approximation of the (III.6) which is solved in finite volume interval I_j by the collocation method for the breakup and coalescence, the approximate solution is then obtained by inserting the function $p_h(\theta, x, v)$ into the weak formulation of (III.6) and multiplying both sides of the aggregation and breakup equation by choosing the test function as Dirac functions $\theta_j(v) = \partial\left(v - v_j^c\right)$ with v_j^c the collocation points.

In this section we briefly display the application of this discretizations. For more details the reader should consult Hasseine and Bart, 2015; Sandu, 2004; Sandu and Borden, 2003.

III.5   Application and results

Let us consider the spatially distributed in one-dimensional population balance equation Eq. (III.6) subject to the boundary condition $p(\theta, 0, v) = ve^{-v}$. The studied

Table III.1: Summary of the test cases.

Case	Feed distribution p_{in}	Droplet velocity v_d	Breakage functions	Coalescence function $\omega(v,u)$	Growth function $G(v)$
Pure breakage (2 cases)	ve^{-v}	Cte	$g(v) = v$ $\beta(\frac{v}{u}) = \frac{2}{v}$		
		v	$g(v) = v^2$ $\beta(\frac{v}{u}) = \frac{2}{v}$		
Pure coalescence (3 cases)	ve^{-v}	Cte		Cte $v + u$	
		v		vu	
Pure growth	ve^{-v}	Cte			v
Growth with breakage	ve^{-v}	Cte	$g(v) = v^2$ $\beta(\frac{v}{u}) = \frac{2}{v}$		v
Growth with coalescence	ve^{-v}			Cte	v
Growth with breakage with coalescence	ve^{-v}	Cte	$g(v) = v^2$ $\beta(\frac{v}{u}) = \frac{2}{v}$	Cte	v

Cte: constant.

cases are summarized in the Table III.1:

III.5.1   Case 1. Breakage with $g(v) = v, \beta(v/u) = 2/v$ and $v_d = constant$

In the following, we solve this problem by the variational iteration method. Integrating Eq.(III.8) with respect to x we have

$$p_{i+1} = p_i - \int_0^x \left(\frac{\partial p_i}{\partial x} - 2v \int_v^\infty \frac{p_i}{u} du + vp_i \right) dx \tag{III.23}$$

$$e^{-v}v \tag{III.24}$$

$$-e^{-v}v^2 x + v \left(e^{-v} + 2e^{-v}x \right) \tag{III.25}$$

$$\frac{1}{2}e^{-v}v^3 x^2 + v^2 \left(-e^{-v}x - 2e^{-v}x^2 \right) + v \left(e^{-v} + 2e^{-v}x + e^{-v}x^2 \right) \tag{III.26}$$

Hence, we calculate the general term as:

$$p_n\left(\theta, x, v\right) = -\frac{e^{-v}\left(2 - 3n + n^2 + 2v - 2nv + v^2\right)\left(-vx\right)^n}{v^2 x \Gamma\left[n\right]} \tag{III.27}$$

Then:

$$p\left(\theta, x, v\right) = \sum_{n=0}^{\infty} -\frac{e^{-v}\left(2 - 3n + n^2 + 2v - 2nv + v^2\right)\left(-vx\right)^n}{v^2 x \Gamma\left[n\right]} \tag{III.28}$$

$$= e^{-v(1+x)} v(1 + x)^2 \mathbf{u}\left[\theta\right] \tag{III.29}$$

which converges to the exact solution.

Now rewriting this equation in terms of the original variables we get

$$p\left(t, z, v\right) = e^{-v(1+z-z_d)} v(1 + z - z_d)^2 \mathbf{u}\left[t - \frac{z - z_d}{v_d}\right] \tag{III.30}$$

The *unit step u* [.] function is defined as:

$$u\left[t - \frac{z - z_d}{v_d}\right] = \begin{cases} 1, & \left(t - \frac{z - z_d}{v_d}\right) \geq 0, \\ 0, & \textit{otherwise,} \end{cases} \tag{III.31}$$

Figure III.1 shows the prediction of the number density by the variational iteration method at z_d=0.3 (inlet) and z=2.5 (outlet). It must be noted from these profiles that the outlet number density with linear breakage rate gives much production of particles compared to the inlet density as expected.

Figure III.2 concerns the total number of particles, Figure III.2(a) and Sauter diameter and Figure III.2(b) as a function of column height for the case of pure breakage process. This leads to smaller drops which have a lower slip-velocity and greater residence time. Therefore, the total number of particles in the column increases and the Sauter diameter decreases, as shown in Figures III.2(a) and III.2(b), respectively. As can be seen from the figure, the semi-analytical and numerical results of VIM and collocation, respectively, are very distinguishable. The solid line in Figure III.3 shows the holdup versusbcolumn height obtained by the VIM method and the markers by the collocation approach.

Figure III.1: Number density for the pure breakage by the variational iteration method at z=0.3 (inlet) and z=2.5 (outlet).

III.5.2 Case 2. Aggregation with $\omega(v, u) = Cte$ and $v_d = Cte$

$$p_{i+1} = p_i - \int_0^x \left(\frac{\partial p_i}{\partial x} - \frac{v}{2} \int_0^v \frac{p_i(v-u)}{v-u} \frac{p_i(u)}{u} du - p_i \int_0^\infty \frac{p_i(u)}{u} du \right) dx \qquad \text{(III.32)}$$

$$p_0 = e^{-v}v, \qquad \text{(III.33)}$$

$$p_1 = \frac{1}{2}e^{-v}v^2 x + v\left(e^{-v} - e^{-v}x\right), \qquad \text{(III.34)}$$

$$p_2 = \frac{1}{2}e^{-v}v^2 x + v\left(e^{-v} - e^{-v}x\right) + \frac{3}{4}e^{-v}vx^2 - \frac{3}{4}e^{-v}v^2 x^2 + \frac{1}{8}e^{-v}v^3 x^2 + \dots, \qquad \text{(III.35)}$$

then we calculate the general term as:

$$p_n = \frac{4e^{-v}v^{n+1}x^n}{\Gamma(1+n)(2+x)^{n+2}} \qquad \text{(III.36)}$$

The closed-form solution can be written as:

$$p(\theta, x, v) = \sum_{n=0}^{\infty} \frac{4e^{-v}v^{n+1}x^n}{\Gamma(1+n)(2+x)^{n+2}} \qquad \text{(III.37)}$$

$$= \frac{4v\,e^{-\frac{2v}{2+x}}}{(2+x)^2}u[\theta] \qquad \text{(III.38)}$$

(a)

(b)

Figure III.2: Total number of particles (a), and Sauter diameter (b), as function of column height for the case of pure breakage process.

Figure III.3: Holdup versus column height for the pure breakage.

The solution in terms of the original variables is given by:

$$p\left(t,z,v\right) = \frac{4v\, e^{-\frac{2v}{2+z-z_d}}}{\left(2+z-z_d\right)^2}\mathrm{u}\left[t - \frac{z-z_d}{v_d}\right] \tag{III.39}$$

Figure. III.4 shows the prediction of the number density by the VIM at z_d=0.3 (inlet) and $z = 2.5$ (outlet). It must be noted from these profiles that the outlet number density with constant aggregation rate gives low production of drops compared with the inlet density, as expected. Figure. III.5 concerns the total number of particles;Figure III.5(a) Sauter diameter Figure III.5(b) versus column height for the case of pure aggregation process. For the inverse case with aggregation, larger particles are seen to be present. This leads to a. lower total number of particles and a higher Sauter diameter, as shown in Figures III.5(a) and III.5(b), respectively. Again, it can be seen from the figure that the semi-analytical and numerical results of VIM and collocation, respectively, are in good agreement. The solid line in Figure III.6 shows the holdup versus column height obtained by the VIM method and the markers by the collocation approach.
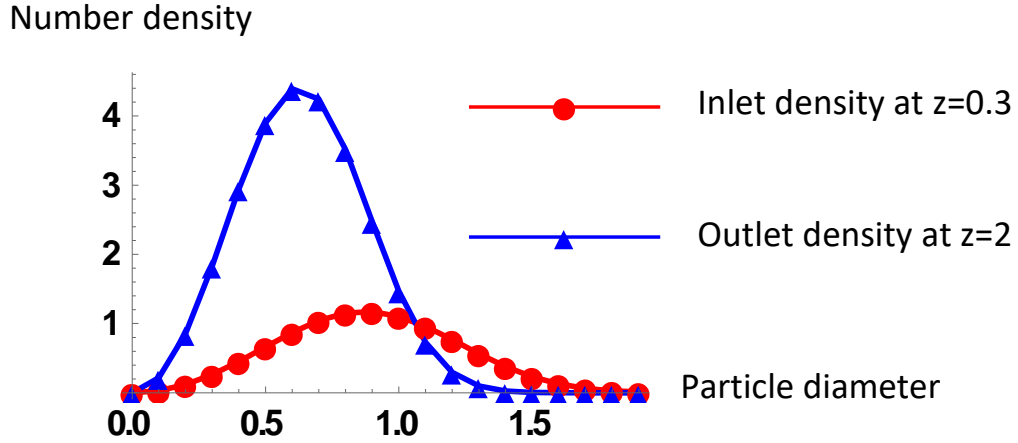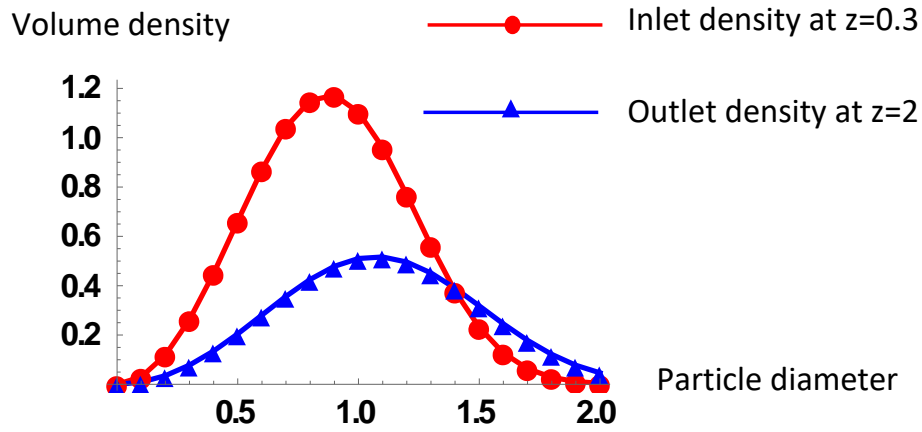
Figure III.4: Number density for the pure aggregation by the variational iteration method at z=0.3 (inlet) and z=2.5 (outlet).

III.5.3   Case 3. Growth with $G(v) = v$ and $v_d = constant$

$$p_{i+1} = p_i - \int_0^x \left(\frac{\partial p_i}{\partial x} + v \frac{\partial p_i}{\partial v} \right) dx \tag{III.40}$$

$$p_0 = e^{-v} v \tag{III.41}$$

$$p_1 = e^{-v} v^2 x + v \left(e^{-v} - e^{-v} x \right), \tag{III.42}$$

$$p_2 = \frac{1}{2} e^{-v} v^3 x^2 + v^2 (e^{-v} x - \frac{3}{2} e^{-v} x^2) + v(e^{-v} - e^{-v} x + \frac{1}{2} e^{-v} x^2) \ldots \tag{III.43}$$

then the general can be obtained as:

$$p_n = \frac{v^{n+1} e^{-(n+1)x - v} (-1 + e^x)^n}{n!} \tag{III.44}$$

The solution can be written as

$$p(\theta, x, v) = \sum_{n=0}^{\infty} \frac{v^{n+1} e^{-(n+1)x - v} (-1 + e^x)^n}{n!} \tag{III.45}$$

$$= v \, e^{-x - e^{-x} v} u[\theta] \tag{III.46}$$
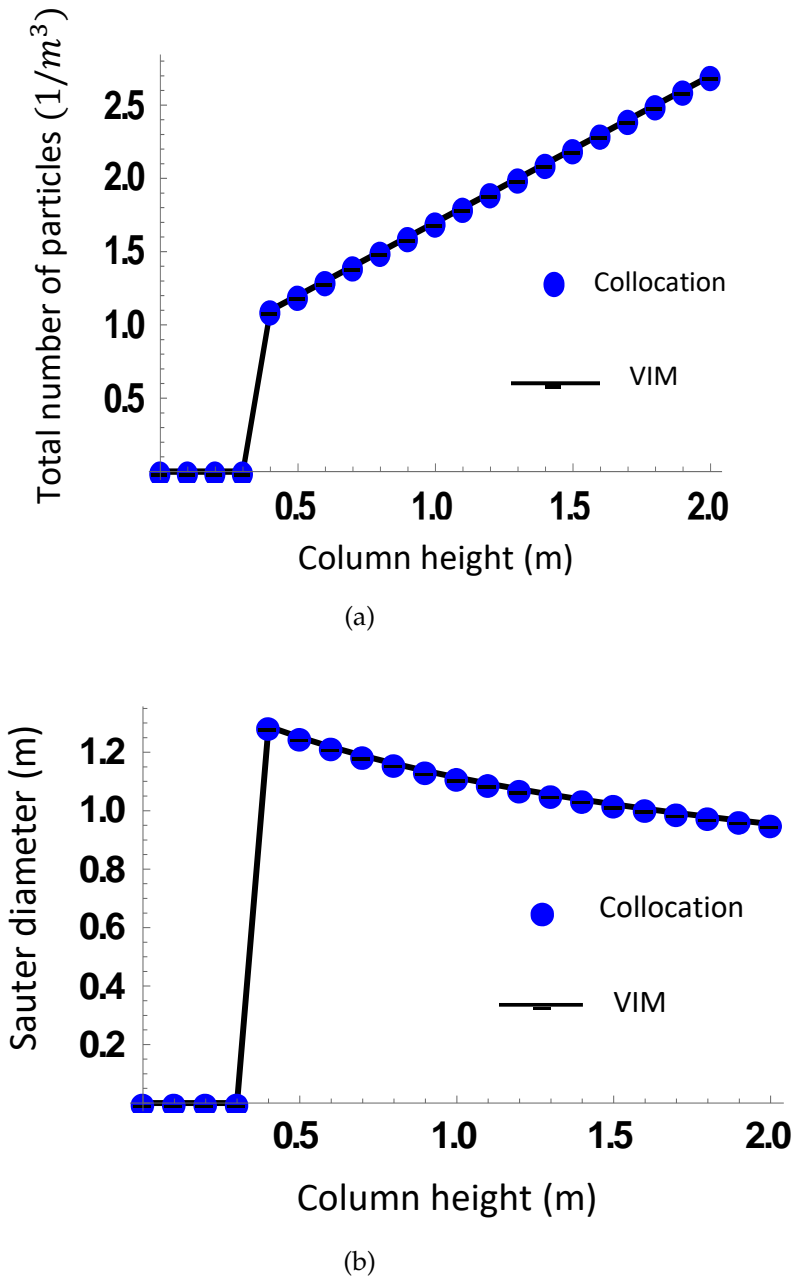
(a)

(b)
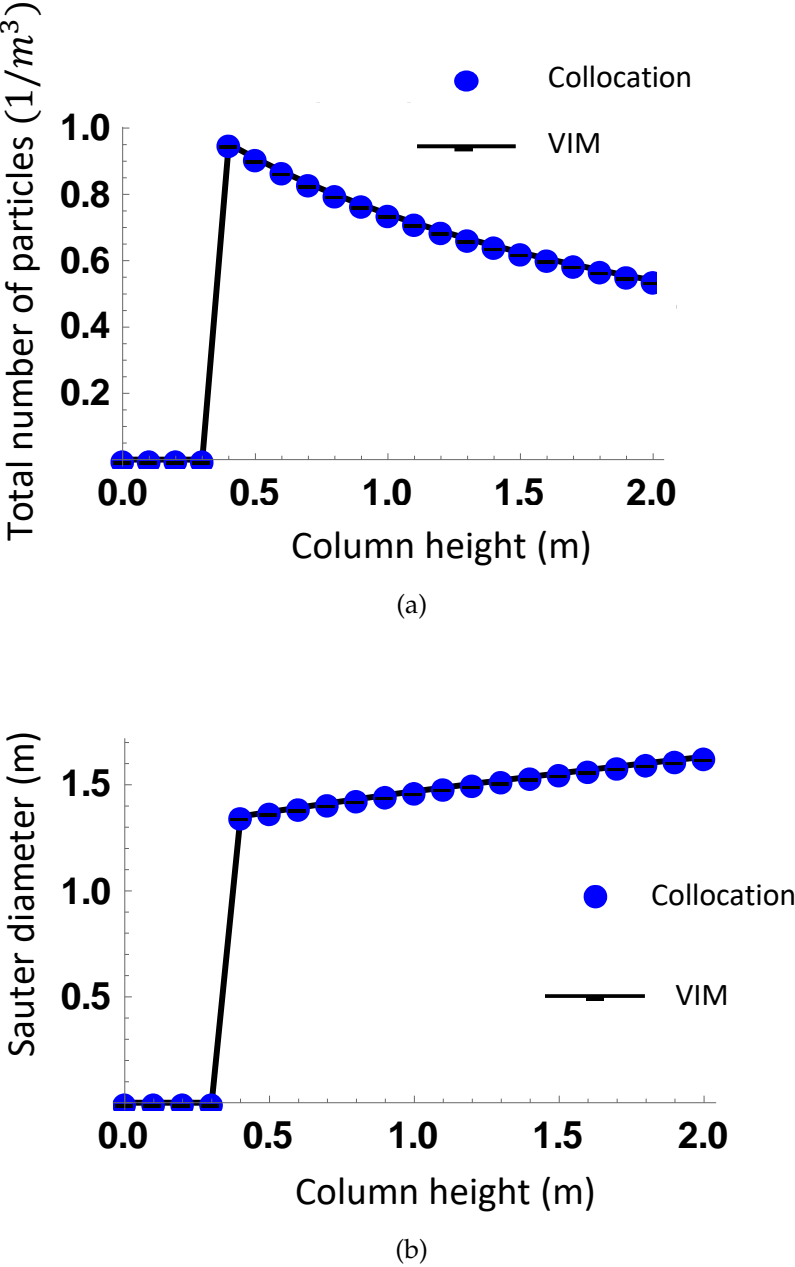
Figure III.5: Total number of particles (a), and Sauter diameter (b), as function of column height for the case of pure aggregation process.
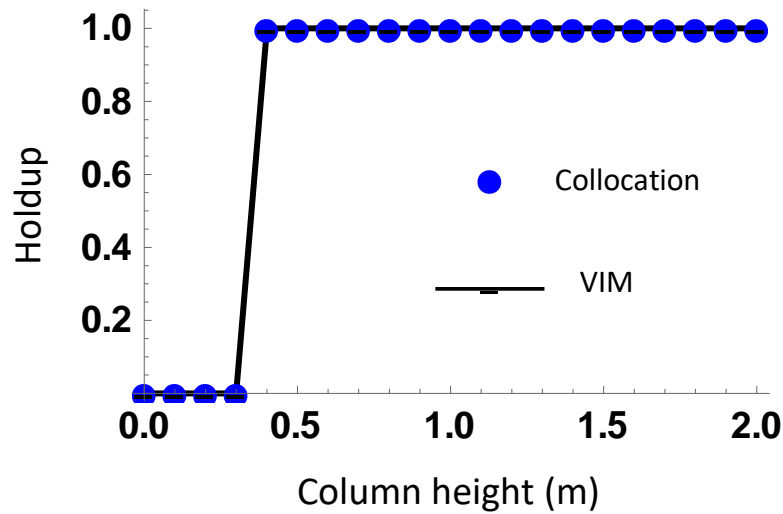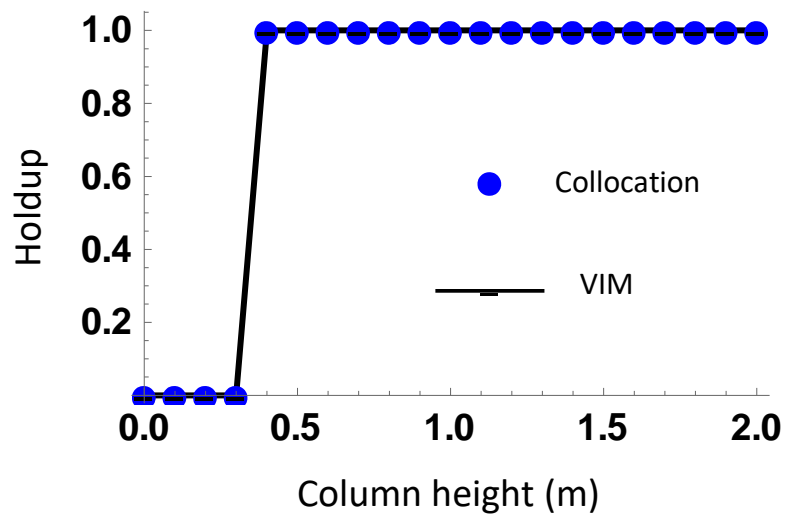
Figure III.6: Holdup versus column height for the pure aggregation.

which can be written as:

$$p\left(t,z,v\right) = v\, e^{-(z-z_d)-e^{-(z-z_d)}v}\mathbf{u}\left[t - \frac{z-z_d}{v_d}\right] \qquad \text{(III.47)}$$

Figure III.7 presents a comparison between discontinuous Galerkin method and variational iteration method results for particle growth Eq.(III.10).
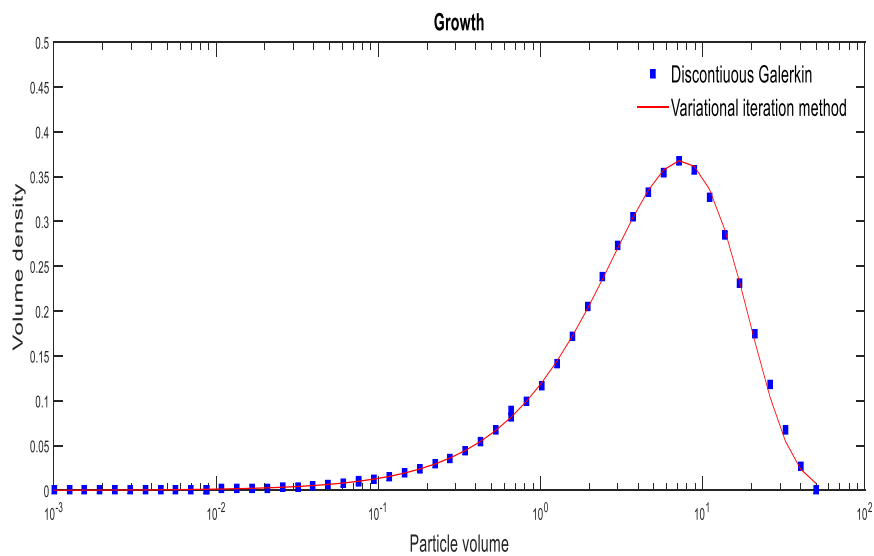
Figure III.7: Comparison between the discontinuous Galerkin and Vim for the case of pure growth process.

III.5.4   Case 4. Coalescence and growth with $\omega(v,u) = constant$, $G(v) = v$ and $v_d = constant$

$$p_{i+1} = p_i - \int_0^x \left(\frac{\partial p_i}{\partial x} + v \frac{\partial p_i}{\partial v} - \frac{v}{2} \int_0^v \frac{p_i(v-u)}{v-u} \frac{p_i(u)}{u} du + p_i \int_0^\infty \frac{p_i(u)}{u} du \right) dx, \quad \text{(III.48)}$$

$$p_0 = e^{-v}v, \quad \text{(III.49)}$$

$$p_1 = v \left(e^{-v} - 2e^{-v}x \right) + \frac{3}{2}e^{-v}v^2x, \quad \text{(III.50)}$$

$$p_2 = v \left(e^{-v} - 2e^{-v}x + \frac{9}{4}e^{-v}x^2 \right) + v^2 \left(\frac{3e^{-v}x}{2} - \frac{17}{4}e^{-v}x^2 \right) + \frac{9}{8}e^{-v}v^3x^2 + \dots \quad \text{(III.51)}$$

$$
\begin{aligned}
p_3 &= v \left(e^{-v} - 2e^{-v}x + \frac{9}{4}e^{-v}x^2 - \frac{23}{12}e^{-v}x^3 \right) \\
&\quad + v^2 \left(\frac{3e^{-v}x}{2} - \frac{17}{4}e^{-v}x^2 + \frac{20}{3}e^{-v}x^3 \right) \\
&\quad + v^3 \left(\frac{9}{8}e^{-v}x^2v^3 - \frac{33}{8}e^{-v}x^3 \right) + \dots
\end{aligned}
\quad \text{(III.52)}
$$

· .,

we therefore suggest that e^{-v} be expressed in Taylor series of finite components for p_3, and then we obtain by substitution the following expression

$$
\begin{aligned}
p_3 &= v \left(1 - 2x + \frac{9x^2}{4} - \frac{23x^3}{12} \dots \right) \\
&\quad + v^2 \left(-1 + \frac{7x}{2} - \frac{13x^2}{2} + \frac{103x^3}{12} \dots \right) \\
&\quad + v^3 \left(\frac{1}{2} - \frac{5x}{2} + \frac{13x^2}{2} - \frac{47x^3}{4} \dots \right) + \dots
\end{aligned}
\quad \text{(III.53)}
$$

This gives:

$$
\begin{aligned}
p_3 &= v \left(\sum_{n=0}^\infty \sum_{m=0}^\infty \frac{(-1)^{n+m}(1+n)}{2^n m!} x^{n+m} \right) \\
&\quad + v^2 \left(\sum_{n=0}^\infty \sum_{m=0}^\infty (-1)^n 2^{-1-n}(1+n)(2+n)\frac{(-2)^m}{m!}x^{n+m} \right) \\
&\quad + v^3 \left(\sum_{n=0}^\infty \sum_{m=0}^\infty \frac{(-3)^m}{m!}\frac{1}{3}(-1)^n 2^{-2-n}(1+n)(2+n)(3+n)x^{n+m} \right) + \dots
\end{aligned}
\quad \text{(III.54)}
$$

and the closed form by

$$p_3 = v \frac{4e^{-x}v}{(2+x)^2} - v^2 \frac{8e^{-2x}v^2}{(2+x)^3} + v^3 \frac{8e^{-3x}}{(2+x)^4} + \dots \tag{III.55}$$

Therefore, we have:

$$p(\theta, x, v) = \lim_{n \to \infty} p_n (\theta, x, v) \tag{III.56}$$

$$= \sum_{n=1}^{\infty} \left(-\frac{2}{2+x}\right)^{n+1} \frac{e^{-nx}v^n}{\Gamma[n]}, \tag{III.57}$$

$$= \frac{4e^{-x - \frac{2e^{-x}v}{2+x}}v}{(2+x)^2} u[\theta] \tag{III.58}$$

This is an exact solution, and in terms of the original variables we get

$$p(t, z, v) = \frac{4e^{-(z-z_d) - \frac{2e^{-(z-z_d)}v}{2+(z-z_d)}}v}{(2+z-z_d)^2} u\left[t - \frac{z-z_d}{v_d}\right] \tag{III.59}$$

Figure. III.8 presents a comparison between discontinuous Galerkin method and variational iteration method results for particle growth and aggregation Eq.(III.11).
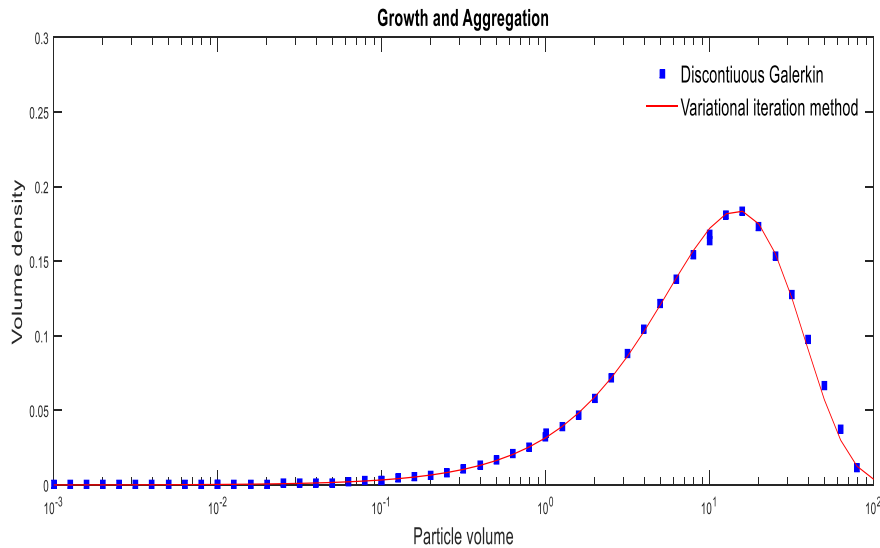
Figure III.8: Comparison between the discontinuous Galerkin and Vim for the case of pure growth process.

III.5.5   Case 5. Simultaneous breakage and growth with $G(v) = v$ and $v_d = constant$

$$p_{i+1} = p_i - \int_0^x \left(\frac{\partial p_i}{\partial x} + v\frac{\partial p_i}{\partial v} - 2\int_v^\infty p_i(u)\,du + vp_i \right) dx \qquad \text{(III.60)}$$

$$p_0 = e^{-v}v \qquad \text{(III.61)}$$

$$p_1 = v\left(e^{-v} + e^{-v}x\right) \qquad \text{(III.62)}$$

$$p_2 = v\left(e^{-v} + e^{-v}x + \frac{1}{2}e^{-v}x^2\right)\ldots \qquad \text{(III.63)}$$

then the general term is obtained as:

$$p_n = \frac{e^{-v}vx^{-1+n}}{\text{Pochhammer}\,[1, -1+n]}. \qquad \text{(III.64)}$$

With the closed solution written as:

$$p(\theta, x, v) = \sum_{n=0}^\infty \frac{e^{-v}vx^{-1+n}}{\text{Pochhammer}\,[1, -1+n]} \qquad \text{(III.65)}$$

$$= e^{-v+x}v\,\mathrm{u}\,[\theta] \qquad \text{(III.66)}$$

With the closed solution written as:

$$p(t, z, v) = ve^{-v+z-z_d}\mathrm{u}\left[t - \frac{z - z_d}{v_d}\right] \qquad \text{(III.67)}$$

Figure III.9 shows a comparison between the discontinuous Galerkin method and variational iteration method results for particle growth and breakage Eq.(III.12).

III.5.6   Case 6. Simultaneous breakup and coalescence and growth with $G(v) = v$, $\omega(v, u) = constant$ and $v_d = constant$

$$p_{i+1} = p_i - \int_0^x \left(\begin{array}{c} \frac{\partial p_i}{\partial x} + v\frac{\partial p_i}{\partial v} - 2\int_v^\infty p_i(u)\,du + vp_i \\ -\frac{1}{2}\int_0^v p_i(v-u)\,p_i(u)du + p_i\int_0^\infty p_i(u)\,du \end{array} \right) dx \qquad \text{(III.68)}$$
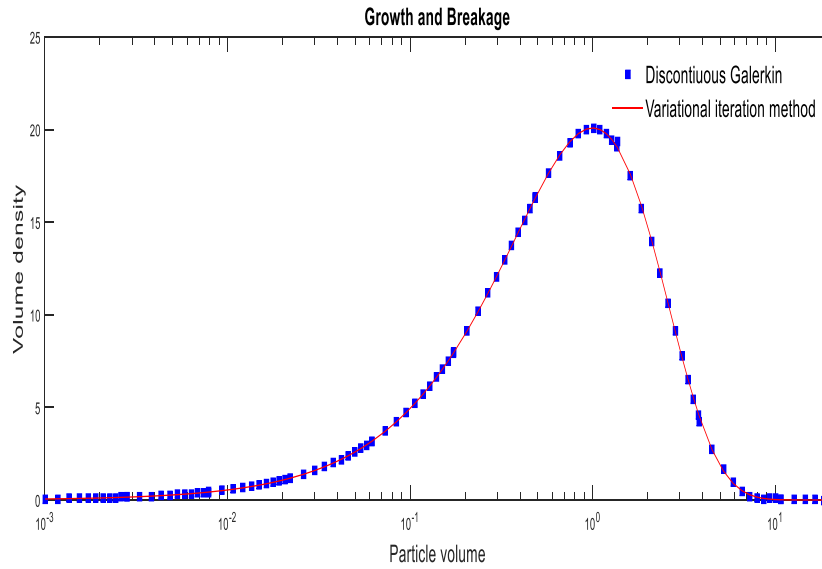
Figure III.9: Comparison between the discontinuous Galerkin and Vim for the case of simultaneous growth and breakage process

$$p_0 = e^{-v}v \tag{III.69}$$

$$p_1 = e^{-v}v + \frac{1}{2}e^{-v}v^2x \tag{III.70}$$

$$p_2 = v\left(e^{-v} + \frac{1}{4}e^{-v}x^2\right) + v^2\left(\frac{e^{-v}x}{2} - \frac{1}{4}e^{-v}x^2\right) + \frac{1}{8}e^{-v}v^3x^2\ldots \tag{III.71}$$

Figure.III.10 shows different cases for the total number of particles such as pure breakage, pure aggregation,pure growth, aggregation and growth, and simultaneous breakage and aggregation and growth are considered.The results can be regarded as a sensitivity analysis of the base concept of a population balance. It is clear from the comparison between all these processes that the pure breakage gives a greater total number of particles. It is evident that in growth-dominated systems, the total number of particles is relatively insensitive to the particular aggregation mechanism. For the semi-analytical solution a very good approximation can be achieved by adding new terms to the decomposition series. A comparison of numerical (collocation approach) and semi-analytical (VIM) results is also made, and they are hardly distinguishable.
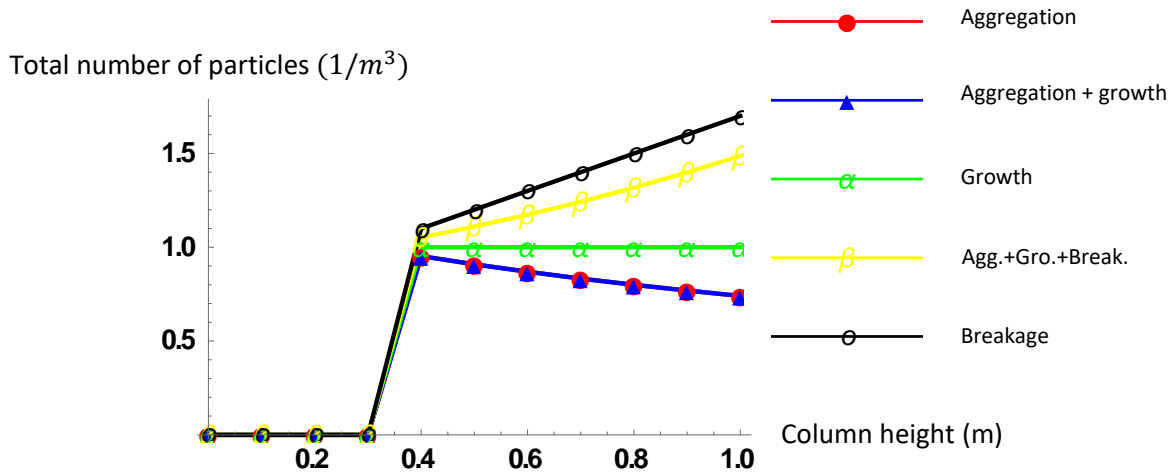
Figure III.10: Total number of particles as function of column height for the case of breakage only, aggregation only, growth only, growth + aggregation, and simultaneous all process. Solid lines vim and markers collocation approach

III.5.7   Case 7. Coalescence with $\omega(v, u) = v + u$ and $v_d = constant$

$$
p_{i+1} = p_i - \int_0^x \left(
\begin{array}{c}
\frac{\partial p_i}{\partial x} - (\frac{v^2}{2} \int_0^v p_i\,(v - u)\,p_i\,(u)\,/((v - u)\,u)du) \\
- p_i \int_0^\infty (v + u)\,p_i\,(u)\,/u du)
\end{array}
\right) dx \tag{III.72}
$$

$$
p_0 = e^{-v}v \tag{III.73}
$$

$$
p_1 = v\left(e^{-v} - e^{-v}x\right) - e^{-v}v^2 x + \frac{1}{2}e^{-v}v^3 x \tag{III.74}
$$

$$
\begin{aligned}
p_2 =& v\left(e^{-v} - e^{-v}x + \frac{1}{2}e^{-v}x^2\right) \\
&+ v^2\left(-e^{-v}x + \frac{3}{2}e^{-v}x^2 - \frac{1}{3}e^{-v}x^3\right) \\
&+ v^3\left(\frac{e^{-v}x}{2} - \frac{1}{4}e^{-v}x^2 - \frac{1}{6}e^{-v}x^3\right) \dots
\end{aligned} \tag{III.75}
$$

Then and with the same suggestion for the case 4 we calculate the exact solution as:

$$
p\left(\theta, x, v\right) = \sum_{m=0}^\infty \sum_n^\infty \frac{e^{-x}(-2 + e^{-x})^m (1 - e^{-x})^k v^{2k+m+1}}{m!k!\Gamma\left[k + 2\right]} \tag{III.76}
$$

$$= \frac{e^{-e^{-x}(-1+2e^x)v-\frac{x}{2}}\mathrm{BesselI}\left[1,2e^{-x/2}\sqrt{-1+e^x}v\right]}{\sqrt{-1+e^x}}\mathrm{u}\left[\theta\right] \qquad \text{(III.77)}$$

with original variable we get:

$$p\left(t,z,v\right) = \frac{e^{-e^{-(z-z_d)}\left(-1+2?^{(z-z_d)}\right)v-\frac{(z-z_d)}{2}}\mathrm{BesselI}\left[1,2e^{-(z-z_d)/2}\sqrt{-1+e^{z-z_d}}v\right]}{\sqrt{-1+e^{z-z_d}}} \qquad \text{(III.78)}$$

$$\times u\left[t-\frac{z-z_d}{v_d}\right]$$

Figure III.11 shows the comparison between the total number of drops versus column height for the case of the pure aggregation process with constant aggregation rate and linear aggregation rate. It is clear that the total number of particles decreases more rapidly with linear aggregation rate than with constant aggregation rate because aggregation becomes more efficient as particles grow when $\omega\left(v,u\right)$ is volume dependent. The linear aggregation mechanism is clearly more efficient in removing particles than is the constant aggregation mechanism Gelbard and Seinfeld, 1978.
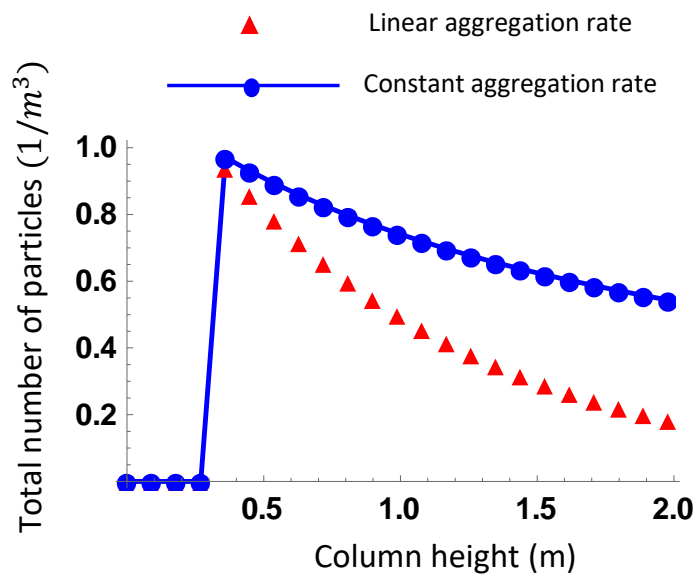
Figure III.11: Comparison between the total number of particles versus column height for the case of pure aggregation process with constant aggregation rate and linear aggregation rate.

III.5.8   Case 8. Breakage $g(v) = v^2, \beta(v/u) = 2/v$ and $v_d = v$

$$p_{i+1} = p_i - \int_0^x \left(\frac{\partial p_i}{\partial x} - 2 \int_v^\infty p_i(u)\, du + v p_i \right) dx \tag{III.79}$$

$$p_0 = e^{-v} v \tag{III.80}$$

$$p_1 = 2e^{-v} x - e^{-v} v^2 x + v \left(e^{-v} + 2e^{-v} x \right) \tag{III.81}$$

$$p_2 = 2e^{-v} x + 2e^{-v} x^2 + \frac{1}{2} e^{-v} v^3 x^2 + v^2 \left(-e^{-v} x - 2e^{-v} x^2 \right)$$
$$+ v \left(e^{-v} + 2e^{-v} x - e^{-v} x^2 \right) + \ldots \tag{III.82}$$

we calculate the general term as:

$$p_n = \frac{(-1)^n x^{n-1}}{n!} e^{-v} v^n (1+x) \left(-n - nx + 2x^2 \right) \tag{III.83}$$

Then the closed form solution can be written as

$$p(\theta, x, v) = \sum_{n=0}^\infty \frac{(-1)^n x^{n-1}}{n!} e^{-v} v^n (1+x) \left(-n - nx + 2x^2 \right) \tag{III.84}$$

$$= e^{-v(1+x)} (1+x) (2x + v + xv)\, \mathrm{u}\,[\theta] \tag{III.85}$$

So we can write

$$p(t, z, v) = e^{-v(1+z-z_d)} (1 + z - z_d) (2(z - z_d) + v + (z - z_d) v)$$
$$\mathrm{u} \left[t - \frac{z - z_d}{v} \right] \tag{III.86}$$

III.5.9   Case 9. Coalescence with $\omega(v, u) = vu$ and $v_d = v$

$$p_{i+1} = p_i - \int_0^x \left(\frac{\partial p_i}{\partial x} - \frac{1}{2} \int_0^v p_i(v-u) p_i(u) du + p_i \int_0^\infty p_i(u)\, du \right) dx \tag{III.87}$$

$$p_0 = e^{-v} v \tag{III.88}$$

$$p_1 = \frac{1}{12}e^{-v}v^3x + v\left(e^{-v} - e^{-v}x\right), \tag{III.89}$$

$$
\begin{aligned}
p_2 = \frac{e^{-v}v^7x^3}{120960} &+ v\left(e^{-v} - e^{-v}x + \frac{3}{4}e^{-v}x^2 - \frac{1}{6}e^{-v}x^3\right) \\
&+ v^5\left(\frac{1}{480}e^{-v}x^2 - \frac{1}{720}e^{-v}x^3\right) \\
&+ v^3\left(\frac{e^{-v}x}{12} - \frac{1}{8}e^{-v}x^2 + \frac{1}{24}e^{-v}x^3\right)
\end{aligned}
\tag{III.90}
$$

Using the above terms, the general term is deduced as:

$$p_n = \frac{4\,x^{n-1}(2+x)^{-n-1}v^{2n-1}}{Gamma(2n)}e^{-v} \tag{III.91}$$

The above series can be generalized as follows:

$$p\left(\theta, x, v\right) = \frac{4\sqrt{x}}{(2+x)^{\frac{3}{2}}}e^{-v}\text{Sinh}\left(\sqrt{\frac{x}{2+x}}v\right)\text{u}\left[\theta\right] \tag{III.92}$$

Therefore the solution is:

$$p\left(t, z, v\right) = \frac{4\sqrt{z - z_d}}{(2+z-z_d)^{\frac{3}{2}}}e^{-v}\text{Sinh}\left(\sqrt{\frac{z - z_d}{2+z - z_d}}v\right)\text{u}\left[t - \frac{z - z_d}{v}\right] \tag{III.93}$$

Figures. III.12 and III.13 show the prediction of the volume density by the VIM at $z_d = 0.3$ (inlet) and $z = 2.2$ (outlet) for the breakage and aggregation respectively with linear velocity. These profiles show that the outlet number densities with linear velocity give low production of drops for the aggregation and greater production of drops for the breakage compared with the inlet densities, as expected..
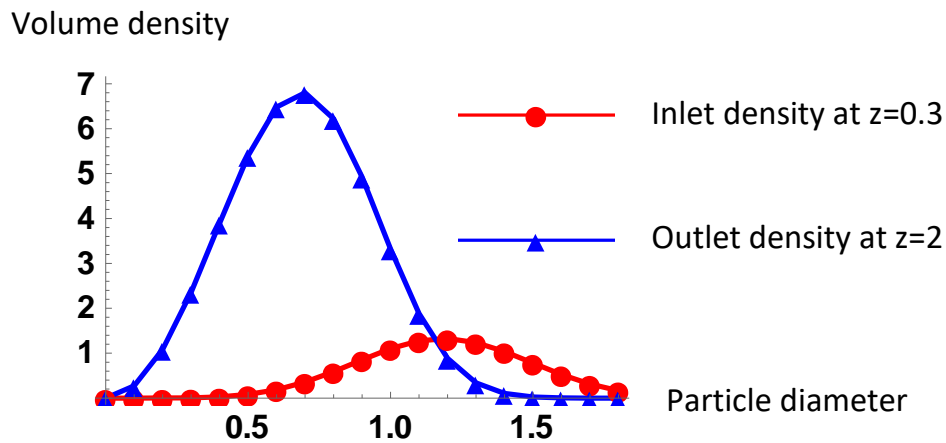
Figure III.12: Volume density for the pure breakage with linear velocity by the variational iteration method at z=0.3 (inlet) and z=2.5 (outlet).
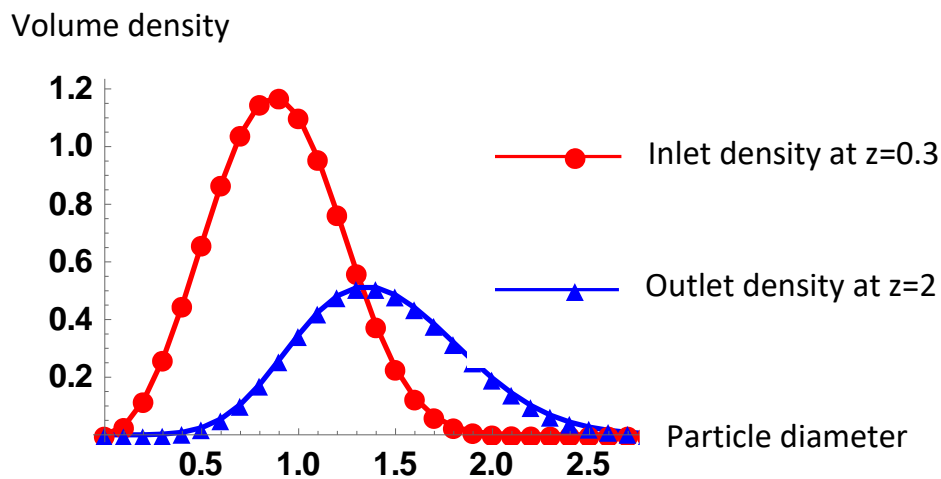
Figure III.13: Volume density for the pure coalescence with linear velocity by the variational iteration method at z=0.3 (inlet) and z=2.5 (outlet).

III.6   Conclusion

In this application, after converting the 1D population balance equation to an integro-ordinary-differential equation, the variational iteration method was examined to solve this equation for breakage, coalescence and growth source terms. From the series that is generated by VIM, the exact solutions are perfectly found for all cases except for the sixth case. Alternatively, with a large number of terms, its series gives a good

exactness. The obtained results support that VIM is an efficient method to solve the integro-differential equations with ease and simplicity in coding. Projection method is a powerful numerical technique for predicting population balance equation distribution. VIM solutions will be also compared with DuQMoGeM solutions for certain cases in the next chapter (chapter IV).

Chapter IV

DuQMoGeM application

IV.1 Introduction

In this chapter we applied the DuQMoGeM to solve the population balance equation for liquid-liquid columns using a multi-compartment model that represents a well-mixed vessel as a particular case. The multi-compartment model can either represent a discretization of a continuous contact column or a multiple-staged column. The model must use appropriate correlations for calculating the inter-compartment drop fluxes for a specific kind of extraction column. The calculation of spatial moment fluxes using DuQMoGeM has never been carried out before. Although several other methods can solve this problem, we did not intend to compare them to the DuQMoGeM in the present work. It must be pointed out that the DuQMoGeM was developed and tested previously only using the particle volume as the internal variable P. L. Lage, 2011. As it has never been applied to solve problems using the particle diameter as the internal variable, we first applied it to solve such population balance models for test cases with analytical solutions. These include models for well-mixed reactors in both continuous and closed systems and a liquid-liquid extraction column without diffusion and with constant phase velocities. Finally, a realistic case of a Kühni column was modeled and solved, and the results were compared to available experimental data.

This work has been partially carried out during the PNE scholarship (2019/2020), at the Thermofluid Dynamic Laboratory of the Programa de Engenharia Química at

COPPE/UFRJ, Brazil, during the academic year 2019/2020.

IV.2   Population balance models

IV.2.1   Model for a liquid-liquid extraction column

The population balance equation for the areal-averaged drop number distribution, $n(t,z,d)$, in a liquid-liquid extraction column can be written as Kronberger et al., 1995; Ramkrishna, 2000:

$$\frac{\partial n(t,z,d)}{\partial t} + \frac{\partial F(t,z,d)}{\partial z} = S(t,z,d) + H(t,z,d) \tag{IV.1}$$

where $z \in [0,h]$ is the vertical coordinate, being h the column height, and $d \in [d_{min}, d_{max}] \subset [0,\infty]$ is the drop equivalent diameter, where d_{min} and d_{max} are physically imposed limits for the drop size distribution, that is, $n(t,z,d) = 0$, $\forall d \notin [d_{min}, d_{max}]$. We proceed in this section as if the extraction column is continuous, that is, without internals, but the resulting equations for the multi-compartment model are the same for a multiple-stage column.

The drops move along the z coordinate with velocity v_d, and their axial dispersion is modeled with an effective isotropic dispersion coefficient $D_{d,ef}$. The advective-diffusive flux F of drops of diameter d at any height in the column is given by:

$$F(t,z,d) = v_d(t,z,d,r_d)n(t,z,d) - \mathcal{D}_{d,ef}(t,z,r_d)\frac{\partial n}{\partial z} \tag{IV.2}$$

where

$$r_d(t,z) = c_v \int_{d_{min}}^{d_{max}} d^3 n(t,z,d)d(d) \tag{IV.3}$$

is the dispersed phase fraction (holdup), being c_v a form factor that relates the drop diameter to its volume, $v(d) = c_v d^3$. For spherical drops, $c_v = \pi/6$.

The two-phase flow and mechanical agitation originate from the turbulent fluctuations in the continuous phase, which generate random drops movements. A dispersive

flux is one way of modeling these drop movements. For staged extraction columns, mechanical agitation is the primary source of dispersion. In Eq. (IV.2), we assumed the hypothesis that $\mathcal{D}_{d,ef}$ is independent from d.

In Equation (IV.1), the H term can be written as:

$$H = H_a + H_b \tag{IV.4}$$

where H_a and H_b are the net rate of drop production by coalescence and breakage, respectively, that are assumed to be functions of the dispersed phase fraction see Ramkrishna, 2000, for their general form. The breakage source terms are given by:

$$H_b = \int_d^{d_{max}} \nu(u)B(d|u)g(u,r_d)n(t,z,u)du - g(d,r_d)n(t,z,d) \tag{IV.5}$$

where g, ν and B are, respectively, the breakage frequency, the mean number of daughter drops and the daughter conditional probability distribution. We assumed that the latter depends only on the diameter ratio of daughter and mother drops. The coalescence source terms are given by:

$$\begin{aligned} H_a &= \frac{1}{2}\int_{d_{min}}^d \omega(u,s,r_d)n(t,z,u)n(t,z,s)\mathcal{J}du \\ &\quad - n(t,z,d)\int_{d_{min}}^{u_{max}} \omega(u,d,r_d)n(t,z,u)du \end{aligned} \tag{IV.6}$$

where $u_{max} = (d_{max}^3 - d^3)^{1/3}$ and ω is the coalescence frequency that is assumed to be a function of the disperse phase fraction, and $\mathcal{J}$ is the Jacobian of the transformation of the internal variable differential, $\mathcal{J}d(d) = ds$:

$$\mathcal{J} = \frac{d^2}{[d^3 - u^3]^{(2/3)}} \tag{IV.7}$$

The number rate of drops entering the column can be modeled as a source at a given z_d position that is given by:

$$S(t,z,d) = \frac{Q_{d,in}(t)}{A}\frac{n_{in}(t,d)}{\bar{v}_{in}(t)}\delta(z - z_d) \tag{IV.8}$$

where $Q_{d,in}(t)$ is the volumetric flow rate of the liquid that forms the drops fed to the column at point z_d and time t, A is the cross-section area of the column, and $n_{in}(t,d)$ is

the normalized drop size distribution formed at the injection point, which satisfies:

$$\int_{d_{min}}^{d_{max}} n_{in}(t,d)d(d) = 1.$$ (IV.9)

Thus, the mean drop volume at $z = z_d$ is given by:

$$\bar{v}_{in}(t) = \int_{d_{min}}^{d_{max}} v(d)n_{in}(t,d)d(d)$$ (IV.10)

Boundary conditions

The Danckwerts boundary condition imposes the value of the advective-dispersive flux at the domain's boundaries. For the present model, the disperse phase is fed to the column at z_d, and the large ascending drops can leave the column at $z = h$, while the continuous phase carries the small descending drops that can leave the column at its bottom. We assumed that the dispersion flux is negligible at the top and bottom of the column, which is an adequate approximation for multi-stage columns with bottom and top sections with no mixing, which is the primary source of drop dispersion. Therefore, the imposed boundary conditions are:

$$\begin{aligned} z = 0, \quad F(t,0,d) &= v_d(t,0,d,r_d)n(t,0,d) - \mathcal{D}_{d,ef}(t,0,r_d)\frac{\partial n}{\partial z} \\ &= \min[v_d(t,0,d,r_d),0]n(t,0,d) \end{aligned}$$ (IV.11)

$$\begin{aligned} z = h, \quad F(t,h,d) &= v_d(t,h,d,r_d)n(t,h,d) - \mathcal{D}_{d,ef}(t,h,r_d)\frac{\partial n}{\partial z} \\ &= \max[v_d(t,h,d,r_d),0]n(t,h,d) \end{aligned}$$ (IV.12)

Considering the large ($v_d > 0$) and small ($v_d < 0$) drops, it is easy to prove that Eqs. (IV.11) and (IV.12) are equivalent to:

$$z = 0, \quad \max[v_d(t,0,d,r_d),0]n(t,0,d) - \mathcal{D}_{d,ef}(t,0,r_d)\frac{\partial n}{\partial z} = 0,$$ (IV.13)

$$z = h, \quad \min[v_d(t,h,d,r_d),0]n(t,h,d) - \mathcal{D}_{d,ef}(t,h,r_d)\frac{\partial n}{\partial z} = 0,$$ (IV.14)

which are the expressions given by M. M. Attarakih et al., 2004.

IV.2.2   Drop velocities

The velocity of drops in a swarm significantly depends on the drop diameter and the volume fraction of the dispersed phase. The rising velocity v_d of a droplet of diameter d, is expressed as Gayler et al., 1953:

$$v_d(d, r_d) = v_r(d, r_d) + v_c(r_d) \tag{IV.15}$$

where v_c is the continuous phase velocity. The relative velocity of droplets with diameter d is often called the slip velocity. It is calculated from the single drop terminal velocity, v_t, considering the slowing factor and the swarm effect by the following expression:

$$v_r(d, r_d) = k_v v_t (1 - r_d)^\kappa \tag{IV.16}$$

where $k_v \in (0, 1]$ is the slowing factor and $(1 - r_d)^\kappa$ accounts for the swarm effect. The drop terminal velocity depends on the physical properties of both phases and droplet diameter Garthe, 2006. The steady-state solution of the mass balance equation for the continuous phase for a column operated in counter-current operation provides:

$$v_c(t, z) = \frac{1}{1 - r_d(t, z)} \left\{ (1 - \mathcal{H}(z - z_c)) \frac{Q_c}{A} + \mathcal{D}_{c,ef}(z) \frac{\partial r_d(t, z)}{\partial z} \right\} \tag{IV.17}$$

where $\mathcal{D}_{c,ef}$ is the dispersion coefficient of the continuous phase that can be used to model backmixing.

IV.2.3   Multi-compartment model for the extraction column

The one-dimensional model of an extraction column can have the external z coordinate domain partitioned to define compartments. These can be actual column stages in a multi-stage column or simply discretization subdomains in a continuous contact column. We consider a multi-compartment column with J sections operated in counter-current mode, where each section has a height h_j, as it is schematically represented in Figure. IV.1.

Its governing equation is given by Eq. (IV.1), which can be integrated using the operator
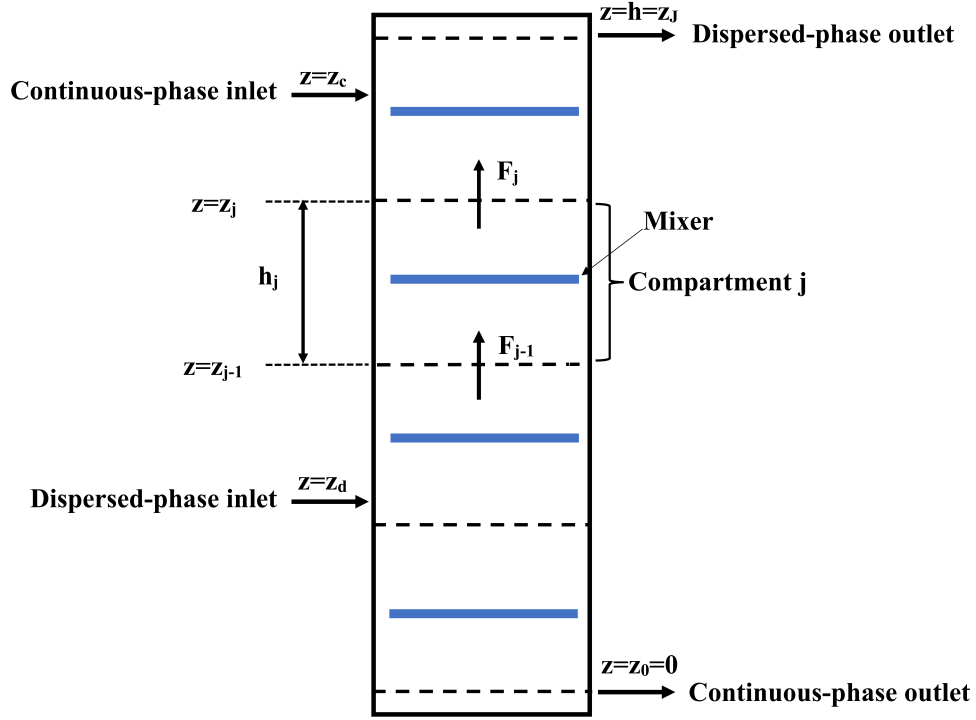
Figure IV.1: Multi-compartment extraction column.

$\frac{1}{h_j} \int_{z_{j-1}}^{z_j} (\cdot) dz$ to give:

$$\frac{\partial}{\partial t} \left[\frac{1}{h_j} \int_{z_{j-1}}^{z_j} n \, dz \right] + \frac{1}{h_j} (F_j - F_{j-1}) = \frac{1}{h_j} \int_{z_{j-1}}^{z_j} S \, dz$$
$$+ \frac{1}{h_j} \int_{z_{j-1}}^{z_j} H \, dz, \quad j = 1, \ldots, J \qquad \text{(IV.18)}$$

where

$$F_j(t,d) = F(t, z_j, d) = v_d(t, z_j, d, r_d(t, z_j)) n(t, z_j, d)$$
$$- \mathcal{D}_{d,ef}(t, z_j, r_d(t, z_j)) \left[\frac{\partial n(t, z, d)}{\partial z} \right]_{z = z_j} \qquad \text{(IV.19)}$$

By defining the average of the generic ψ variable in the j compartment by:

$$\psi_j(t, d) = \frac{1}{h_j} \int_{z_{j-1}}^{z_j} \psi(t, z, d) dz, \qquad \text{(IV.20)}$$

we can write Eq. (IV.18) as:

$$\frac{\partial n_j(t,d)}{\partial t} + \frac{1}{h_j}(F_j - F_{j-1}) = S_j + H_j, \quad J = 1, \ldots, J \tag{IV.21}$$

Equation (IV.21) also represents the population balance model for each stage of a J-staged extraction column. In this case, we have to reinterpret the disperse-phase fluxes given by Eq. (IV.19) as inter-stage fluxes. Then, we must use appropriate correlations Hasseine et al., 2005 or CFD simulation data Weber et al., 2020 for the specific type of staged column to calculate the absolute drop velocity and the drop dispersion coefficient. The j control volume (compartment) is defined to be the column section in the $[z_{j-1}, z_j]$ interval. Therefore, all variables derived from the number size distribution are represented by its volumetric mean at this compartment, $n_j(t,d)$. For instance, the mean dispersed phase fraction in the j compartment is given by:

$$r_{d,j}(t) = c_v \int_{d_{min}}^{d_{max}} d^3 n_j(t,d) d(d) \tag{IV.22}$$

If any variable has a linear behavior within a compartment, then the value at its center is equal to the average, that is, $\psi(t, z_{j-1} + h_j/2, d) = \psi_j(t,d)$. In Eq. (IV.21), the source term S_j exists only for $j = j_d$, defined by $z_{j_d-1} < z_d < z_{j_d}$, where the drops are formed, which is given by:

$$S_j = S_{j_d} \delta_{j,j_d}, \quad S_{j_d} = \frac{1}{h_{j_d}} \int_{z_{j_d-1}}^{z_{j_d}} S dz = \frac{1}{t_{h,j_d}} \frac{n_{in}(t,d)}{\bar{v}_{in}} \tag{IV.23}$$

where

$$t_{h,j_d} = \frac{h_{j_d} A}{Q_{d,in}} = \frac{V_{d_{j_d}}}{Q_{d,in}}, \quad V_{d_{j_d}} = h_{j_d} A \tag{IV.24}$$

It should be noted that F_j must be computed at the boundary z_j between the j and $j+1$ compartments. Therefore, some approximations have to be made as the distribution n_j is a mean value for the j compartment. As small drops can descend along the column dragged by the continuous phase, we must consider drop effluxes at z_0 and z_J. Moreover, every compartment boundary may have upward and downward drop fluxes. Therefore, we split the advective fluxes accordingly, and Eq. (IV.19) becomes:

$$F(t, z_j, d) = F_j(t,d) = F_j^+(t,d) + F_j^-(t,d) - \mathcal{D}_{d,ef}(t, z_j, r_d(t, z_j)) \left[\frac{\partial n(t,z,d)}{\partial z}\right]_{z=z_j} \tag{IV.25}$$

We use a fully upwind approximation for the advective fluxes, that is,

$$
\begin{aligned}
F_j^-(t,d) &= \min(v_{d,j},0)n_{j+1}(t,d), \quad j=0,\ldots,J-1, \quad F_J^-(t,d)=0 \\
F_j^+(t,d) &= \max(v_{d,j},0)n_j(t,d), \quad j=1,\ldots,J, \quad F_0^+(t,d)=0 \quad\quad \text{(IV.26)}
\end{aligned}
$$

where $n(t,z_j,d) = n_j(t,d)$, $v_{d,j}(t,d) = v_d(t,z_j,d,r_d(t,z_j))$ with $r_d(t,z_j) = r_j(t)$. Equation (IV.26) implies that there is no drop inlet at the column boundaries at z_0 and z_J. Substituting Eqs. (IV.26) into Eq. (IV.25) and applying the boundary conditions given by Eqs. (IV.11) and (IV.12) under the assumption of no dispersive flux at the boundaries, we have:

$$
F_0(t,d) = F_0^-(t,d) = \min(v_{d,0},0)n_1(t,d) \quad\quad \text{(IV.27)}
$$

$$
F_J(t,d) = F_J^+(t,d) = \max(v_{d,J},0)n_J(t,d) \quad\quad \text{(IV.28)}
$$

Equations (IV.27) and (IV.28) are equivalent to the assumption of escape frequencies equal to $-v_{d,0}/h_0$ and $v_{d,J}/h_J$ for, respectively, the descending drops at the lowest compartment and the ascending drops at the highest compartment. For the inter-compartment fluxes inside the column, we approximate the dispersive term by central differences:

$$
\left[\frac{\partial n(t,z,d)}{\partial z}\right]_{z=z_j} = \frac{n_{j+1}(t,d) - n_j(t,d)}{\dfrac{h_{j+1}+h_j}{2}}, \quad\quad \text{(IV.29)}
$$

The weighted harmonic mean is used to obtain the dispersion coefficient at the compartment boundaries:

$$
\mathcal{D}_{d,ef,j+1/2}(t) = \mathcal{D}_{d,ef}(t,z_j) = \left[\frac{1}{h_j+h_{j+1}}\left(\frac{h_j}{\mathcal{D}_{d,ef,j}(t)} + \frac{h_{j+1}}{\mathcal{D}_{d,ef,j+1}(t)}\right)\right]^{-1}, \quad\quad \text{(IV.30)}
$$

where $\mathcal{D}_{d,ef,j}(t)$ is the volumetric mean dispersion coefficient in compartment j. The harmonic mean used in Eq. (IV.30) reduces to the correct limiting dispersive fluxes when $\mathcal{D}_{d,ef,i} \to 0$ or $\mathcal{D}_{d,ef,i} \to \infty$ for $i = j, j+1$ for transport processes in series. Using these approximations, we have

$$
F_j(t,d) = F_j^+(t,d) + F_j^-(t,d) - \mathcal{D}_{d,ef,j+1/2}(t)\frac{2}{h_{j+1}+h_j}\left[n_{j+1}(t,d) - n_j(t,d)\right]. \quad\quad \text{(IV.31)}
$$

Thus, the multi-compartment model consists of the following ODE system for n_j:

$$\frac{\partial n_j}{\partial t} + \frac{1}{h_j}(F_j - F_{j-1}) = H_j + S_j, \quad j = 1, \ldots, J \tag{IV.32}$$

The breakage and coalescence source terms in compartment j can be written as:

$$H_j = H_{a,j} + H_{b,j} \tag{IV.33}$$

Some definitions and approximations must be made to write these terms as functions of n_j. Lets assume that $n(t, z, d) = n_j(t, d)$ for $z \in [z_{j-1}, z_j]$. Then, these distributions can be taken out of the z integral, and mean breakage and aggregation functions can be defined for each compartment. Assuming that $\nu(u)$ and $B(d|u)$ do not depend on z, the breakage source term is given by:

$$H_{b,j} = \int_d^{d_{max}} \nu(u)B(d|u)g_j(u, r_{d,j})n_j(t, u)dudz - g_j(d, r_{d,j})n_j(t, d) \tag{IV.34}$$

The coalescence source term is given by:

$$\begin{aligned}
H_{a,j} &= \frac{1}{2}\int_{d_{min}}^d \omega_j(u, s, r_{d,j})n_j(t, u)n_j(t, s)Jdu \\
&- n_j(t, d)\int_{d_{min}}^{u_{max}} \omega_j(u, d, r_{d,j})n_j(t, u)du
\end{aligned} \tag{IV.35}$$

where

$$g_j(d, r_{d,j}(t)) = \frac{1}{h_j}\int_{z_{j-1}}^{z_j} g(d, r_d(t, z))dz \tag{IV.36}$$

$$\omega_j(u, d, r_{d,j}(t)) = \frac{1}{h_j}\int_{z_{j-1}}^{z_j} \omega(u, d, r_d(t, z))dz \tag{IV.37}$$

IV.2.4   Model for the well-mixed vessel

The behavior of the dispersed phase in a continuous well-mixed vessel is a particular case of Eq. (IV.32), where $J = j_d = 1$, $h_1 = h$, $t_{h,1} = t_h$ and, using Eq. (IV.28), we have:

$$\frac{F_1}{h_1} = \frac{v_{d,1}}{h_1}n_1(t, d) = \frac{Q_{d,in}}{hA}n_1(t, d) = \frac{1}{t_h}n_1(t, d) \tag{IV.38}$$

where in the last two expressions the drop escape frequency was assumed to be independent from its diameter and equal to the inverse of the mean residence time of the dispersed phase, t_h. Therefore, for the well-mixed vessel, the population balance equation can be written as Ramkrishna, 2000:

$$\frac{\partial n(t,d)}{\partial t} = \frac{1}{t_h}\left[\frac{n_{in}(t,d)}{\bar{v}_{in}} - n(t,d)\right] + H_a(t,d) + H_b(t,d) \tag{IV.39}$$

where the subscript 1 was dropped. For a batch well-mixed vessel Eq. (IV.39) takes the simple form:

$$\frac{\partial n(t,d)}{\partial t} = H_a(t,d) + H_b(t,d) \tag{IV.40}$$

IV.3　Generalized moment equations

Consider the generalized moment operator:

$$\langle \phi_k, (\cdot) \rangle = \int_{d_{min}}^{d_{max}} (\cdot)\phi_k(d)d(d), \tag{IV.41}$$

where $\phi_k(d)$ is the Legendre polynomial of k degree defined into the shifted interval $[d_{min}, d_{max}]$, which have the following orthogonality property:

$$\langle \phi_k, \phi_j \rangle = \int_{d_{min}}^{d_{max}} \phi_k(d)\phi_j(d)d(d) = \delta_{kj}\langle \phi_k, \phi_k \rangle = \delta_{kj}\|\phi_k\|^2 \tag{IV.42}$$

IV.3.1　Moment equations for the multi-compartment model

The Legendre generalized moments of $n_j(t,d)$ can be computed from its definition, Eq. (IV.20), and from Eq. (IV.41) and they can be written as:

$$\mu_{j,k}^{(\phi)} = \langle \phi_k, n_j \rangle = \frac{1}{h_j}\int_{z_{j-1}}^{z_j} \langle \phi_k, n \rangle dz \tag{IV.43}$$

Applying the moment operator, Eq. (IV.41), to Eq. (IV.32), we get:

$$\frac{\partial \mu_{j,k}^{(\phi)}}{\partial t} + \frac{1}{h_j}(\langle \phi_k, F_j \rangle - \langle \phi_k, F_{j-1} \rangle) = H_{j,k}^{(\phi)} + \frac{1}{t_{h,j_d}}\frac{\mu_{in_k}^{(\phi)}}{\bar{v}_{in}}\delta_{j,j_d}, \quad j = 1,\dots,J \tag{IV.44}$$

where $\langle \phi_k, F_j \rangle$ are calculated using F_j from Eqs. (IV.27), (IV.28) and (IV.31):

$$
\begin{aligned}
\langle \phi_k, F_0 \rangle &= \langle \phi_k, \min(v_{d,0}, 0) n_1 \rangle \\
\langle \phi_k, F_j \rangle &= \langle \phi_k, \max(v_{d,j}, 0) n_j \rangle + \langle \phi_k, \min(v_{d,j}, 0) n_{j+1} \rangle \\
&\quad - \frac{2 \mathcal{D}_{d,ef,j+1/2}}{h_{j+1} + h_j} \left[\mu_{j+1,k}^{(\phi)} - \mu_{j,k}^{(\phi)} \right], \quad j = 1, \ldots, J - 1 \quad \text{(IV.45)} \\
\langle \phi_k, F_J \rangle &= \langle \phi_k, \max(v_{d,J}, 0) n_J \rangle
\end{aligned}
$$

and

$$
\mu_{in,k}^{(\phi)}(t) = \int_{d_{min}}^{d_{max}} n_{in}(t, d) \phi_k(d) d(d) \tag{IV.46}
$$

The moments of the breakage and coalescence terms in the j compartment are written as:

$$
H_{j,k}^{(\phi)} = \langle \phi_k, H_j \rangle = \langle \phi_k, H_{a,j} \rangle + \langle \phi_k, H_{b,j} \rangle \tag{IV.47}
$$

Using the hypotheses described in section IV.2.3, we can write the moments of the coalescence and breakage terms as:

$$
\langle \phi_k, H_{a,j} \rangle = \frac{1}{2} \int_{d_{min}}^{d_{max}} \int_{d_{min}}^{d_{max}} \left[\phi_k \left([s^3 + u^3]^{1/3} \right) - \phi_k(s) - \phi_k(u) \right]
$$
$$
\omega_j(u, s) n_j(t, u) n_j(t, s) ds du \tag{IV.48}
$$

$$
\langle \phi_k, H_{b,j} \rangle = \int_{d_{min}}^{d_{max}} g_j(u) n_j(t, u) \left[\nu(u) \Pi_k^{(\phi)}(u) - \phi_k(u) \right] du \tag{IV.49}
$$

where

$$
\Pi_k^{(\phi)}(u) = \int_{d_{min}}^{u} \phi_k(d) B(d|u) d(d) \tag{IV.50}
$$

IV.3.2   Moment equations for the well-mixed vessel

This is a particular case of the model presented in the previous section. Thus, considering the same hypotheses described in section IV.2.4, we can write the moments of the corresponding PBE by:

$$
\frac{\partial \mu_k^{(\phi)}}{\partial t} = \frac{1}{t_h} \left[\frac{\mu_{in,k}^{(\phi)}}{\bar{v}_{in}} - \mu_k^{(\phi)} \right] + \langle \phi_k, H_a \rangle + \langle \phi_k, H_b \rangle \tag{IV.51}
$$

where

$$\mu_k^{(\phi)}(t) = \int_{d_{min}}^{d_{max}} n(t,d)\phi_k(d)d(d) \tag{IV.52}$$

and $\langle \phi_k, H_a \rangle$ and $\langle \phi_k, H_b \rangle$ are those obtained from Eqs. (IV.48) to (IV.49) by dropping the j subscript.

IV.4 The usage of a dimensionless internal variable

The internal variable d can be used to defined the dimensionless diameter x in the $[0,1]$ interval:.

$$
\begin{aligned}
x(d) &= \frac{d - d_{min}}{d_{max} - d_{min}} &\Rightarrow\qquad dx &= \frac{d(d)}{d_{max} - d_{min}} & (IV.53)\\
d(x) &= d_{min} + x\left(d_{max} - d_{min}\right) & & & (IV.54)
\end{aligned}
$$

Considering the $n_j(t,d)$ distribution in the multi-compartment model, the transformed distribution $\tilde{n}_j(t,x)$ is given by :

$$n_j(t,d)d(d) = \tilde{n}_j(t,x)dx \quad\Rightarrow\quad \tilde{n}_j(t,x) = n_j(t,d)\left(d_{max} - d_{min}\right) \tag{IV.55}$$

Defining $\varphi_k(x) = \phi_k(d(x))$, the following relation between the moment operators can be established:

$$
\begin{aligned}
\langle \varphi_k, (\cdot) \rangle = \int_0^1 (\cdot)\varphi_k(x)dx &= \frac{1}{d_{max} - d_{min}} \int_{d_{min}}^{d_{max}} (\cdot)\phi_k(d)d(d)\\
&= \frac{1}{d_{max} - d_{min}} \langle \phi_k, (\cdot) \rangle & (IV.56)
\end{aligned}
$$

where $\langle (\cdot), (\cdot) \rangle$ indicates the inner product between two functions relatively to their internal variable, d or x. It should be pointed out that $\varphi_k(x)$ is just an expression for $\phi_k(d(x))$ and, therefore, both have the same dimensions, even though x is dimensionless. Therefore, Eqs. (IV.55) and (IV.56) shows that:

$$\langle \varphi_k, \tilde{n}_j \rangle = \langle \phi_k, n_j \rangle \tag{IV.57}$$

Similarly

$$\tilde{n}_{in}(t,x) = (d_{max} - d_{min})n_{in}(t,d) \quad \Rightarrow \quad \langle \varphi_k, \tilde{n}_{in} \rangle = \langle \phi_k, n_{in} \rangle \tag{IV.58}$$

If we define:

$$\tilde{F}_j(t,x) = (d_{max} - d_{min})\, F_j(t,d), \tag{IV.59}$$

$$\tilde{H}_{a,j}(t,x) = (d_{max} - d_{min})\, H_{a,j}(t,d) \tag{IV.60}$$

$$\tilde{H}_{b,j}(t,x) = (d_{max} - d_{min})\, H_{b,j}(t,d) \tag{IV.61}$$

then

$$\langle \varphi_k, \tilde{F}_j \rangle = \langle \phi_k, F_j \rangle \tag{IV.62}$$

$$\langle \varphi_k, \tilde{H}_{a,j} \rangle = \langle \phi_k, H_{a,j} \rangle \tag{IV.63}$$

$$\langle \varphi_k, \tilde{H}_{b,j} \rangle = \langle \phi_k, H_{b,j} \rangle \tag{IV.64}$$

IV.4.1   Moment equations of the multi-compartment model

Considering Eqs. (IV.57), (IV.58), (IV.62), (IV.63) and (IV.64), the moment equations of the multi-compartment model, given by Eq. (IV.44), can be written as:

$$\frac{\partial \mu_{j,k}^{(\varphi)}}{\partial t} + \frac{1}{h_j}\left(\langle \varphi_k, \tilde{F}_j \rangle - \langle \varphi_k, \tilde{F}_{j-1} \rangle \right) = \langle \varphi_k, \tilde{H}_j \rangle + \frac{1}{t_{h,j_d}}\frac{\mu_{in,k}^{(\varphi)}}{\bar{v}_{in}}\delta_{j,j_d}, \quad j = 1, \dots, J \tag{IV.65}$$

where

$$\langle \varphi_k, \tilde{F}_0 \rangle = \langle \varphi_k, \min(v_{d,0}, 0)\tilde{n}_1 \rangle,$$

$$\begin{aligned}
\langle \varphi_k, \tilde{F}_j \rangle = {} & \langle \varphi_k, \max(v_{d,j}, 0)\tilde{n}_j \rangle + \langle \varphi_k, \min(v_{d,j}, 0)\tilde{n}_{j+1} \rangle \\
& - \frac{2\mathcal{D}_{d,ef,j+1/2}}{h_{j+1} + h_j}\left[\mu_{j+1,k}^{(\varphi)} - \mu_{j,k}^{(\varphi)} \right], \quad j = 1, \dots, J-1,
\end{aligned} \tag{IV.66}$$

$$\langle \varphi_k, \tilde{F}_J \rangle = \langle \varphi_k, \max(v_{d,J}, 0)\tilde{n}_J \rangle,$$

and

$$\begin{aligned}
\langle \varphi_k, \tilde{H}_{a,j} \rangle = \frac{1}{2}\int_0^1 \int_0^1 {} & \left[\varphi_k\left(q(x,y)\right) - \varphi_k(y) - \varphi_k(x) \right] \\
& \tilde{\omega}_j(x,y)\tilde{n}_j(t,x)\tilde{n}_j(t,y)\,dy\,dx
\end{aligned} \tag{IV.67}$$

where $q(x,y)$ is the value of the dimensionless diameter of the daughter drop formed by the coalescence of drops with dimensionless diameters $x(d)$ and $y(u)$ and $\tilde{\omega}_j(x(d), y(u)) = \omega_j(d, u)$. The breakage term becomes:

$$\langle \varphi_k, \tilde{H}_{b,j} \rangle = \int_0^1 \tilde{g}_j(x) \tilde{n}_j(t, x) \left[\tilde{v}(x) \tilde{\Pi}_k^{(\varphi)}(x) - \varphi_k(x) \right] dx \tag{IV.68}$$

where $\tilde{g}_j(x(d)) = g_j(d)$ and

$$\begin{aligned}
\Pi_k^{(\phi)}(u(x)) &= \int_{d_{min}}^{u(x)} \phi_k(d(y)) B\left(d(y) | u(x)\right) d(d) \\
&= \int_0^x \varphi_k(y) \tilde{B}\left(y | x\right) dy = \tilde{\Pi}_k^{(\varphi)}(x).
\end{aligned} \tag{IV.69}$$

IV.4.2 Moment equations for the continuous well-mixed vessel

As before, this is a special case of the multicompartment model with just one compartment. Therefore, the moment equations in the dimensionless internal variable come from Eq. (IV.65) with $J = 1$. Using the same approximations described in section IV.2.4, we have:

$$\frac{\partial \mu_k^{(\varphi)}}{\partial t} = \frac{1}{t_h} \left[\frac{\mu_{k,in}^{(\varphi)}}{\bar{v}_{in}} - \mu_k^{(\varphi)} \right] + \langle \varphi_k, \tilde{H}_a \rangle + \langle \varphi_k, \tilde{H}_b \rangle \tag{IV.70}$$

and $\langle \psi_k, \tilde{H}_a \rangle$ and $\langle \psi_k, \tilde{H}_b \rangle$ are those obtained from Eqs. (IV.67) to (IV.69) by dropping the j subscript.

IV.5   Application of the DuQMoGeM to the models

The DuQMoGeM employs two quadrature rules P. L. Lage, 2011. The first one is the N_q-point Gauss–Christoffel quadrature based on the $2N_q$ moments of the particle number distribution function. It is used to discretize the distribution. The second quadrature rule is a M-point Gaussian quadrature based on an orthogonal polynomial family that is used to calculate the integrals related to the internal variable with controlled accuracy. It is strongly recommended that $M > 2N_q$ to guarantee the correct

integration of the expansion coefficients of Eq. (IV.74) when it is substituted into Eq. (IV.75).

For continuous distributions, the $2N_q$ generalized moments of the distribution are directly related to a $(2N_q - 1)$-order series expansion using the orthogonal polynomial family employed to generate the second quadrature. Here, all models were solved using the dimensionless internal variable x, and, therefore, we employed the Legendre polynomials shifted to the $[0, 1]$ interval, $\varphi_k(x)$.

IV.5.1   The Gauss-Legendre quadrature

The Gauss-Legendre quadrature in the $[0, 1]$ interval approximates the following integral of a generic function G:

$$\int_0^1 G(x)dx \approx \sum_{i=1}^{M} w_i G(\xi_i) \tag{IV.71}$$

where w_i are the weights and ξ_i are the abscissas of the quadrature rule. As it gives the correct value of the integral when G is a polynomial whose order is equal to or less than $2M - 1$, the result for $G(x) = 1$ gives that:

$$\sum_{i=1}^{M} w_i = 1 \tag{IV.72}$$

If an integral in the incomplete interval $[0, x]$ is necessary, one just has to define $Y = y/x$:

$$\int_0^x G(y)dy = x \int_0^1 G(xY)dY = x \sum_{i=1}^{M} w_i G(\xi_i x) = \sum_{i=1}^{M} w_{x,i} G(\xi_{x,i}) \tag{IV.73}$$

where $w_{x,i} = xw_i$ and $\xi_{x,i} = x\xi_i$.

IV.5.2   DuQMoGeM solution for the multi-compartment extraction column

For this case, the mean distribution function at each compartment, $\tilde{n}_j(t, x)$, is approximated by the polynomial series of $2N_q - 1$ order:

$$\tilde{n}_j(t, x) = \sum_{i=0}^{2N_q-1} c_{j,i}(t)\varphi_i(x) \tag{IV.74}$$

where

$$c_{j,i}(t) = \frac{\langle \tilde{n}_j, \varphi_i \rangle}{\langle \varphi_i, \varphi_i \rangle} = \frac{1}{\|\varphi_i\|^2} \int_0^1 \tilde{n}_j(t, x)\varphi_i(x)dx = \frac{\mu_{j,i}^{(\varphi)}(t)}{\|\varphi_i\|^2}, \quad i = 0, 1, \ldots, 2N_q - 1 \tag{IV.75}$$

Although Eq. (IV.74) provides an approximate representation of the drop number distribution, it must be emphasized that the DuQMoGeM is a moment method, and its solution consists of the generalized moments, $\mu_{j,i}^{(\varphi)}$. Substitution (IV.74) and (IV.75) in (IV.65) gives:

$$\begin{aligned}
\| \varphi_k \|^2 \frac{\partial c_{j,k}(t)}{\partial t} &= \frac{1}{h_j}(\langle \varphi_k, \tilde{F}_{j-1} \rangle - \langle \varphi_k, \tilde{F}_j \rangle) + \frac{1}{t_{h,j_d}} \frac{\mu_{in,k}^{(\varphi)}}{\bar{v}_{in}} \delta_{j,j_d} \\
&+ \sum_{i=0}^{2N_q-1} \sum_{l=0}^{2N_q-1} \mathcal{A}_{jkli} c_{j,l} c_{j,i} + \sum_{i=0}^{2N_q-1} \mathcal{L}_{jki} c_{ji}, \quad j = 1, \ldots, J
\end{aligned} \tag{IV.76}$$

where, from Eq. (IV.66):

$$\begin{aligned}
\langle \varphi_k, \tilde{F}_0 \rangle &= \langle \varphi_k, \min(v_{d,0}, 0)\tilde{n}_1 \rangle \\
\langle \varphi_k, \tilde{F}_j \rangle &= \langle \varphi_k, \max(v_{d,j}, 0)\tilde{n}_j \rangle + \langle \varphi_k, \min(v_{d,j}, 0)\tilde{n}_{j+1} \rangle \\
&\quad - \frac{2\mathcal{D}_{d,ef,j+1/2}}{h_{j+1} + h_j} \| \varphi_k \|^2 \left[c_{j+1,k} - c_{j,k} \right], \, j = 1, \ldots, J - 1 \\
\langle \varphi_k, \tilde{F}_J \rangle &= \langle \varphi_k, \min(v_{d,J})\tilde{n}_J \rangle
\end{aligned} \tag{IV.77}$$

The advective terms in Eq. (IV.77) can be approximated by:

$$\langle \varphi_k, \max(v_{d,j}, 0)\tilde{n}_j \rangle = \sum_{i=0}^{2N_q-1} c_{j,i} \mathcal{V}_{jki}^+, \tag{IV.78}$$

$$\langle \varphi_k, \min(v_{d,j}, 0)\tilde{n}_{j+1} \rangle = \sum_{i=0}^{2N_q-1} c_{j+1,i} \mathcal{V}_{jki}^- \tag{IV.79}$$

where

$$\mathcal{V}_{jki}^+ = \langle \varphi_k, \max(v_{d,j}, 0)\varphi_i \rangle = \int_0^1 \varphi_k(x)\varphi_i(x)\max[v_{d,j}(t, d(x)), 0]dx, \tag{IV.80}$$

$$\mathcal{V}_{jki}^- = \langle \varphi_k, \min(v_{d,j}, 0)\varphi_i \rangle = \int_0^1 \varphi_k(x)\varphi_i(x)\min[v_{d,j}(t, d(x)), 0]dx. \tag{IV.81}$$

Using Eqs. (IV.67) and (IV.68), the breakage and coalescence terms can be written as:

$$\mathcal{L}_{jki} = \left\langle \tilde{g}_j \left[\tilde{v}\tilde{\Pi}_k^{(\varphi)} - \varphi_k \right], \varphi_i \right\rangle = \int_0^1 \tilde{g}_j(x)\varphi_i(x) \left[\tilde{v}(x)\tilde{\Pi}_k^{(\varphi)}(x) - \varphi_k(x) \right] dx, \tag{IV.82}$$

$$\mathcal{A}_{jkli} = \left\langle \left\langle \left[\varphi_k\left(q(x,y)\right) - \varphi_k(y) - \varphi_k(x) \right] \tilde{\omega}_j(x,y), \varphi_l(y) \right\rangle, \varphi_i(x) \right\rangle$$
$$= \frac{1}{2}\int_0^1\int_0^1 \left[\varphi_k\left(q(x,y)\right) - \varphi_k(y) - \varphi_k(x) \right] \tilde{\omega}_j(x,y)\varphi_i(x)\varphi_l(y)dydx \tag{IV.83}$$

Applying the Gauss-Legendre quadrature given by Eq. (IV.71) to the above integrals, we have:

$$\mathcal{V}_{jki}^+ = \sum_{\substack{r=1 \\ v_{d,j}(t,d(\xi_r))\geq 0}}^M w_r\varphi_k(\xi_r)\varphi_i(\xi_r)v_{d,j}(t, d(\xi_r)), \tag{IV.84}$$

$$\mathcal{V}_{jki}^- = \sum_{\substack{r=1 \\ v_{d,j}(t,d(\xi_r))<0}}^M w_r\varphi_k(\xi_r)\varphi_i(\xi_r)v_{d,j}(t, d(\xi_r)), \tag{IV.85}$$

$$\mathcal{L}_{jki} = \sum_{r=1}^M w_r\tilde{g}_j(\xi_r)\varphi_i(\xi_r) \left[\tilde{v}(\xi_r)\tilde{\Pi}_k^{(\varphi)}(\xi_r) - \varphi_k(\xi_r) \right], \tag{IV.86}$$

$$\mathcal{A}_{jkli} = \frac{1}{2}\sum_{r=1}^M\sum_{p=1}^M w_r w_p \left[\varphi_k\left[q(\xi_p,\xi_r)\right] - \varphi_k(\xi_p) - \varphi_k(\xi_r) \right] \tilde{\omega}_j(\xi_r,\xi_p)\varphi_i(\xi_r)\varphi_l(\xi_p). \tag{IV.87}$$

For the moments of the daughter distribution function, defined in eq. (IV.69), the quadrature rule in the incomplete interval given by Eq. (IV.73) gives:

$$\tilde{\Pi}_k^{(\varphi)}(\xi_r) = \xi_r \sum_{m=1}^{M} w_m \varphi_k(\xi_r \xi_m) \tilde{B}\left(\xi_r \xi_m | \xi_r\right). \tag{IV.88}$$

IV.5.3   DuQMoGeM solution for the well-mixed vessel

This solution can be obtained by applying the multi-compartment model with $J = j_d = 1$. Using Eq. (IV.77) and the same simplifications described in section IV.2.4, we have:

$$\| \varphi_k \|^2 \frac{\partial c_k(t)}{\partial t} = \frac{\mu_{in,k}^{(\varphi)}}{t_h \bar{v}_{in}} - \frac{1}{t_h} \| \varphi_k \|^2 c_k(t) + \sum_{i=0}^{2N_q-1} \sum_{l=0}^{2N_q-1} \mathcal{A}_{kli} c_l c_i + \sum_{i=0}^{2N_q-1} \mathcal{L}_{ki} c_i \tag{IV.89}$$

where

$$\tilde{n}(t,x) = \sum_{i=0}^{2N_q-1} c_i(t) \varphi_i(x), \quad c_i(t) = \frac{\mu_i^{(\varphi)}(t)}{\|\varphi_i\|^2} \tag{IV.90}$$

where $\mathcal{L}_{ki}$ and $\mathcal{A}_{kli}$ are calculated as given by Eqs. (IV.86) and (IV.87) after dropping the j subscript.

IV.6   Results

In order to present the results clearly, we divided this section into four subsections, each one devoted to presenting results for one of the following systems: batch extraction vessel, continuous flow extraction vessel, extraction columns, all of them solved for problems with known analytical solutions, and an extraction column with available experimental data.

The batch extraction vessel section shows DuQMoGeM results for problems with pure breakage, pure coalescence, and simultaneous breakage and coalescence. The continuous flow extraction vessel section presents DuQMoGeM results for pure breakage

and pure coalescence problems. The convergence of the lowest order moments regarding the number of points in the first quadrature, N_q, was studied for these well-mixed vessel solutions. Analytical solutions exist for extraction column problems with no drop dispersion and constant drop ascension velocity assumptions. The extraction column section presents DuQMoGeM solutions for three such cases: pure breakage, pure coalescence, and simultaneous breakage and coalescence. The convergence of results regarding the number of compartments was analyzed. In the final section, we compared the DuQMoGeM prediction of the hold up of the dispersed phase with available experimental data for a Kühni column operated with the toluene-water system. We modeled the Kühni column, including drop advective and dispersive transport, breakage, and coalescence.

In fact, the verification problems were solved analytically in the semi-finite range, $[0, \infty)$, while the DuQMoGeM solutions were solved for the range $[d_{min}, d_{max}]$. However, we guaranteed that the supports of the number density distributions given by the analytical solutions were always within the $[d_{min}, d_{max}]$ range for the analyzed time interval. We also assumed spherical droplets.

IV.6.1   Batch extraction vessel

For the batch extraction vessel, we applied the DuQMoGeM solution to Eq. IV.40, for which three cases with available analytical solutions were considered: a pure breakage, a pure coalescence, and a simultaneous breakage and coalescence problems. In fact, the last two cases were solved previously by P. L. Lage, 2011 using the DuQMoGeM, but employing the particle volume in the semi-infinite domain as the internal variable. In this section, all variables are considered dimensionless.

Pure coalescence in finite domain, $d \in [0, 6.0]$

When the drops undergo coalescence with a constant kernel ($\omega = 1$ for this case) and with an exponential initial distribution given by

$$n(0, d) = v'(d) \exp[-v(d)], \tag{IV.91}$$

the analytical solution was reported by Gelbard and Seinfeld, 1978 as:

$$n(t, d) = \frac{4v'(d)}{(\omega t + 2)^2} \exp\left(-\frac{2v(d)}{\omega t + 2}\right), \tag{IV.92}$$

where $v(d) = c_v d^3$ and $v'(d) = dv/d(d) = 3c_v d^2$. Under these conditions, we investigated the effect of the number of the Gauss–Christoffel quadrature points on the absolute errors of the first four moments. Figure IV.2 shows that the absolute error decreases by increasing the number of the Gauss–Christoffel quadrature N_q, being the best results generated for $N_q = 6$. This figure shows that the DuQMoGeM accuracy for the zeroth-order moment is better than for the first and second-order moments. The third-order moment has an error close to the machine's accuracy because it is unchanged throughout the evolution of the distribution as the breakage phenomenon conserves the total volume (mass) of the particles. Figure IV.3 presents the analytical solution and the numerical distribution function computed with $N_q = 6$ and $M = 12$ for this case for three instants, showing perfect agreement between the analytical distributions and their DuQMoGeM approximations.

Pure breakage in finite domain, $d \in [0, 2]$

In this case, a normal Gaussian distribution with mean $m = 0.9$ and standard deviation $\alpha = 0.8$ was used as the initial condition as given by:

$$n(0, d) = \frac{v'(d)}{\sqrt{2\pi\alpha}} \exp\left[-\frac{(v(d) - m)^2}{\Lambda}\right] \tag{IV.93}$$

where $\Lambda = 2\alpha^2$. For a daughter drop distribution given by $B(d|u) = 6d^2/u^3$ and a breakage frequency linear in drop volume, $g(d) = v(d)$, Hasseine et al., 2020 provided
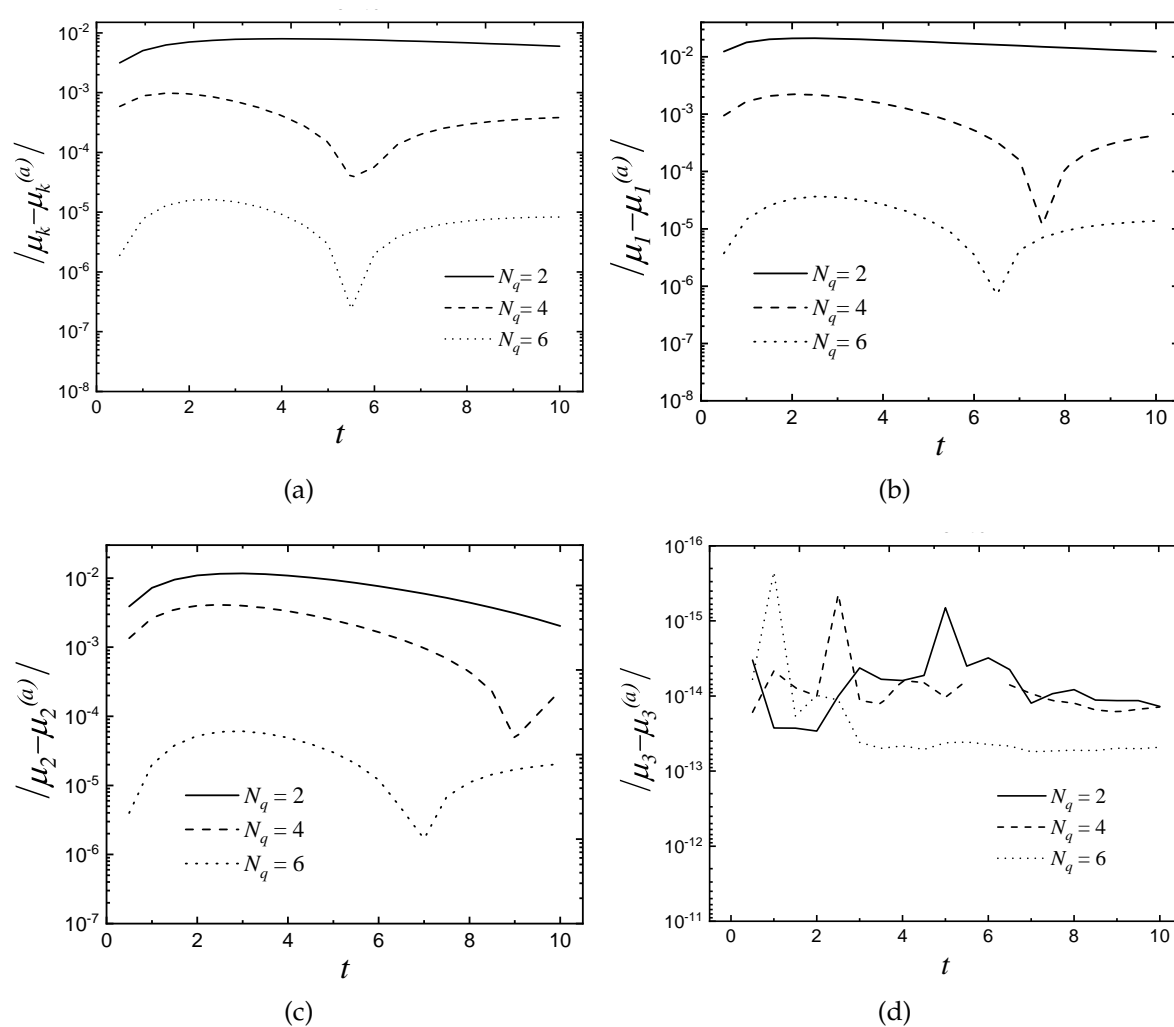
Figure IV.2: Pure coalescence problem in a batch extraction vessel: absolute errors for the first four regular moments for the DuQMoGeM solutions with $N_q = 2, 4$ and 6 using the same number of Gauss-Legendre quadrature points, $M = 12$.
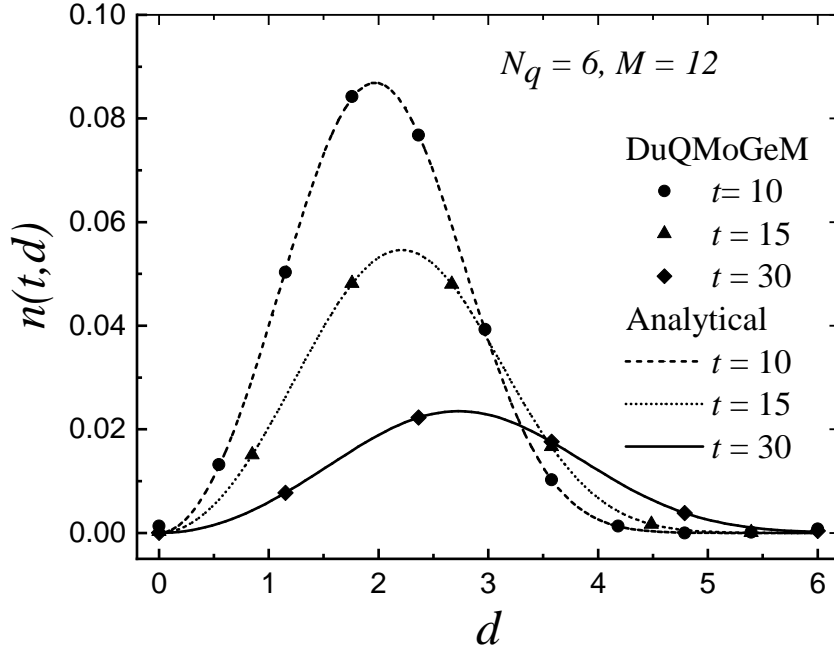
Figure IV.3: Pure coalescence problem in a batch extraction vessel: comparison of the analytical and numerical distributions.

the exact solution that can be writen as:

$$n(t,d) = v'(d)\frac{2\chi + \Lambda t^2\chi + \sqrt{\Lambda}\sqrt{\pi}\Phi\left(2t + mt^2 - t^2v(d)\right)}{2\sqrt{2\pi}\alpha}\exp\left[-tv(d)\right] \qquad \text{(IV.94)}$$

where

$$\chi = \exp\left[-\frac{(v(d)-m)^2}{2\alpha^2}\right] \quad \text{and} \quad \Phi = 1 + \text{erf}\left[\frac{m-v(d)}{\sqrt{\Lambda}}\right] \qquad \text{(IV.95)}$$

Figure IV.4(a) shows a comparison between the analytical moments of $n(t,d)$ with those obtained from DuQMoGeM solution for $N_q = 4$ and $M = 8$, which show excellent agreement. The results show that the total volume of the droplets μ_3 remains constant. The moments of the order lower than three increase, whereas μ_4 and μ_5 decrease. Figure IV.4(b) shows the good agreement between the exact and the numerical distributions obtained from DuQMoGeM at different times using $N_q = 6$ and $M = 12$.

Simultaneous breakage and coalescence in finite domain, $d \in [0, 2.8]$

We considered here the combined coalescence and breakage problem with $\omega(v,u) = 1$, $g(d) = g_0v(d)$, $g_0 = 2$, and $B(d/u) = 6d^2/u^3$. For the initial condition described by
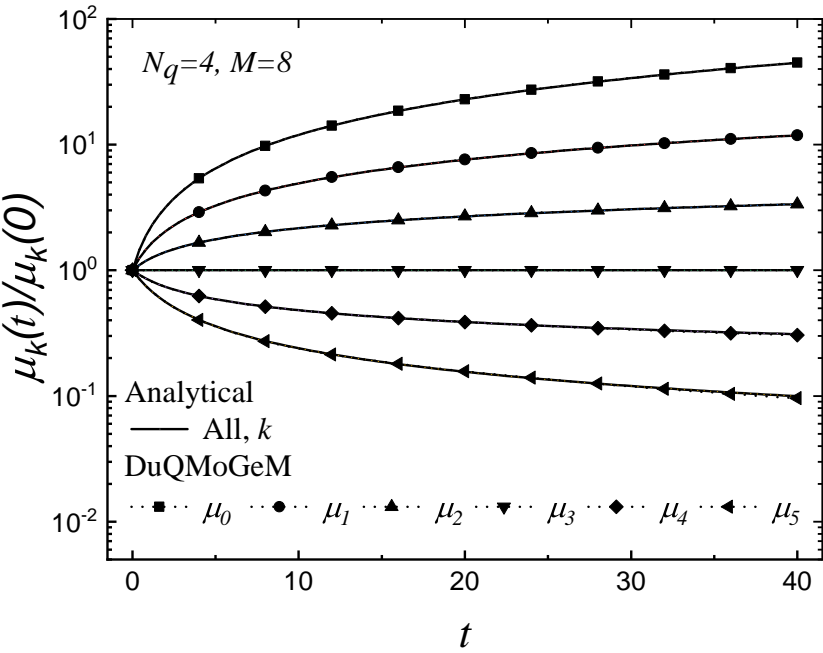
(a)
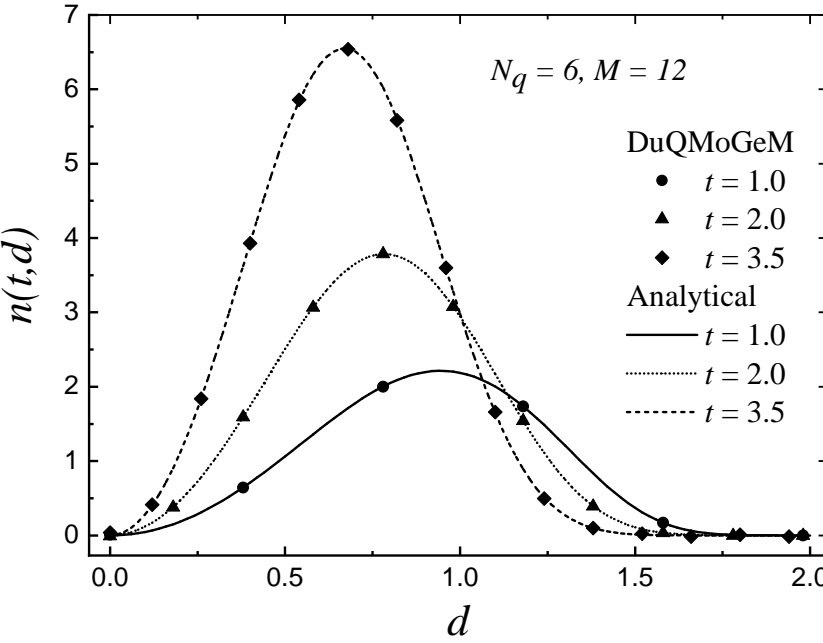
(b)

Figure IV.4: Pure breakage problem in a batch extraction vessel: comparison of the analytical and numerical results.
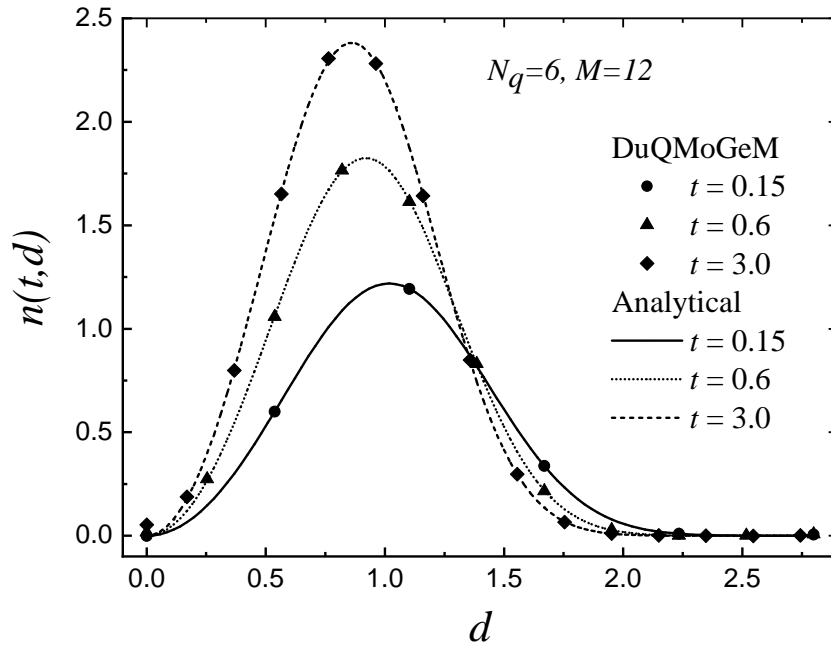
Figure IV.5: Simultaneous breakage and coalescence problem in batch extraction vessel: comparison of the analytical and numerical distributions.

Eq. (IV.91), McCoy and Madras, 2003 gave the following analytical solution:

$$n(t,d) = v'(d)[\Phi(t)]^2 \exp\left[-\Phi(t)v(d)\right] \tag{IV.96}$$

where

$$\Phi(t) = \Phi(\infty)\frac{1 + \Phi(\infty)\tanh(\Phi(\infty)t/2)}{\Phi(\infty) + \tanh(\Phi(\infty)t/2)}, \quad \Phi(\infty) = \sqrt{2g_0} \tag{IV.97}$$

Figure IV.5 shows the series approximation of the number density distribution for the numerical solution with $N_q = 6$ and $M = 12$ at different values of t, showing a good agreement with the analytical solution.

IV.6.2   Continuous flow extraction vessel

The performance of the DuQMoGeM to solve the PBE in the continuous flow well-mixed extraction vessel is tested for two different cases: one with droplet coalescence and other with droplet breakage. In this section, all variables are considered dimensionless.

Pure breakage in finite domain, $d \in [0, 1.9]$

This case is similar to first case of pure breakage but in a continuous flow extraction vessel with $t_h = 10^3$. The inlet drop number distribution, $n_{in}(t, d)$, is the normal Gaussian distribution with mean $m = 0.9$ and standard deviation $\alpha = 0.8$ given by equation (IV.93). Initially, there is no drop in the reactor, and, thus, $n(0, d) = 0$. This problem comes from Hasseine et al., 2020 and its analytical solution is:

$$
\begin{aligned}
n(t, d) = \frac{v'(d)a}{2\sqrt{2\pi}\alpha\beta(t,d)[a + v(d)]^3} &\Big\{ 2\left[-1 + \beta(t,d)\right][v(d)]^2 \chi \\
&+ \Lambda\left[-2 + 2\beta(t,d) - 2tv(d) - t^2[v(d)]^2\right]\chi \\
&+ \sqrt{\Lambda}\sqrt{\pi}\left[t^2[v(d)]^3 + m(-2 + 2\beta(t,d) - 2tv(d) - t^2[v(d)]^2)\right]\Phi \\
&+ a^2\left[(-2 + 2\beta(t,d) - \Lambda t^2)\chi + \sqrt{\Lambda}\sqrt{\pi}t(-2 - mt + tv(d))\Phi\right] \\
&- 2a\Big[-2(-1 + \beta(t,d))v(d)\chi + \Lambda t(1 + tv(d))\chi \\
&- \sqrt{\Lambda}\sqrt{\pi}\{-1 + \beta(t,d) - tv(d) + t^2(v(d))^2 - mt[1 + tv(d)]\}\Phi\Big] \Big\}
\end{aligned}
$$ (IV.98)

where $a = t_h^{-1}$ and $\beta(t, d) = \exp\{t[a + v(d)]\}$. Figure IV.6(a) shows the regular moments obtained from DuQMoGeM solution with $N_q = 6$ and $M = 12$ together with those computed from the exact solution. The results demonstrate that all moments increase with time. The numerical and analytical results for all moments are in good agreement. Figure IV.6(b) shows the exact and the numerical distribution obtained from DuQMoGeM at different values of t. The agreement between the numerical and analytical distributions is excellent.

Pure coalescence in finite domain, $d \in [0, 4.6]$

The population balance equation in a continuous flow well-mixed extraction vessel was solved dynamically using the DuQMoGeM for a pure coalescence problem with a constant aggregation kernel ($\omega = 1$). The initial condition is zero, $n(0, d) = 0$, while the drop number distribution at the inlet, $n_{in}(t, d)$, has the same distribution given by equation (IV.91). M. J. Hounslow, 1990 solved this problem at the steady state and found

(a)
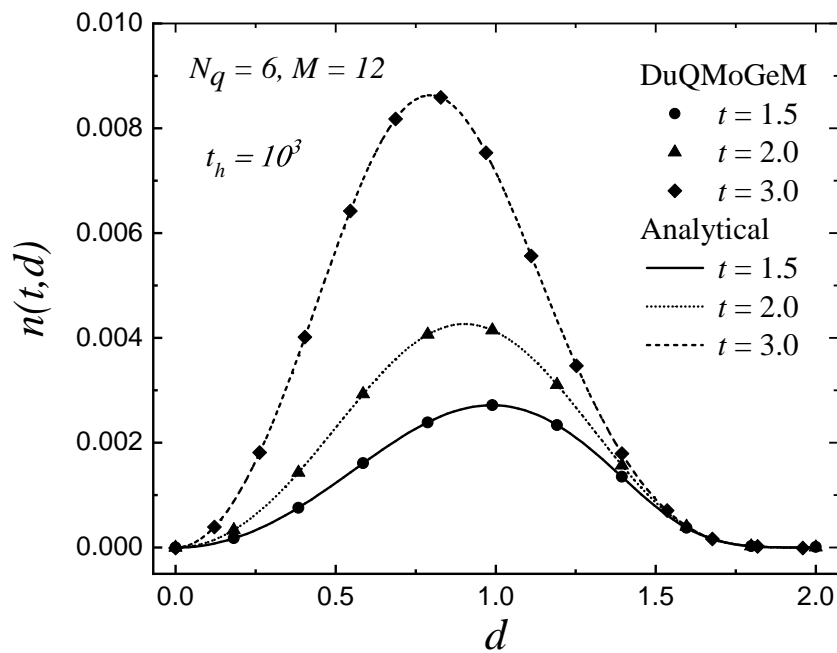
(b)

Figure IV.6: Pure breakage problem in a continuous flow extraction vessel: comparison of the analytical and numerical results.
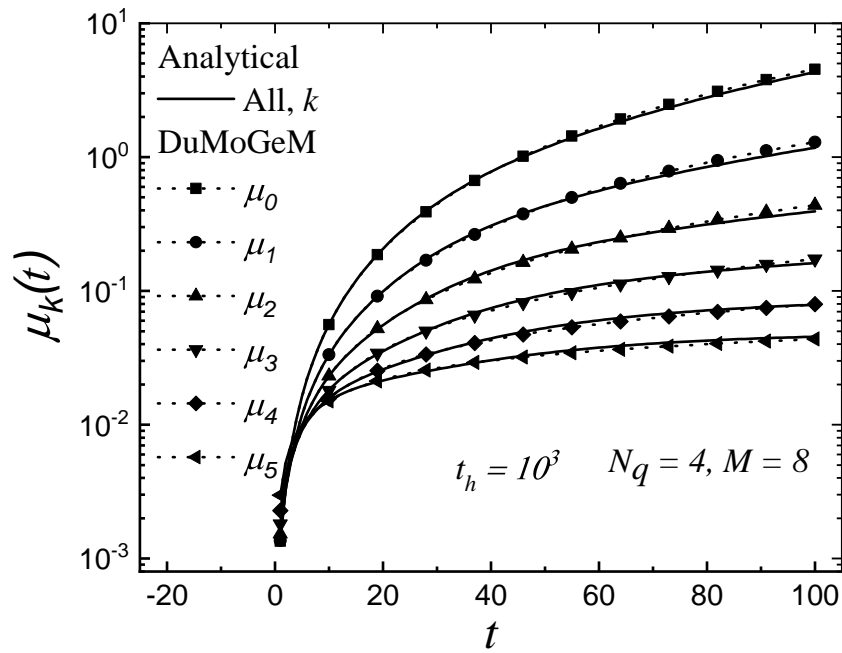
the following exact solution:

$$n(\infty, d) = \frac{v'(d)}{\sqrt{1 + 2t_h}} \exp\left[-\frac{(1 + t_h)v(d)}{1 + 2t_h}\right] \left[I_0\left(\frac{-t_h v(d)}{1 + 2t_h}\right) + I_1\left(\frac{-t_h v(d)}{1 + 2t_h}\right)\right] \quad \text{(IV.99)}$$

where I_0 and I_1 are the modified Bessel functions of the first kind and zeroth and first orders, respectively.

The simulation was implemented with $N_q = 3$ and $M = 6$ and $t_h = 10$. In order to verify the DuQMoGeM results, for different values of t, the distributions obtained by the DuQMoGeM are presented with the exact solution described by the above equation in Figure. IV.7(a). The numerical distributions for $t \geq 30$ conform with its steady-state analytical solution. The dynamically predicted and the analytical steady-state moments are presented in Figure. IV.7(b). As expected for a first-order system, the process reaches the steady state for $t/t_h \approx 4$.

IV.6.3   Hydrodynamics simulation of extraction columns

The DuQMoGeM solution of the multi-compartment model was obtained for three test cases: pure breakage, pure coalescence and breakage with coalescence. We assumed pure drop advection with a constant velocity because the analytical solutions are known for these three cases under this assumption, being provided by M. M. Attarakih et al., 2004 and Hasseine et al., 2018. In this section, all variables are considered dimensionless. All simulations assumed no drops initially present in the column, $Q_d/A = 1$, $v_d = 1$, and inlet drop number distribution given by:

$$N_0 n_{in}(t, d) = v'(d)\frac{N_0}{\bar{v}_{in}} \exp\left[-\frac{v(d)}{\bar{v}_{in}}\right] \quad \text{(IV.100)}$$

where the drop number density, N_0, and the mean volume, $\bar{v}_{in}$, were chosen to be 0.05 and 1, respectively. For each case, the employed breakage and coalescence functions are reported in Table IV.1. Solutions are presented along the dimensionless vertical coordinate, $\zeta = z/h$ and the injection point of the disperse phase is located at $\zeta = 0.1$. For all cases, the simulation results were obtained assuming an uniform compartment height.
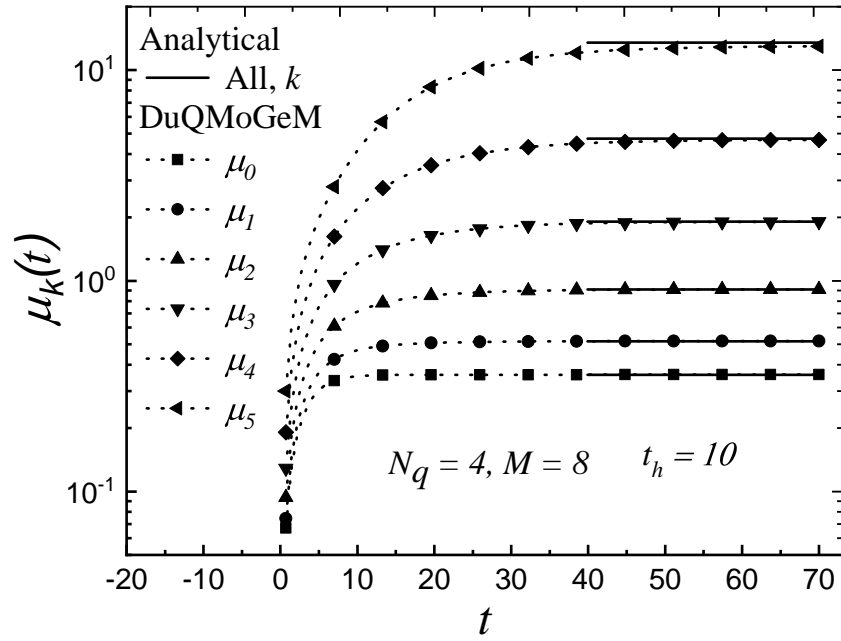
(a)
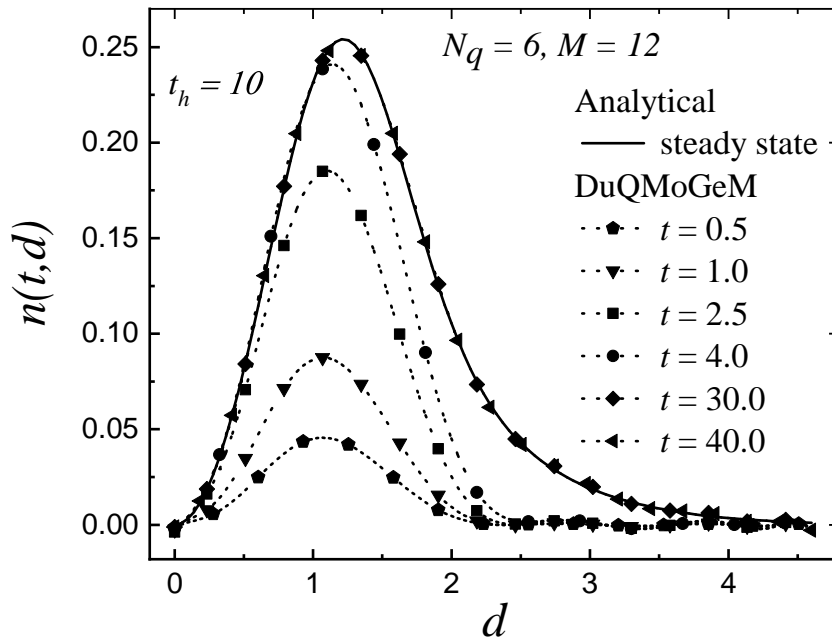
(b)

Figure IV.7: Pure coalescence problem in a continuous flow extraction vessel: comparison of the analytical and numerical results.

Table IV.1: Breakage and coalescence functions.

Case	$B(d/u)$	$g(d) = g_0 v(d)$	$\omega(d,u) = \omega_0$
1	$6d^2/u^3$	$g_0 = 10^{-2}$	$\omega_0 = 0$
2	0	$g_0 = 0$	$\omega_0 = 0.5$
3	$6d^2/u^3$	$g_0 = 1.92 \times 10^{-2},$	$\omega_0 = 0.3$

Case 1: pure breakage, $d \in [0, 2.5]$

The analytical solution is described as follows:

$$n(t,z,d) = v'(d)\frac{N_0}{\bar{v}_{in}}\exp\left[-(1+g_0\Delta z)\frac{v(d)}{\bar{v}_{in}}\right](1+g_0\Delta z)^2\mathcal{H}\left[t-\frac{\Delta z}{v_d}\right] \qquad \text{(IV.101)}$$

where $\Delta z = z - z_d$ and $\mathcal{H}$ is the Heaviside step function.

Case 2: pure coalescence, $d \in [0, 3.8]$

The exact solution for this case is written as:

$$n(t,z,d) = v'(d)\frac{N_0}{\bar{v}_{in}}\frac{4}{(2+N_0\omega\Delta z)^2}\exp\left[-\frac{2}{(2+N_0\omega\Delta z)}\frac{v(d)}{\bar{v}_{in}}\right]\mathcal{H}\left[t-\frac{\Delta z}{v_d}\right] \qquad \text{(IV.102)}$$

Case 3: breakage and coalescence, $d \in [0, 2.7]$

Using the technique reported in the chapter III, we can derive the analytical solution from that developed by McCoy and Madras, 2003 for the batch problem, leading to:

$$n(t,z,d) = v'(d)\frac{N_0}{\bar{v}_{in}}[\Phi(z)]^2\exp\left[-\Phi(z)\frac{v(d)}{\bar{v}_{in}}\right]\mathcal{H}\left[t-\frac{\Delta z}{v_d}\right] \qquad \text{(IV.103)}$$

where

$$\Phi(z) = \Phi(\infty)\frac{1+\Phi(\infty)\tanh(\Phi(\infty)\omega\Delta z N_0/2)}{\Phi(\infty)+\tanh(\Phi(\infty)\omega\Delta z N_0/2)}, \quad \Phi(\infty) = \left[\frac{2g_0\bar{v}_{in}}{\omega_0 N_0}\right]^{1/2} \qquad \text{(IV.104)}$$

For this solution, N_0 and $\bar{v}_{in}$ are constants for all t and z.

Convergence regarding the number of compartments

For $N_q = 3$ and $M = 6$, the effect of the number of compartments in the DuQMo-GeM solution for Case 1 was studied for $J = 50, 100$ and 200 compartments. The results for the first four regular moments are presented in Figure. IV.8, which shows that the DuQMoGeM accuracy improves by increasing the number of compartments. However,
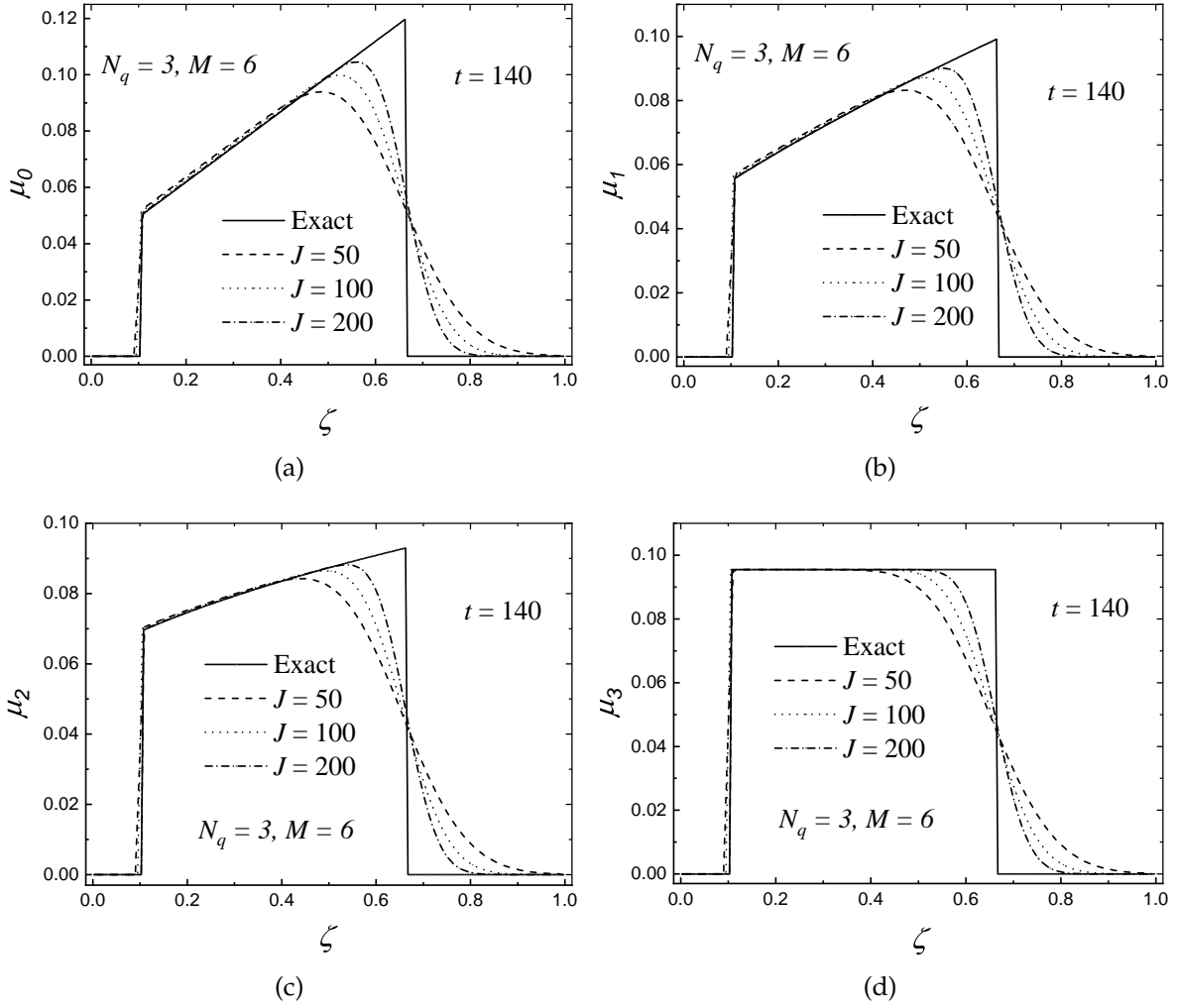
Figure IV.8: DuQMoGeM convergence regarding the number of compartments for the pure breakage problem.

$J = 200$ is still not enough to accurately capture the sharp moving front of the solution due to the numerical diffusion of the upwind scheme used for the advective part of F_j.

Prediction of the steady-state solution

Using $N_q = 4$, $M = 8$ and $J = 100$, the DuQMoGeM steady-state results for the moments of order $k = 1, 2, 3$ and 4 are compared with the analytical solution for the pure breakage, pure coalesence, and simultaneous breakage and coalescence in Figure. IV.9. The accuracy of the moments predicted by DuQMoGeM is very good. The third moment, μ_3, is constant after the injection point ($\zeta = 0.1$) in all cases due to the absence of mass transfer.
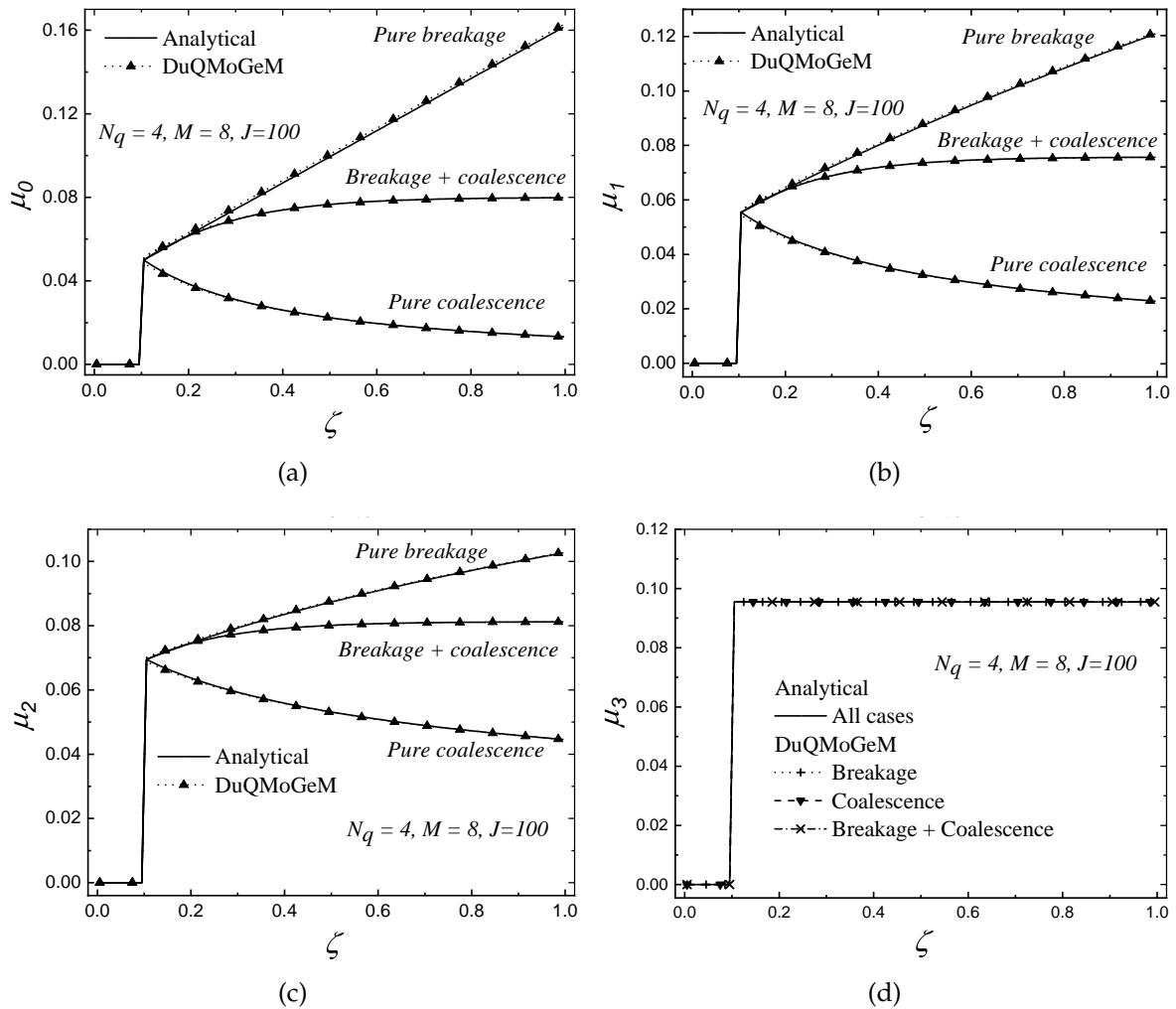
Figure IV.9: Comparison of the analytical and numerical moments for steady-state solutions in an extraction column.

The numerical and analytical distributions are shown in Figure. IV.10 at steady state at several ζ points. The DuQMoGeM results were obtained with $N_q = 6$, $M = 12$ and $J = 100$. The agreement between the simulated and analytical distributions is quite good, showing the ability of the DuQMoGeM to predict the drop number distributions in an extraction column.

Table IV.2 shows the mean CPU times and their standard deviations computed for 20 runs of case 3 simulation using each one of five sets of values for N_q, M, and J, which were defined as variations of the base case ($N_q = 3$, $M = 6$ and $J = 100$). When J doubled, the computational cost increased about 2.4 times. A 10-fold increase in M, added 38% in the CPU time. The simulation with $N_q = 3$ is about 67% more costly than that with $N_q = 2$. Therefore, the cost increase with M is mild, but it is superlinear with

Table IV.2: CPU times for simulating Case 3.*

Conditions	CPU time (s)	Standard deviation (s)
$N_q = 3, M = 6, J = 50$	0.85	0.02
$N_q = 3, M = 6, J = 100$	2.15	0.20
$N_q = 3, M = 6, J = 200$	5.06	0.11
$N_q = 3, M = 60, J = 100$	2.97	0.10
$N_q = 2, M = 6, J = 100$	1.28	0.03

*CodeBlocks 20.03 (Windows 10) on a Intel(R) Core(TM) i3-2348@2.30 GHz.

J or N_q for this simple problem.

IV.6.4   Experimental validation of an extraction column

As a final test, we compared the DuQMoGeM results with the experimental data of Hasseine et al., 2005 for the hydrodynamic behavior of a laboratory-scale Kühni column without mass transfer. It was operated in countercurrent mode with water as the continuous phase and toluene forming the drops of the dispersed phase. Many researchers widely used this chemical system that is recommended by the EFCE (European Federation of Chemical Engineering) as a test system for liquid extraction studies. This column has 44 compartments. The dispersed-phase was fed at compartment five ($j_d = 5$ and $z_d/h = 0.091$), and the continuous phase inlet is at the bottom of compartment 43 ($z_c = 294$ cm). The active height of the column, where there is mechanical agitation, consists of compartments 5 to 41. Table IV.3 shows the operating conditions and column dimensions, while Table IV.4 presents the physical properties of both phases. We reported the details of the Kühni column modeling in the following.

IV.6.5   Drop velocity correlations

The drop terminal velocity, v_t, was calculated according to the value of Morton number using the correlations given by J. C. Godfrey and Slater, 1994, Klee and Treybal, 1956, Grace, TH, et al., 1976, and Vignes, 1965.
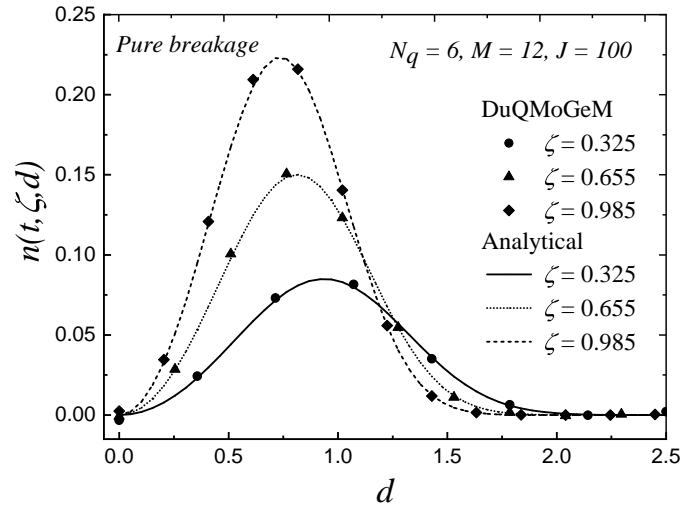
(a)
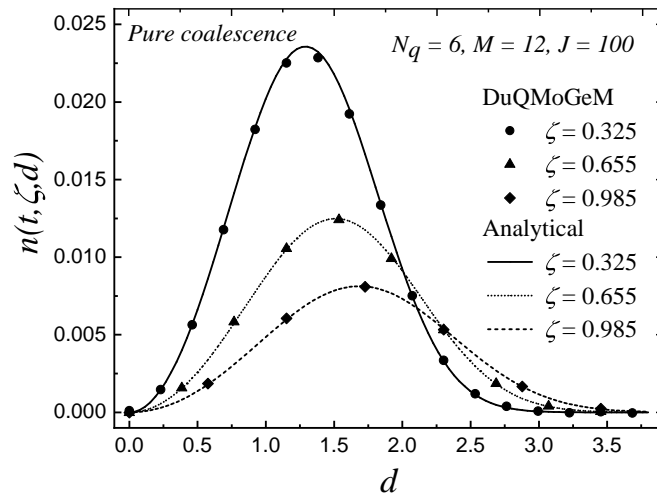
(b)

(c)

Figure IV.10: Comparison of the analytical and numerical distributions in an extraction column.

The slowing factor values for the Kühni column are provided by Fang et al., 1995:

$$k_v = 1 - (1 - \theta) \left(\frac{7.1810^{-5} Re_R / \theta}{1 + 7.1810^{-5} Re_R / \theta} \right) \tag{IV.105}$$

where θ is the relative free cross-sectional stator area and Re_R is defined by:

$$Re_R = \frac{\rho_c D_R^2 N_R}{\eta_c} \tag{IV.106}$$

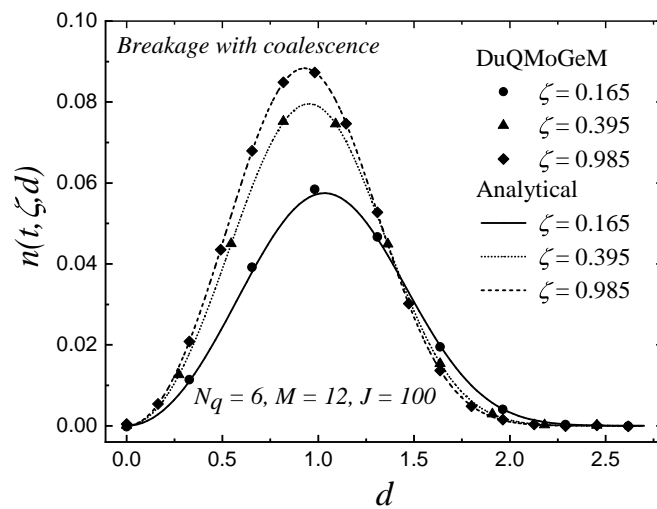The exponent in the swarm effect term was calculated from Bailes et al., 1986 correlation:

$$\kappa = 4.45 Re_p^{-0.1} - 1, \quad Re_p = \frac{\rho_c d v_t k_v}{\eta_c} \tag{IV.107}$$

IV.6.6   Initial and feed conditions

There are no drops in the column at $t = 0$, and the inlet drop distribution n_{in} is the experimental piecewise constant distribution employed by Hasseine et al., 2005, whose mean Sauter diameter is 0.294 cm.

IV.6.7   Dispersion coefficient correlations

We employed the dispersion coefficient correlations given by Steiner et al., 1988. For the continuous phase, the correlation is applied to each compartment:

$$\mathcal{D}_{c,j}(t) = \bar{v}_{c,j} h_j \left[0.188 + 0.0267 \theta^{0.5} \frac{D_R N_R}{\bar{v}_{c,j}} \right] \tag{IV.108}$$

where $\bar{v}_{c,j} = Q_c / [A(1 - r_{d,j}(t))]$ is the interstitial continuous-phase velocity and h_j is the actual height of the compartment j in the Kühni column. For the disperse phase, Steiner et al., 1988 also provided a correlation, but they recommended its usage with caution:

$$\mathcal{D}_{d,cor} = -3.78 \times 10^{-4} + 0.068 \left[\frac{Q_c}{A N_R} \right]^{0.5} \tag{IV.109}$$

Since $\mathcal{D}_d \to \mathcal{D}_c$ from above as the mixing intensity increases Gourdon et al., 1994, and following Seikova et al., 1992, we used:

$$\mathcal{D}_{d,j}(t) = \max(\mathcal{D}_{d,cor}, \mathcal{D}_{c,j}(t)) \tag{IV.110}$$

It should be noted that $\mathcal{D}_{c,j}$ and $\mathcal{D}_{d,j}$ are assumed null for the non-active sections of the Kühni column.

IV.6.8 Drop breakage

Different breakup mechanisms exist and strongly depend on the column geometry. The drop breakage probability is supposed to be homogeneous in each compartment Hasseine et al., 2005, the breakage frequency and the breakage probability were modeled by Cauwenberg et al., 1997; Simon et al., 2002 and recommended by Modes, 2000:

$$\frac{P(d)}{1 - P(d)} = 0.2148 We_m^{0.7796} \tag{IV.111}$$

where

$$We_m = \frac{\rho_c^{0.8} \eta_c^{0.2} d D_R^{1.6} (\omega^{1.8} - \omega_{crit}^{1.8})}{\sigma} \tag{IV.112}$$

The breakage frequency depends on the residence time:

$$g(z,d) = \frac{P(d) v_d(z,d)}{h_j} \tag{IV.113}$$

where

$$\omega_{crit} = 2\pi \, 0.65 \left(\frac{\rho_c D_R^3}{\sigma} \right)^{-0.5} \left(\frac{d}{D_R} \right)^{-0.72} \tag{IV.114}$$

where D_R is the rotor diameter.

The daughter droplet size distribution is described by a β distribution, based on the mother drop diameter d_0 Bahmanyar and Slater, 1991:

$$B(d_0, d) = 3(\nu - 1) \left(1 - \frac{d^3}{d_0^3} \right)^{\nu - 2} \frac{d^2}{d_0^3} \tag{IV.115}$$

where the mean number of daughter drops is calculated by:

$$\nu = 2 + 0.838 \left[\left(\frac{d_0}{d_{crit}} \right) - 1 \right]^{1.309} \tag{IV.116}$$

The critical diameter at which drops start to break is given by:

$$d_{crit} = 0.65 D_R W e_R^{-0.72} \tag{IV.117}$$

where:

$$We_R = \frac{\rho_c D_R^3 N_R^2}{\sigma} \tag{IV.118}$$

IV.6.9 Drop coalescence

For this process, the system properties at interfaces, the intensity of the collision and the contacting time between the colliding drops are key parameters. It is usual to define the coalescence rate as:

$$\omega\,(d_1, d_2, r_d) = \lambda\,(d_1, d_2, r_d)\, f\,(d_1, d_2, r_d) \tag{IV.119}$$

where λ is the collision efficiency, and f is the collision frequency. From the literature Coulaloglou and Tavlarides, 1977, the expressions for λ and f can be modeled by:

$$\lambda\,(d_1, d_2, r_d) = \exp\left[-\frac{C_2 \eta_c \rho_c \epsilon \left(\frac{d_1 d_2}{d_1 + d_2} \right)^4}{(1 + r_d)^3 \sigma^2} \right] \tag{IV.120}$$

and

$$f\,(d_1, d_2, r_d) = \frac{C_1 \sqrt[3]{\epsilon}\,(d_1 + d_2)^2 \sqrt{d_1^{2/3} + d_2^{2/3}}}{1 + r_d} \tag{IV.121}$$

where ϵ is the specific energy input, $C_1 = 0.01$ and $C_2 = 10^8\,m^{-2} = 10^4\,cm^{-2}$.

Table IV.3: Kühni column parameters.

Turbine diameter	$D_R = 0.085\,m$
Compartment height	$h_j = 0.07\,m, \forall j$
Total height	$h = 3.08m$
Active part	$2.52\,m$
Throughput continuous phase	$Q_c = 125\,L/h$
Throughput through the distributor	$Q_d = 130\,L/h$
Column diameter	$D = 0.15\,m$
Energy dissipation	$\epsilon = 0.0788\,W/kg$

Table IV.4: Chemical system properties.

$\eta_c\,(mPa)$	$\eta_d\,(mPa)$	$\rho_c\,(kg/m^3)$	$\rho_d\,kg/m^3$	$\sigma\,(mNm^{-1})$
0.92	0.6	997.2	862.2	33.7

IV.6.10   Mechanical power dissipation per unit mass

The power dissipation per unit mass is a parameter that affects the drop behavior in agitated systems A. Kumar and Hartland, 1995. The effect of the rotor can be

$$\epsilon = \frac{\mathcal{P}}{\rho_c A h_j} = \frac{4\mathcal{P}}{\pi D^2 h_j \rho_c} \tag{IV.122}$$

The power input per compartment can be calculated by:

$$\mathcal{P} = N_p N_R^3 D_R^5 \rho \tag{IV.123}$$

where N_p is the power number of the column:

$$N_p = 1.08 + \frac{10.94}{Re_R^{0.5}} + \frac{257.37}{Re_R^{1.5}} \tag{IV.124}$$

The numerical simulation of the Kühni column was carried out with $J = 44$, corresponding to the actual number of stages. We verified the convergence of the results by comparing those obtained using $N_q = 3$ and 4 and $M = 16$ and 32. After some preliminary simulations, we chose $[0.01, 0.4]\,cm$ as the diameter range. Sensitivity of the results to these choices of d_{min} and d_{max} was performed, and the results were essentially the same. Minor differences in the drop Sauter mean diameter results occurred only below the disperse-phase inlet, where the holdup is essentially zero. The simulation

reaches the steady-state profiles for the hold up after about 1000 s, but the breakage and coalescence dynamics were much faster. Thus, the results at $t = 1200$ can represent the steady-state. Figure IV.11 shows the simulated holdup profile and drop Sauter mean diameter together with the available experimental data Hasseine et al., 2005. Considering that the Sauter mean diameter data are scattered, the agreement between experimental and simulated data is fairly good. The simulation from $t = 0$ to $1200s$ whose results are shown in Figure. IV.11 took about 930 seconds on an Intel(R) Core(TM) i7-2600K@3.40 GHz (GNU FORTRAN compiler, version 9.3.0).
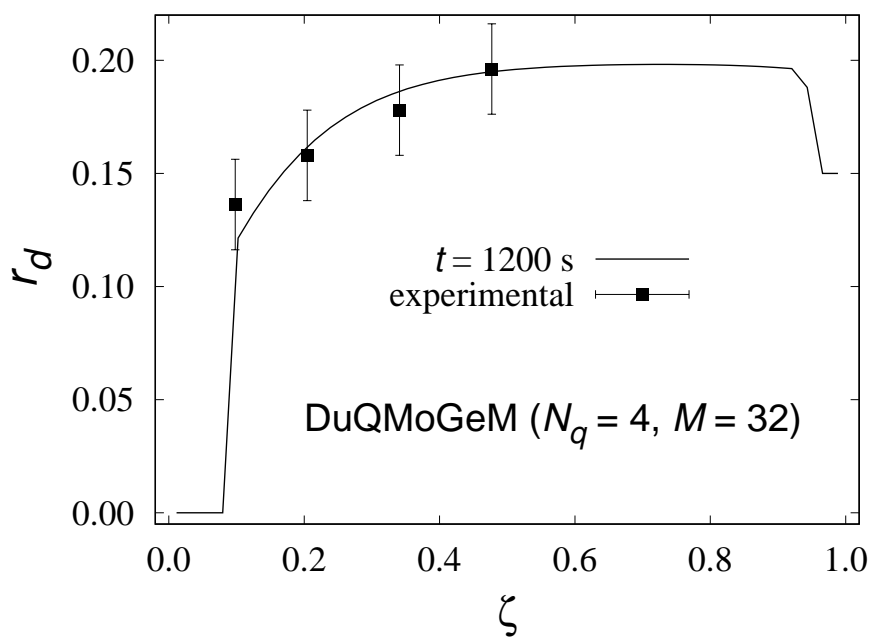
(a)
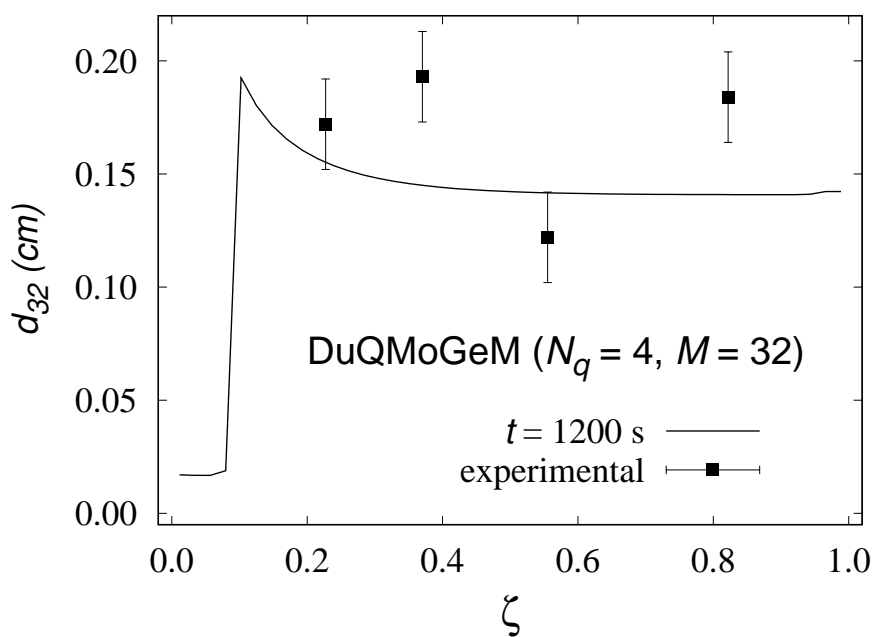
(b)

Figure IV.11: Simulated and experimental data for the Kühni column at steady-state: (a) dispersed phase holdup and (b) Sauter mean diameter.

IV.7   Conclusion

The DuQMoGeM results were compared to analytical solutions for batch and continuous well-mixed vessels and extraction columns, showing that it is accurate for predicting the evolution of the low order moments and the drop number distribution along with the column height. We also modeled a Kühni column for which the simulation accurately predicted the steady-state experimental holdup.

The numerical treatment is summarized as:

- The distribution is discretized by $N_q - point$ Gauss–Christoffel quadrature based on the $2N_q$ moments.

- The integrals related to the internal variable are calculated by $M - point$ Gaussian quadrature based on an orthogonal polynomial family.

- For the spatially discretization, we consider a multi-compartment column with J sections.

- Differential Algebraic System Solver (DASSL) is used as a numerical integration in time.

The results are encouraging the DuQMoGeM usage to solve the population balance equation.

General conclusion

This work explored the use of variational iteration method to applied to hydrodynamics simulation based on droplets population balance model for bubbles or droplets column. The considering equation is reduced by assuming uniform particle velocity (constant, linear in volume), neglecting diffusion flux, and applying chain rule transformation.

The exact solutions are successfully found, comparisons between the present method and the projection method which includes collocation (aggregation, breakage) and discontinuous Galerkin (growth) techniques are made.

The results showed that the variational iteration method eliminated complex calculations and provides highly accurate numerical solutions without spatial discretizations for the population balance equations. It is also worth noting that the advantage of the VIM methodology displays a fast convergence of the solutions. The illustrations show the rapid convergence of the solutions just as in a closed form solution. The numerical solutions obtained by projection method are in excellent agreements with the exact solutions.

Since its solutions are available just for some simple cases, the proposed solutions are very important to test the accurate of numerical methods to solve one dimensional population balance equation including growth, breakage and coalescence source terms.

Population balance models, including breakage and coalescence, were solved using DuQMoGeM for describing the dispersed phase behavior in liquid-liquid dispersed systems. We analyzed DuQMoGeM solutions for batch and continuous flow well-mixed vessels and liquid-liquid extraction columns. We considered problems including break-

age and coalescence for which analytical solutions exist. The moments of the droplet size distribution predicted by the DuQMoGeM were in excellent agreement with the analytical solutions. Besides, the DuQMoGeM approximation for the drop number distribution was also shown to be in good agreement with the analytical solutions.

We modeled and simulated a Kuhni column for which some experimental data exists. The DuQMoGeM results for the disperse phase holdup agreed well with the experimental data at the steady-state, and the simulated drop Sauter mean diameter compared favorably with the scattered experimental data.

Therefore, we showed that the DuQMoGeM is a very efficient technique for solving droplet population balance models, being quite promising for modeling and simulating liquid-liquid extraction columns.

References

Abbasbandy, S. (2006). Numerical solutions of the integral equations: Homotopy perturbation method and adomian's decomposition method. *Applied Mathematics and Computation*, *173*(1), 493–500.

Abdou, M., & Soliman, A. (2005). New applications of variational iteration method. *Physica D: Nonlinear Phenomena*, *211*(1-2), 1–8.

Adomian, G. (1990). A review of the decomposition method and some recent results for nonlinear equations. *Mathematical and Computer Modelling*, *13*(7), 17–43.

Adomian, G., & Rach, R. (1986). On linear and nonlinear integro-differential equations. *Journal of mathematical analysis and applications*, *113*(1), 199–201.

Adomian, G. (1988). *Nonlinear stochastic systems theory and applications to physics* (Vol. 46). Springer Science & Business Media.

Adomian, G. (2013). *Solving frontier problems of physics: The decomposition method* (Vol. 60). Springer Science & Business Media.

Altunok, M., Grömping, T., & Pfennig, A. (2006). Redrop—an efficient simulation tool for describing solvent and reactive extraction columns. *Computer aided chemical engineering* (pp. 665–670). Elsevier.

Athmani, K., da Cunha Lage, P. L., & Hasseine, A. (2022). The duqmogem application to the numerical modeling of liquid-liquid columns. *Chemical Engineering Science*, 117721.

Attarakih, M., Abu-Khader, M., & Bart, H.-J. (2013). Modeling and dynamic analysis of a rotating disc contactor (rdc) extraction column using one primary and one secondary particle method (opospm). *Chemical Engineering Science*, *91*, 180–196.

Attarakih, M., Al-Zyod, S., Abu-Khader, M., & Bart, H.-J. (2012). Ppblab: A new multivariate population balance environment for particulate system modelling and simulation. *Procedia Engineering*, *42*, 1445–1462.

Attarakih, M. M., Bart, H.-J., & Faqir, N. M. (2004). Numerical solution of the spatially distributed population balance equation describing the hydrodynamics of interacting liquid–liquid dispersions. *Chemical Engineering Science*, *59*(12), 2567–2592.

Attarakih, M. M., Bart, H.-J., & Faqir, N. M. (2006a). Solution of the population balance equation using the sectional quadrature method of moments (sqmom). *Computer aided chemical engineering* (pp. 209–214). Elsevier.

Attarakih, M. M., Bart, H.-J., & Faqir, N. M. (2006b). Solution of the population balance equation using the sectional quadrature method of moments (sqmom). *Computer aided chemical engineering* (pp. 209–214). Elsevier.

Attarakih, M. M., Bart, H.-J., Lagar, L., & Faqir, N. M. (2006). Llecmod: A windows-based program for hydrodynamics simulation of liquid–liquid extraction columns. *Chemical Engineering and Processing: Process Intensification*, *45*(2), 113–123.

Attarakih, M. M., Drumm, C., & Bart, H.-J. (2009). Solution of the population balance equation using the sectional quadrature method of moments (sqmom). *Chemical Engineering Science*, *64*(4), 742–752.

Babolian, E., & Biazar, J. (2002). Solving the problem of biological species living together by adomian decomposition method. *Applied Mathematics and computation*, *129*(2-3), 339–343.

Bahmanyar, H., & Slater, M. J. (1991). Studies of drop break-up in liquid-liquid systems in a rotating disc contactor. part i: Conditions of no mass transfer. *Chemical Engineering & Technology: Industrial Chemistry-Plant Equipment-Process Engineering-Biotechnology*, *14*(2), 79–89.

Bailes, P. J., Gledhill, J., Godfrey, J. C., & Slater, M. J. (1986). Hydrodynamic behaviour of packed, rotating disc and kühni liquid/liquid extraction columns. *Chemical engineering research & design*, *64*(1), 43–55.

Bart, H.-J., Jildeh, H., & Attarakih, M. (2020). Population balances for extraction column simulations—an overview. *Solvent Extraction and Ion Exchange*, *38*(1), 14–65.

Cabassud, M., Gourdon, C., & Casamatta, G. (1990). Single drop break-up in a kühni column. *The Chemical Engineering Journal*, *44*(1), 27–41.

Campos, F., & Lage, P. (2003). A numerical method for solving the transient multidimensional population balance equation using an euler–lagrange formulation. *Chemical Engineering Science*, *58*(12), 2725–2744.

Casamatta, G. (1981). *Comportement de la population des gouttes dans une colonne d'extraction: Transport, rupture, coalescence, transfert de matière.* (Doctoral dissertation).

Cauwenberg, V., Degrève, J., & Slater, M. J. (1997). The interaction of solute transfer, contaminants and drop break-up in rotating disc contactors: Part i. correlation of drop breakage probabilities. *The Canadian Journal of Chemical Engineering, 75*(6), 1046–1055.

Chesters, A. (1991). Modelling of coalescence processes in fluid-liquid dispersions: A review of current understanding. *Chemical engineering research and design*, *69*(A4), 259–270.

Cockburn, B. (2003). An introduction to the discontinuous galerkin method for convection-dominated problems lecture notes. *University of Minnesotta*.

Cockburn, B., & Shu, C.-W. (1989). Tvb runge-kutta local projection discontinuous galerkin finite element method for conservation laws. ii. general framework. *Mathematics of computation*, *52*(186), 411–435.

Coulaloglou, C., & Tavlarides, L. L. (1977). Description of interaction processes in agitated liquid-liquid dispersions. *Chemical Engineering Science*, *32*(11), 1289–1297.

Dudek, M., Fernandes, D., Herø, E. H., & Øye, G. (2020). Microfluidic method for determining drop-drop coalescence and contact times in flow. *Colloids and Surfaces A: Physicochemical and Engineering Aspects*, *586*, 124265.

Dutta, B. K. (2007). *Principles of mass transfer and seperation processes*. PHI Learning Pvt. Ltd.

El-Shahed, M. (2005). Application of he's homotopy perturbation method to volterra's integro-differential equation. *International Journal of Nonlinear Sciences and Numerical Simulation*, *6*(2), 163–168.

Fang, J., Godfrey, J., Mao, Z.-Q., Slater, M., & Gourdon, C. (1995). Single liquid drop breakage probabilities and characteristic velocities in kühni columns. *Chemical engineering & technology*, *18*(1), 41–48.

Fernandez-Diaz, J., & Gomez-Garcia, G. (2007). Exact solution of smoluchowski's continuous multi-component equation with an additive kernel. *EPL (Europhysics Letters)*, *78*(5), 56002.

Fox, R. O. (2003). *Computational models for turbulent reacting flows*. Cambridge university press.

Garthe, D. (2006). *Fluiddynamics and mass transfer of single particles and swarms of particles in extraction columns* (Doctoral dissertation). Technische Universität München.

Gayler, R., Roberts, N., & Pratt, H. R. (1953). *Liquid-liquid extraction. part 4. a further study of hold-up in packed columns* (tech. rep.). Atomic Energy Research Establishment, Harwell, Berks (England).

Gelbard, F., & Seinfeld, J. H. (1978). Numerical solution of the dynamic equation for particulate systems. *Journal of Computational Physics*, *28*(3), 357–375.

Godfrey, J. (1991). Slip velocity relationships for liquid-liquid extraction columns. *Trans. Instn. Chem. Engrs.*, *69*, 130–141.

Godfrey, J., Slater, M., & Liquid-liquid Extraction Equipment, J. W. (1994). Sons. *New York*.

Godfrey, J. C., & Slater, M. J. (1994). *Liquid-liquid extraction equipment*. Wiley New York.

Gordon, R. G. (1968). Error bounds in equilibrium statistical mechanics. *Journal of Mathematical Physics*, *9*(5), 655–663.

Gourdon, C., Casamatta, G., & Muratet, G. (1994). Population balance based modelling. In J. Godfrey & M. Slater (Eds.), *Liquid-liquid extraction equipment* (pp. 141–226). John Wiley & Sons.

Grace, J., TH, N. et al. (1976). Shapes and velocities of single drops and bubbles moving freely through immiscible liquids. *Chemical engineering*, *54*, 167–173.

Hančil, V., & Rod, V. (1988). Break-up of a drop in a stirred tank. *Chemical Engineering and Processing: Process Intensification*, *23*(3), 189–193.

Hasseine, A., Barhoum, Z., Attarakih, M., & Bart, H.-J. (2015). Analytical solutions of the particle breakage equation by the adomian decomposition and the variational iteration methods. *Advanced Powder Technology*, *26*(1), 105–112.

Hasseine, A., & Bart, H.-J. (2015). Adomian decomposition method solution of population balance equations for aggregation, nucleation, growth and breakup processes. *Applied Mathematical Modelling*, *39*(7), 1975–1984.

Hasseine, A., Bellagoun, A., & Bart, H.-J. (2011). Analytical solution of the droplet breakup equation by the adomian decomposition method. *Applied Mathematics and Computation*, *218*(5), 2249–2258.

Hasseine, A., Meniai, A.-H., Lehocine, M. B., & Bart, H.-J. (2005). Assessment of drop coalescence and breakup for stirred extraction columns. *Chemical Engineering & Technology: Industrial Chemistry-Plant Equipment-Process Engineering-Biotechnology*, *28*(5), 552–560.

Hasseine, A., Bechka, I., Attarakih, M., & Bart, H.-J. (2017). Applications of he's methods to the steady-state population balance equation in continuous flow systems. *Journal of Applied Engineering Science & Technology*, *3*(2), 71–78.

Hasseine, A. (2007). Modèlisation des colonnes d'extraction liquide-liquide à base de la résolution du bilan de population. incorporation des phénomènes de rupture et de coalescence des gouttes.

Hasseine, A., Athmani, K., & Bart, H. J. (2018). Variational iteration method and projection method solution of the spatially distributed population balance equation. *Arab Journal of Basic and Applied Sciences*, *25*(3), 132–141.

Hasseine, A., Hlawitschka, M. W., Omar, W., & Bart, H.-J. (2020). New analytical and numerical solutions of the particle breakup process. *The Open Chemical Engineering Journal*, *14*(1).

Hasseine, A., Senouci, S., Attarakih, M., & Bart, H.-J. (2015). Two analytical approaches for solution of population balance equations: Particle breakage process. *Chemical Engineering & Technology*, *38*(9), 1574–1584.

He, J.-H. (1998). Approximate analytical solution for seepage flow with fractional derivatives in porous media. *Computer Methods in Applied Mechanics and Engineering*, *167*(1-2), 57–68.

He, J.-H. (1999a). Homotopy perturbation technique. *Computer methods in applied mechanics and engineering*, *178*(3-4), 257–262.

He, J.-H. (1999b). Variational iteration method–a kind of non-linear analytical technique: Some examples. *International journal of non-linear mechanics*, *34*(4), 699–708.

He, J.-H. (2000a). A coupling method of a homotopy technique and a perturbation technique for non-linear problems. *International journal of non-linear mechanics*, *35*(1), 37–43.

He, J.-H. (2000b). Variational iteration method for autonomous ordinary differential systems. *Applied mathematics and computation*, *114*(2-3), 115–123.

He, J.-H. (2003). Homotopy perturbation method: A new nonlinear analytical technique. *Applied Mathematics and computation*, *135*(1), 73–79.

He, J.-H. (2004a). The homotopy perturbation method for nonlinear oscillators with discontinuities. *Applied mathematics and computation*, *151*(1), 287–292.

He, J.-H. (2004b). Variational principles for some nonlinear partial differential equations with variable coefficients. *Chaos, Solitons & Fractals*, *19*(4), 847–851.

He, J.-H. (2005a). Application of homotopy perturbation method to nonlinear wave equations. *Chaos, Solitons & Fractals*, *26*(3), 695–700.

He, J.-H. (2005b). Homotopy perturbation method for bifurcation of nonlinear problems. *International Journal of Nonlinear Sciences and Numerical Simulation*, *6*(2), 207–208.

He, J.-H. (2006). Some asymptotic methods for strongly nonlinear equations. *International journal of Modern physics B*, *20*(10), 1141–1199.

He, J.-H. (2007). Variational iteration method—some recent results and new interpretations. *Journal of computational and applied mathematics*, *207*(1), 3–17.

He, J. (1997). A new approach to nonlinear partial differential equations. *Communications in Nonlinear Science and Numerical Simulation*, *2*(4), 230–235.

Henschke, M. (2004). *Auslegung pulsierter siebboden-extraktionskolonnen*. Shaker.

Hounslow, M. (1998). The population balance as a tool for understanding particle rate processes. *KONA Powder and Particle Journal*, *16*, 179–193.

Hounslow, M. J. (1990). A discretized population balance for continuous systems at steady state. *AIChE journal*, *36*(1), 106–116.

Hounslow, M., Ryall, R., & Marshall, V. (1988). A discretized population balance for nucleation, growth, and aggregation. *AIChE journal*, *34*(11), 1821–1832.

Hulburt, H. M., & Katz, S. (1964). Some problems in particle technology: A statistical mechanical formulation. *Chemical engineering science*, *19*(8), 555–574.

Jafari, H., Zabihi, M., & Saidy, M. (2008). Application of homotopy perturbation method for solving gas dynamics equation. *Applied Mathematical Sciences*, *2*(48), 2393–2396.

Jaradat, M. (2012). Dynamic modelling and simulation of (pulsed and stirred) liquid-liquid extraction columns using the population balance equation.

John, V., Angelov, I., Öncül, A., & Thévenin, D. (2007). Techniques for the reconstruction of a distribution from a finite number of its moments. *Chemical Engineering Science*, *62*(11), 2890–2904.

Klee, A. J., & Treybal, R. E. (1956). Rate of rise or fall of liquid drops. *AIChE Journal*, *2*(4), 444–447.

Kopriwa, N., Buchbender, F., Ayesterán, J., Kalem, M., & Pfennig, A. (2012). A critical review of the application of drop-population balances for the design of solvent extraction columns: I. concept of solving drop-population balances and modelling breakage and coalescence. *Solvent Extraction and Ion Exchange*, *30*(7), 683–723.

Kronberger, T., Ortner, A., Zulehner, W., & Bart, H.-J. (1995). Numerical simulation of extraction columns using a drop population model. *Computers & chemical engineering*, *19*, 639–644.

Kumar, A., & Hartland, S. (1992). Prediction of axial mixing coefficients in rotating disc and asymmetric rotating disc extraction columns. *The Canadian Journal of Chemical Engineering*, *70*(1), 77–87.

Kumar, A., & Hartland, S. (1995). A unified correlation for the prediction of dispersed-phase hold-up in liquid-liquid extraction columns. *Industrial & engineering chemistry research*, *34*(11), 3925–3940.

Kumar, S., & Ramkrishna, D. (1997). On the solution of population balance equations by discretization—iii. nucleation, growth and aggregation of particles. *Chemical Engineering Science*, *52*(24), 4659–4679.

Kumar, S., & Ramkrishna, D. (1996a). On the solution of population balance equations by discretization—i. a fixed pivot technique. *Chemical Engineering Science*, *51*(8), 1311–1332.

Kumar, S., & Ramkrishna, D. (1996b). On the solution of population balance equations by discretization—ii. a moving pivot technique. *Chemical Engineering Science*, *51*(8), 1333–1342.

Lage, P. L. (2011). On the representation of qmom as a weighted-residual method—the dual-quadrature method of generalized moments. *Computers & Chemical Engineering*, *35*(11), 2186–2203.

Lage, P. (2002). Comments on the"an analytical solution to the population balance equation with coalescence and breakage-the special case with constant number of particles"by dp patil and jrg andrews [chemical engineering science 53 (3) 599-601]. *Chemical Engineering Science*, *19*(57), 4253–4254.

Laitinen, A. T., Penttilä, K. J., Manninen, M. T., Syrjänen, J. K., Kaunisto, J. M., & Murtomäki, L. S. (2019). Axial dispersion and cfd models for the extraction of lev-

ulinic acid from dilute aqueous solution in a kühni column with 2- methylte-trahydrofuran solvent. *Chemical Engineering Research and Design*, *146*, 518–527.

Li, N., & Ziegler, E. (1967). Effect of axial mixing on mass transfer in extraction columns. *Industrial & Engineering Chemistry*, *59*(3), 30–36.

Liou, J.-J., Srienc, F., & Fredrickson, A. (1997). Solutions of population balance models based on a successive generations approach. *Chemical Engineering Science*, *52*(9), 1529–1540.

Mantzaris, N. V., Daoutidis, P., & Srienc, F. (2001a). Numerical solution of multi-variable cell population balance models: I. finite difference methods. *Computers & Chemical Engineering*, *25*(11-12), 1411–1440.

Mantzaris, N. V., Daoutidis, P., & Srienc, F. (2001b). Numerical solution of multi-variable cell population balance models. iii. finite element methods. *Computers & Chemical Engineering*, *25*(11-12), 1463–1481.

Marchal, P., David, R., Klein, J., & Villermaux, J. (1988). Crystallization and precipitation engineering—i. an efficient method for solving population balance in crystallization with agglomeration. *Chemical Engineering Science*, *43*(1), 59–67.

Marchisio, D. L., & Fox, R. O. (2005). Solution of population balance equations using the direct quadrature method of moments. *Journal of Aerosol Science*, *36*(1), 43–73.

Marchisio, D. L., Vigil, R. D., & Fox, R. O. (2003a). Implementation of the quadrature method of moments in cfd codes for aggregation–breakage problems. *Chemical Engineering Science*, *58*(15), 3337–3351.

Marchisio, D. L., Vigil, R. D., & Fox, R. O. (2003b). Quadrature method of moments for aggregation–breakage processes. *Journal of colloid and interface science*, *258*(2), 322–334.

McCoy, B. J., & Madras, G. (2003). Analytical solution for a population balance equation with aggregation and fragmentation. *Chemical Engineering Science*, *58*(13), 3049–3051.

McGraw, R. (1997). Description of aerosol dynamics by the quadrature method of moments. *Aerosol Science and Technology*, *27*(2), 255–265.

Modes, G. (2000). *Grundsätzliche studie zur populationsdynamik einer extraktionskolonne auf basis von einzeltropfenuntersuchungen*. Shaker.

Mohyud-Din, S. T., Sikander, W., Khan, U., & Ahmed, N. (2017). Optimal variational iteration method for nonlinear problems. *Journal of the Association of Arab Universities for Basic and Applied Sciences*, *24*, 191–197.

Momani, S., & Abuasad, S. (2006). Application of he's variational iteration method to helmholtz equation. *Chaos, Solitons & Fractals*, *27*(5), 1119–1123.

Momani, S., & Odibat, Z. (2006). Analytical solution of a time-fractional navier–stokes equation by adomian decomposition method. *Applied Mathematics and Computation*, *177*(2), 488–494.

Muralidhar, R., & Ramkrishna, D. (1986). Analysis of droplet coalescence in turbulent liquid-liquid dispersions. *Industrial & engineering chemistry fundamentals*, *25*(4), 554–560.

Nicmanis, M., & Hounslow, M. (1996). A finite element analysis of the steady state population balance equation for particulate systems: Aggregation and growth. *Computers & chemical engineering*, *20*, S261–S266.

Nicmanis, M., & Hounslow, M. (1998). Finite-element methods for steady-state population balance equations. *AIChE Journal*, *44*(10), 2258–2272.

Odibat, Z., & Momani, S. (2008). Modified homotopy perturbation method: Application to quadratic riccati differential equation of fractional order. *Chaos, Solitons & Fractals*, *36*(1), 167–174.

Patil, D., & Andrews, J. (1998). An analytical solution to continuous population balance model describing floc coalescence and breakage—a special case. *Chemical Engineering Science*, *53*(3), 599–601.

Rajabi, A., Ganji, D., & Taherian, H. (2007). Application of homotopy perturbation method in nonlinear heat conduction and convection equations. *Physics Letters A*, *360*(4-5), 570–573.

Ramkrishna, D. (2000). *Population balances: Theory and applications to particulate systems in engineering*. Elsevier.

Ramkrishna, D., & Singh, M. R. (2014). Population balance modeling: Current status and future prospects. *Annual review of chemical and biomolecular engineering*, *5*, 123–146.

Reddy, C. R., Surender, O., Rao, C. V., & Pradeepa, T. (2017). Adomian decomposition method for hall and ion-slip effects on mixed convection flow of a chemically reacting newtonian fluid between parallel plates with heat generation/absorption. *Propulsion and Power Research*, *6*(4), 296–306.

Roul, P. (2010). Application of homotopy perturbation method to biological population model. *Applications and Applied Mathematics: An International Journal (AAM)*, *5*(2), 2.

Sandu, A. (2004). Piecewise polynomial solutions of aerosol dynamic equations. *Computer Science technical report*, *CS-TR-04-01*(-), -.

Sandu, A., & Borden, C. (2003). A framework for the numerical treatment of aerosol dynamics. *Applied Numerical Mathematics*, *45*(4), 475–497.

Santos, F., Favero, J., & Lage, P. (2013). Solution of the population balance equation by the direct dual quadrature method of generalized moments. *Chemical Engineering Science*, *101*, 663–673.

Schmidt, S., Simon, M., & Bart, H.-J. (2003). Tropfenpopulationsmodellierung–einfluss von stoffsystem und technischen geometrien. *Chemie Ingenieur Technik*, *75*(1-2), 62–68.

Seikova, I., Gourdon, C., & Casamatta, G. (1992). Single-drop transport in a kühni extraction column. *Chemical Engineering Science*, *47*(15), 4141–4154. https://doi.org/https://doi.org/10.1016/0009-2509(92)85164-7

Simon, M., Schmidt, S., & Bart, H.-J. (2002). Bestimmung von zerfalls-und koaleszenzparametern in flüssig/flüssig-systemen auf der grundlage von einzeltropfenexperimenten. *Chemie Ingenieur Technik*, *74*(3), 247–256.

Simon, M., Schmidt, S. A., & Bart, H.-J. (2003). The droplet population balance model–estimation of breakage and coalescence. *Chemical Engineering & Technology: Industrial Chemistry-Plant Equipment-Process Engineering-Biotechnology*, *26*(7), 745–750.

Smoluchowski, M. v. (1916). Drei vortrage uber diffusion, brownsche bewegung und koagulation von kolloidteilchen. *Zeitschrift fur Physik*, *17*, 557–585.

Steiner, L., Kumar, A., & Hartland, S. (1988). Determination and correlation of axial-mixing parameters in an agitated liquid-liquid extraction column. *The Canadian Journal of Chemical Engineering*, *66*, 241–247.

Strand, C., Olney, R., & Ackerman, G. (1962). Fundamental aspects of rotating disk contactor performance. *AIChE Journal*, *8*(2), 252–261.

Su, J., Gu, Z., & Xu, X. Y. (2009). Advances in numerical methods for the solution of population balance equations for disperse phase systems. *Science in China Series B: Chemistry*, *52*(8), 1063–1079.

Tsouris, C., & Tavlarides, L. (1994). Breakage and coalescence models for drops in turbulent dispersions. *AIChE Journal*, *40*(3), 395–406.

Valentas, K. J., & Amundson, N. R. (1966). Breakage and coalescence in dispersed phase systems. *Industrial & Engineering Chemistry Fundamentals*, *5*(4), 533–542.

Valentas, K. J., Bilous, O., & Amundson, N. R. (1966). Analysis of breakage in dispersed phase systems. *Industrial & engineering chemistry fundamentals*, *5*(2), 271–279.

Vignes, A., & Globule, H. D. D.-M. D. (1965). Dans un fluide immobile et infini. *Genie Chim*, *93*(5), 129–142.

Vignes, A. (1965). Hydrodynamique des dispersions. *Genie Chimique*, *93*, 129–142.

Wazwaz, A.-M. (2007). The variational iteration method for rational solutions for kdv, k (2, 2), burgers, and cubic boussinesq equations. *Journal of Computational and Applied Mathematics*, *207*(1), 18–23.

Weber, B., Schneider, M., Görtz, J., & Jupke, A. (2020). Compartment model for liquid-liquid extraction columns. *Solvent Extraction and Ion Exchange*, *38*(1), 66–87.

Yuan, C., Laurent, F., & Fox, R. (2012). An extended quadrature method of moments for population balance equations. *Journal of Aerosol Science*, *51*, 1–23.

Appendix A

MATHEMATICAL FUNCTIONS

A.1 Dirac delta function

$\delta(x)$ returns 0 for all real numeric x except 0 .

A.2 Gamma function

$$\Gamma(x) = \int_0^\infty t^{x-1} e^{-t} dt, \quad (\Re(x) > 0)$$

A.3 Unit step function

$$u[x] = \begin{cases} 1, & x \geq 0 \\ 0, & x \text{ otherwise} \end{cases}$$

A.4   Modified Bessel functions Modified Bessel functions of the first kind

$$\text{BesselI}\,[n,z] = I_n(z) = \sum_{k=0}^{\infty} \frac{1}{\Gamma(k+1)\Gamma(k+n+1)} \left(\frac{z}{2}\right)^{2k+1}, \quad n \in \Re \text{ and } z \in \mathbb{C}$$

A.5   Modified Bessel functions of the second kind

$$\text{BesselK}[n,z] = K_n(z) = \frac{\pi}{2} \frac{I_{-n}(z) - I_n(z)}{\sin(n\pi)}, \quad n \in \Re \text{ and } z \in \mathbb{C}$$

A.6   Pochhammer symbol

$$\text{Pochhammer}\,[n,z] = (z)_n = \frac{\Gamma(z+n)}{\Gamma(z)}$$

Appendix B

ORAL AND POSTER PRESENTATIONS

1. *Study of the droplet population in liquid-liquid extraction columns.* Fifth International Conference on Energy, Materials, Applied Energetics and Pollution (ICEMAEP'I9), Constantine, Algeria. 22-24/10/2019.
   Iman Bechka, Khaled Athmani and Abdelmalek Hasseine.

2. *Solution of Two-component Aggregation Population Balance Equation (PBE) for Sum Kernel by Adomian Decomposition Method (ADM).* 4th International Symposium on Materials and Sustainable Development (ISMSD2019). M'hamed Bougara University of Boumerdes, Algeria. 12-14/11/2019.
   Khaled Athmani, Abdelmalek Hasseine and Iman Bechka.

3. *Solution of two-component aggregation population balance equation by Adomian decomposition method.* The international conference on waste treatment and valorization ICWTV2019.University Salah Boubnider Constantine 3, Constontine, Algeria. 26-27/11/2019.
   Khaled Athmani, Abdelmalek Hasseine and Iman Bechka.

4. *Solution of two-component population balance equation for the simultaneous growth and aggregation by the variational iteration method.* International seminar on green chemistry and sustainable engineering ISGCSE. University Echahid Hamma Lakhdar,

124

El-Oued, Algeria. 17-18/12/2019.

Khaled Athmani, Abdelmalek Hasseine and Iman Bechka.

5. *Solution of two-component aggregation population balance equation for a constant kernel by Variational Iteration Method* . The 1st National Virtual Conference on Chemical Process and Environmental Engineering NVCCPEE University of Biskra, Algeria, 15-16/12/2021.

Khaled Athmani and Abdelmalek Hasseine.

Appendix C

LIST OF PUBLICATIONS

1. **Article:** Variational iteration method and projection method solution of the spatially distributed population balance equation, 2018. Arab Journal of Basic and Applied Sciences, 25(3): 132-141.
   Abdelmalek Hasseine, Khaled Athmani and Hans Joerg Bart.
   doi: 10.1080/25765299.2018.1517485

2. **Article:** The DuQMoGeM application to the numerical modeling of liquid-liquid columns, 2022. Chemical Engineering Science, 257.
   Khaled Athmani, Paulo Laranjeira da Cunha Lage and Abdelmalek Hasseine.
   doi: https://doi.org/10.1016/j.ces.2022.117721